
DNA Damage-Induced Degradation of Elongating RNA Polymerase II by a SUMO-Dependent Mechanism

DISSERTATION DER FAKULTÄT FÜR BIOLOGIE DER
LUDWIG-MAXIMILIANS-UNIVERSITÄT MÜNCHEN



vorgelegt von

Irina Heckmann

München, 2016

Die vorliegende Arbeit wurde zwischen Mai 2011 und Juli 2016 unter der Anleitung von Prof. Dr. Stefan Jentsch am Max-Planck-Institut für Biochemie in Martinsried durchgeführt.

Erstgutachter: Prof. Dr. Stefan Jentsch

Zweitgutachter: Prof. Dr. Angelika Böttger

Tag der Abgabe: 7.07.2016

Tag der mündlichen Prüfung: 3.11.2016

EIDESSTATTLICHE ERKLÄRUNG

Hiermit erkläre ich an Eides statt, dass ich die vorliegende Dissertation selbstständig und ohne unerlaubte Hilfe angefertigt habe. Ich habe weder anderweitig versucht, eine Dissertation einzureichen oder eine Doktorprüfung durchzuführen, noch habe ich diese Dissertation oder Teile derselben einer anderen Prüfungskommission vorgelegt.

München, den 24.11.2016

.....
Irina Heckmann

TABLE OF CONTENTS

1	SUMMARY	1
2	INTRODUCTION	2
2.1	The Consequences of DNA Damage	2
2.2	DNA Repair in the Context of Stalled Replication Machinery	3
2.3	DNA Repair in the Context of Stalled Transcription Machinery	4
2.3.1	The Nucleotide Excision Repair (NER) Pathway	5
2.4	Degradation of RNA Polymerase II upon DNA Damage	8
2.4.1	Posttranslational Modifications of Rpb1	8
2.4.2	Ubiquitin and the Small Ubiquitin-Like Modifier (SUMO)	10
2.4.3	Functions of Ubiquitylation and SUMOylation	12
2.4.4	Mechanism of Proteasomal Degradation of Rpb1	13
2.4.5	SUMO-Targeted Ubiquitin Ligases (STUbLs)	16
3	AIMS OF THIS STUDY	18
4	RESULTS	19
4.1	DNA damage-induced degradation of Rpb1 from the elongating pool of RNA polymerase II	19
4.2	Degradation of Rpb1 is dependent on the proteasome and the ubiquitin/SUMO-specific segregase Cdc48	22
4.3	Rpb1 ubiquitylation upon DNA damage involves the ubiquitin ligases Rsp5 and Elc1-Cul3	24
4.4	Rpb1 is SUMOylated upon DNA damage and thereby marked for degradation	27
4.5	Rpb1 SUMOylation is not restricted to previously identified lysine residues	29
4.6	Degradation of Rpb1 is mediated by a SUMO-dependent pathway involving the SUMO-targeted ubiquitin ligase Slx5/Slx8	31
4.7	The kinases CTDK1 and Bur1/Bur2 are not degraded upon DNA damage	32
4.8	Transcription-coupled repair (TCR) is important for DNA damage-induced Rpb1 degradation	34
4.9	RNAPII accumulates on chromatin after DNA damage if Rpb1 is not removed by proteasomal degradation	35
4.10	Interference with the nuclear pore complex influences Rpb1 degradation	37

5	DISCUSSION	39
5.1	Potential loss of Rpb1 phosphorylation after DNA damage	39
5.2	Rpb1 is degraded in a SUMOylation- and ubiquitylation-dependent manner	40
5.3	Influence of the nuclear pore complex on Rpb1 degradation.....	42
5.4	Rpb1 is monoubiquitylated by previously identified ubiquitin ligases.....	43
5.5	Role of Rad26 in RNAPII removal from chromatin upon DNA damage	45
5.6	Parallels of Rpb1 modification and degradation to other SUMO- and STUbL- dependent pathways.....	46
6	MATERIALS AND METHODS	47
6.1	Microbiological Techniques.....	47
6.1.1	<i>Escherichia coli</i> (<i>E. coli</i>) Techniques	47
6.1.2	<i>Saccharomyces cerevisiae</i> (<i>S. cerevisiae</i>) Techniques	48
6.2	Molecular Biological Techniques	54
6.2.1	General Buffers and Solutions.....	54
6.2.2	Purification of DNA	54
6.2.3	Molecular Cloning	55
6.2.4	Polymerase Chain Reaction (PCR)	56
6.3	Biochemical Techniques	57
6.3.1	General Buffers and Solutions.....	57
6.3.2	Protein Methods.....	58
6.3.3	Chromatin Methods	62
6.4	Computer-aided Analysis.....	64
7	REFERENCES	65
8	ABBREVIATIONS	76

1 Summary

DNA damage induced by various means can trigger mutagenesis and genome instability, if remained unrepaired. Especially bulky DNA lesions interfere with protein machineries that trek along the DNA. In contrast to DNA replication, the RNA transcription machinery is highly sensitive to such 'road-blocks' as translesion synthesis is rare. Upon stalling of the transcribing RNA polymerase II (RNAPII) in front of the DNA lesion, the lesion itself is often shielded by the RNAPII complex and is therefore inaccessible for repair. If the RNAPII complex cannot be dislodged from the lesion by backwards movement, the last option is complete removal of RNAPII from the chromatin to allow repair. Previous work showed that removal involves degradation of Rpb1, the largest subunit of RNAPII, which presumably triggers disassembly of the whole complex. Rpb1 is targeted by several enzymes and thereby becomes modified by ubiquitin and the small ubiquitin-like modifier (SUMO) in response to DNA damage. While ubiquitylation of Rpb1 was described to trigger proteasomal degradation, the fate of SUMOylated Rpb1 remained elusive.

Taking advantage of different Rpb1 antibodies to study Rpb1 degradation upon DNA damage, it turned out that the elongating pool of Rpb1 is preferentially targeted for degradation. However, the previously identified ubiquitin ligases Rsp5 and Elc1-Cul3 do not contribute to ubiquitin-dependent degradation of elongating Rpb1 upon DNA damage. Instead, the stalled RNAPII complex is recognized by the SUMO machinery to target Rpb1 and possibly other subunits for SUMOylation. SUMOylated Rpb1 might function as a recruiting factor to assemble remodeling factors like Rad26 and other proteins required for DNA repair. However, SUMOylated Rpb1 also recruits the so-called SUMO-targeted ubiquitin ligase (STUbL) Slx5/Slx8. Binding of Slx5/Slx8 to SUMOylated Rpb1 leads to subsequent polyubiquitylation. Rpb1, modified in this manner, is recognized by the ubiquitin/SUMO-selective segregase Cdc48. Finally, Cdc48 extracts Rpb1 from the chromatin-bound RNAPII complex and delivers it to the proteasome for degradation.

Although the mechanism proposed in this study is distinctly different from the previously identified Rpb1 degradation mechanism, it reveals striking parallels with the removal of other chromatin-bound proteins.

2 Introduction

2.1 The Consequences of DNA Damage

The genomic information stored in DNA is the basis for life and its faithful propagation to the next generation is essential for cell survival. To achieve this, the integrity of cellular processes like DNA replication, DNA transcription and RNA translation have to be maintained. However, cells are constantly challenged by exogenous stressors like ultraviolet (UV) light irradiation or alkylating agents, which can cause various forms of DNA damage. Additionally, endogenous metabolic compounds, like reactive oxygen species (ROS), can induce DNA breaks or base oxidations, which promote the formation of bulky lesions¹. If DNA lesions are left unrepaired, they can interfere with crucial cellular processes. For instance, damaged DNA can block progression of the replicating or transcribing machineries, leading to persistent stalling on chromatin². This in turn can trigger genomic instability, consequently leading to cancer or aging in multicellular organisms³. Therefore, all living cells have evolved repair mechanisms to deal with different forms of DNA damage and, via these mechanisms, aid in maintaining genomic stability¹. In the course of this, repair of damaged DNA, which is occupied by a stalled protein complex, represents a special challenge for the cell. Not only does the damaged template DNA have to be recognized and repaired in a time-dependent manner, but also the cellular machineries for DNA and RNA synthesis must be maintained to some degree to allow potential restart after repair. Additionally, in the case of replication, the newly synthesized DNA must be preserved until the replication machinery can be restarted to prevent gross-chromosomal rearrangements⁴. Therefore, it is not surprising that DNA repair progression is tightly connected with protein remodeling, protein disassembly and protein turnover processes to get access to the damaged site and, whenever possible, to maintain the catalytic activity of stalled machineries.

2.2 DNA Repair in the Context of Stalled Replication Machinery

The replication machinery, consisting of DNA polymerase and several auxiliary factors like the minichromosome maintenance (MCM) helicase complex and the proliferating cell nuclear antigen (PCNA), fulfills two functions – it replicates DNA and scans it for damaged sites simultaneously⁵⁻⁷. Stalling of the replicating DNA polymerase can occur at modified bases, single- and double-strand breaks, upon depletion of the nucleotide pool or at highly transcribed regions⁸. A stalled DNA polymerase can lead to the accumulation of single-stranded DNA (ssDNA), because the replicative helicase proceeds with DNA unwinding while DNA synthesis is interrupted⁹. The replication protein A (RPA) subsequently binds the ssDNA and recruits the replication checkpoint kinase ATR (Mec1 in yeast). In contrast, stalled replication machinery at DNA double-strand breaks (DSBs) leads to the activation of the checkpoint kinase ATM (Tel1 in yeast). Phosphorylation of downstream targets by both checkpoint kinases results in p53-dependent cell cycle arrest and DNA repair by different mechanisms according to the nature of the DNA lesion⁴. Interestingly, the stalled replicative DNA polymerases are not removed, but remain bound to the DNA for 40-60 minutes after DNA damage treatment in a replication competent state. Thus, the replication fork is stabilized and DNA replication can be potentially reactivated after repair completion¹⁰⁻¹².

To avoid potential cell cycle arrest upon stalling of the replication machinery, cells have evolved bypass mechanisms¹³. Upon replication stalling, the sliding clamp PCNA becomes modified by posttranslational modifications to govern the choice of bypass mechanism. Due to an uncoupling of DNA unwinding and DNA replication, accumulation of RPA-coated ssDNA triggers recruitment of the ubiquitin ligase Rad18 together with the ubiquitin-conjugating enzyme Rad6¹⁴. This leads to monoubiquitylation of PCNA at lysine (K) 164, which in turn recruits the translesion synthesis (TLS) polymerases Pol η , Pol ζ and Rev1¹³. In contrast to the accurate replicative DNA polymerases, TLS polymerases have a larger active site and no proofreading mechanism, allowing accommodation of bulky lesions into their active center and incorporation of the correct or incorrect nucleotide opposite to the lesion¹⁵, therefore, this mechanism is error-prone. On the other hand, PCNA can also be modified with K63-linked polyubiquitin chains by the heterodimeric ubiquitin-conjugating enzyme Ubc13/Mms2 and the ubiquitin ligase Rad5, which promotes an error-free template switching mechanism¹⁶. For that, the information of the undamaged sister chromatid is used to replicate through the damaged template¹⁷. The precise

switching mechanism from replicative to translesion DNA polymerases is still unknown. A recent study proposed that proteasomal degradation of Pol3, the catalytic subunit of the replicative polymerase δ , is crucial to allow DNA binding by the TLS polymerase¹⁸.

Interestingly, the prolonged stalled replication machinery itself can lead to DSB formation and subsequent repair by homologous recombination (HR). However, SUMOylated PCNA usually blocks unwanted sister chromatid recombination, which can lead to gross-chromosomal rearrangements. Usually, PCNA SUMOylation takes place under non-damage conditions and in turn recruits Srs2, an antirecombinogenic helicase, which disrupts Rad51 filaments and thereby inhibits HR¹³.

2.3 DNA Repair in the Context of Stalled Transcription Machinery

Transcribing RNA polymerases (RNAPs) are particularly susceptible to stalling at bulky DNA adducts. Exposure to UV light leads to the dimerization of adjacent pyrimidines resulting in cyclobutane pyrimidine dimers (CPDs) within the DNA. These CPDs, but not other bulky DNA lesions, can enter the active site of transcribing RNAPII and lead to stalling upon nucleotide misincorporation opposite to the lesion¹⁹. A prolonged stalled RNAPII can activate the checkpoint kinase ATR and, subsequently, trigger p53-dependent cell cycle arrest and DNA repair, similarly to a stalled replicative DNA polymerase²⁰. In yeast, a special enzyme called photolyase removes CPDs in a light-dependent manner. Yet, CPD repair by photolyase is more efficient in the non-transcribed strand compared to the transcribed strand, indicating that the stalled RNAPII complex shields the CPD from recognition and repair²¹. A key mechanism to remove bulky DNA adducts, to avoid cell cycle arrest and cell death in yeast and higher organisms, is the nucleotide excision repair (NER) pathway^{22,23}.

2.3.1 The Nucleotide Excision Repair (NER) Pathway

Bulky DNA adducts, such as those caused by UV light, are preferentially repaired by the nucleotide excision repair (NER) pathway. Several syndromes are linked to mutations in NER genes. Among them are the genetic disorders *Xeroderma Pigmentosum* (XP)²⁴, Cockayne syndrome (CS)²⁵ and Trichothiodystrophy (TDD)²⁶, which are associated with a predisposition towards cancer and accelerated aging.

The NER pathway is initiated through lesion recognition, which differs in the two NER subpathways called global genome repair (GGR) and transcription-coupled repair (TCR). GGR removes DNA lesions genome wide, whereas TCR functions preferentially in the transcribed strand of actively transcribed genes (Figure 1).

In the GGR pathway, lesion recognition is achieved through probing of the DNA for helix-distortions through the XPC-Rad23B-CETN2 complex (Rad4-Rad23 in yeast), which subsequently binds opposite to the lesion to ssDNA. This enables the GGR pathway to target a broad range of damage types²⁷. Recognition is also possible through the UV-DDB complex, which binds directly to the UV light-induced lesion and stimulates recruitment of the XPC complex²⁸. In turn, XPC binding stimulates recruitment of the transcription factor II H (TFIIH), which is a multi-subunit complex with DNA helicase activity²⁹. The TFIIH helicase subunits XPB (Rad25) and XPD (Rad3) are implicated in DNA unwinding and damage detection³⁰. Upon lesion detection, the damaged bases must be removed. Thus, XPA (Rad14), which is presumably recruited together with TFIIH, displaces the XPC complex and recruits the endonucleases XPF-ERCC1 (Rad1-Rad10) and XPG (Rad2). After dual incision from the 5'- and 3'-site, roughly 30 nucleotides, including the damaged bases, are removed. However, 5'-incision by XPF-ERCC1 is sufficient to initiate gap filling by DNA synthesis³¹. Binding of RPA to the undamaged ssDNA opposite to the lesion protects this part from cleavage by the endonucleases. Finally, depending on the cell cycle stage, DNA Pol δ , Pol ϵ or Pol κ fills the gap and DNA ligase 1 or 3 completes DNA repair^{32,33}.

The lesion recognition and verification steps differ in the two NER subpathways. In contrast to GGR, the TCR subpathway is activated through a prolonged stalled RNAPII complex and the DNA damage must be detected and subsequently repaired in the context of the stalled complex. Therefore, in humans, activation of the TCR pathway is controlled by the Cockayne syndrome (CS) proteins A and B, UV-stimulated scaffold protein A (UVSSA) and the ubiquitin-specific processing protease 7 (USP7), which transiently interact with the elongating RNAPII^{34,35}. These factors recognize the stalled RNAPII

complex and are responsible for the recruitment of further TCR factors, which are important for DNA damage detection. In yeast, Rad26, the homolog of human CSB, and Rpb4/Rpb9, two non-essential subunits of RNAPII, are implicated in TCR activation³⁶⁻³⁹. Although CSB/Rad26 is crucial for TCR, it is still unclear how it recognizes stalled RNAPII. Data suggest that CSB/Rad26 travels with the elongating RNAPII and this interaction gets stabilized upon DNA damage^{40,41}. Interestingly, Rad26, but apparently not CSB, becomes phosphorylated and is thereby activated upon DNA damage by the checkpoint kinase Mec1⁴².

Theoretically, once the DNA damage is detected in the TCR pathway the further repair steps, including DNA incision, gap filling and ligation, are identical for both NER pathways. However, the stalled RNAPII occupies roughly 35 nucleotides of the transcribed DNA strand and might hinder the endonucleases and other TCR factors to access the lesion⁴³. There are three different possibilities of how the repair machinery can gain access to the lesion (Figure 1). First, the RNA polymerase can simply be released from the DNA to allow access. This has been shown to occur for RNAPII and RNAPI, but the underlying mechanism is poorly understood^{44,45}. Second, RNAPII backtracking from the lesion can facilitate repair without dissociation. This is possible because RNAPII has a proofreading mechanism, which allows the complex to backtrack during transcription⁴⁶⁻⁴⁸. After RNAPII backtracking and successful DNA repair, reactivation of transcription requires RNA transcript cleavage for repositioning of the 3'-end with the active center of RNAPII^{46,49}. RNAPII itself possesses an internal RNA cleavage activity, which is required for this step. Moreover, reactivation of RNAPII is stimulated by the transcription factor II S (TFIIS), which is recruited in a CS-dependent manner in humans³⁴. Interestingly, also RNAPII backtracking is thought to be activated by CSB^{50,51}. Finally, as a last resort, RNAPII can be actively removed from the lesion by proteasomal degradation of its catalytic subunit Rpb1⁵².

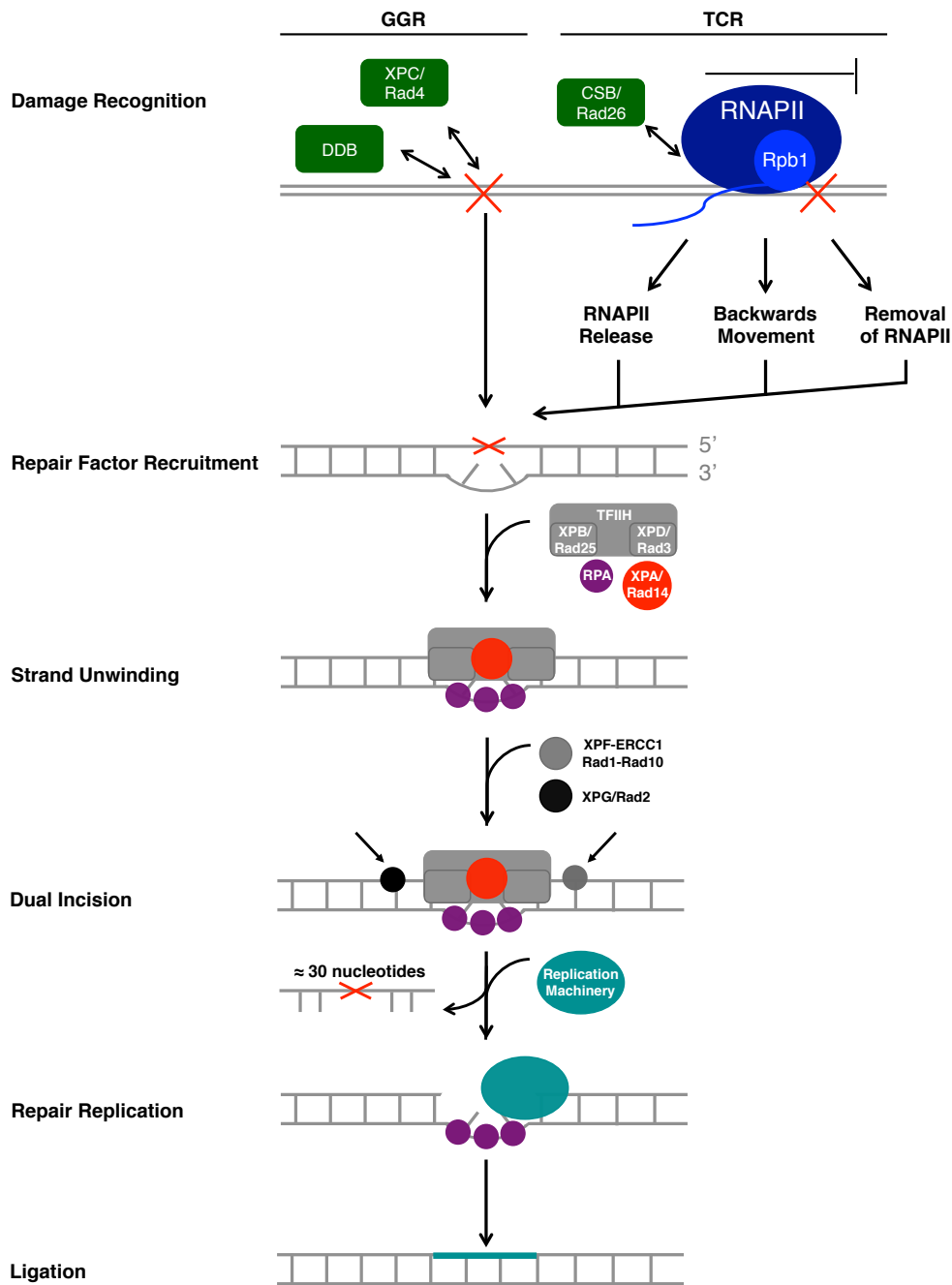


Figure 1: Removal of DNA lesions by the nucleotide excision repair (NER) pathway.

DNA lesions throughout the genome are recognized and removed by the global genome repair (GGR) pathway. The lesion is detected through the XPC (Rad4) complex or the DDB1 complex. DNA lesions in the transcribed strand force RNA polymerase II (RNAPII) to halt. CSB (Rad26) recognizes the stalled RNAPII and activates the transcription-coupled repair (TCR) branch. To get access to the DNA damage site, RNAPII can be released, displaced by backwards movement or removed from chromatin. After DNA damage detection, both subpathways, TCR and GGR, converge to the following NER steps. The transcription factor II H (TFIIH) is recruited to DNA lesion sites. This multi-subunit complex contains the helicases XPB (Rad25) and XPD (Rad3) to allow DNA unwinding. XPA (Rad14) and RPA have lesion detection functions. RPA binds to the undamaged ssDNA to avoid unwanted endonuclease cleavage. XPF-ERCC1 (Rad1-Rad10) incises at the 5'-site, whereas XPG (Rad2) acts on the 3'-site. Roughly 30 nucleotides are removed by dual incision, whereas 5'-site incision is enough to start gap filling by DNA polymerases. The repair process is completed after strand ligation.

2.4 Degradation of RNA Polymerase II upon DNA Damage

In order to get access to DNA lesions, which are occupied by an irreversibly stalled RNAPII complex, the last resort is to remove RNAPII from chromatin. This is achieved through turnover of its catalytic subunit Rpb1, whereas other subunits are not affected⁵³. Over the last decades, a multistep mechanism has been described in yeast and humans, including ubiquitylation of Rpb1 to induce proteasomal degradation⁵². Additionally, Rpb1 is targeted for other posttranslational modifications under DNA damage conditions as well as during the transcription cycle. In the following, general posttranslational modifications of Rpb1 will be described first. Next, specifically the posttranslational modifications by ubiquitin and the small ubiquitin-like modifier (SUMO) will be explained more in detail, since they are of special interest for this work. Finally, the DNA damage-triggered Rpb1 degradation pathway will be introduced.

2.4.1 Posttranslational Modifications of Rpb1

RNA polymerase II is a 12-subunit complex important for transcription of protein-coding genes, as well as for synthesis of non-coding RNAs⁵⁴⁻⁵⁶. To ensure efficient and faithful transcription, the largest subunit, Rpb1, is targeted for diverse posttranslational modifications. These modifications influence the recruitment of binding partners to catalyze and synchronize transcription progression with mRNA processing⁵⁷. The main target for posttranslational modifications throughout the transcription cycle is the carboxy-terminal domain (CTD) of Rpb1 (Figure 2).

The CTD consists of repeating peptides of the consensus sequence Tyr₁-Ser₂-Pro₃-Thr₄-Ser₅-Pro₆-Ser₇. The number of repeats is species-dependent, with 26 copies in *S. cerevisiae* and 52 repeats in humans. However, not every repeat follows the consensus sequence^{58,59}. Moreover, not every repeat within the CTD is equally modified at any given time^{60,61}. The CTD can be targeted for acetylation, glycosylation, proline *cis/trans* isomerization, methylation, phosphorylation and ubiquitylation⁵⁹. The phosphorylation pattern at serine (Ser) 2 and Ser5 has been extensively studied and is probably the most well-understood Rpb1 modification.

Rpb1 is phosphorylated at Ser5 by Kin28 (CDK7 in humans), which belongs to the TFIIH complex⁶². In contrast, Ser2 is targeted by two different kinases, Bur1 (CDK9 in humans) and the CTDK1 complex⁶³. Both belong to the cyclin-dependent kinase family.

However, Srb10 (CDK8 in humans) can also phosphorylate Ser5 and Ser2 *in vitro*^{62,64}. The phosphorylation patterns at Ser5 or Ser2 follow opposite trends. When Rpb1 is bound to the promoter and the 5'-region of genes, it is preferentially phosphorylated at Ser5. However, when RNA polymerase travels through the gene body, this modification on Rpb1 declines due to the activity of the phosphatases Ssu72 and Rtr1^{65,66}. In contrast, Ser2 phosphorylation is associated with transcription elongation and levels increase towards the 3'-region of the gene and then decrease beyond the polyA site⁶¹. After transcription termination, the phosphatase Fcp1 removes residual phosphorylations⁶⁷⁻⁶⁹.

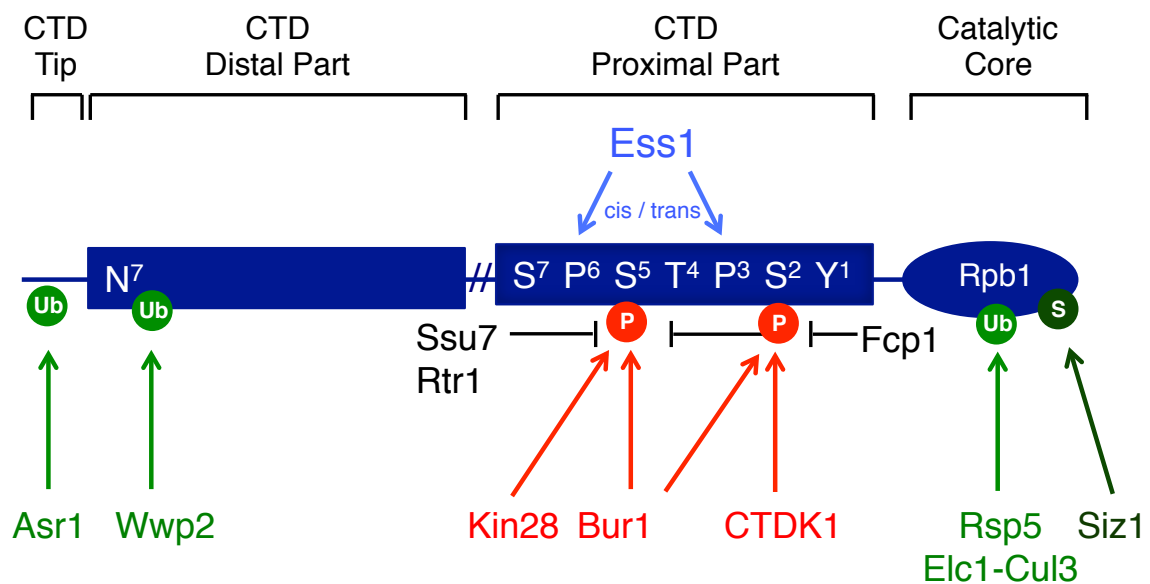


Figure 2: Posttranslational modifications of Rpb1.

Rpb1 can be modified at different regions. The enzymes involved are color-coded according to the modification. The consensus sequence of the C-terminal domain (proximal part) is targeted by phosphorylation (P) at serine 5 (S⁵) and serine 2 (S²) during transcription, whereas dephosphorylation is important to proceed in the transcription cycle. Cis/trans isomerization between proline 3 (P³) and proline 6 (P⁶) controls binding of proteins for transcription progression. Ubiquitylation (Ub) can take place at the 7th residue (N⁷) of non-consensus sequences (distal part) in humans or at the very C-terminus (CTD tip), observed in yeast cells. Ubiquitylation in the catalytic core region is thought to induce proteasomal degradation of Rpb1.

Although the CTD consensus sequence lacks lysine residues, the tail can be ubiquitylated at non-consensus sites⁵⁸ (Figure 2, CTD distal part). In humans, the ubiquitin ligase Wwp2 ubiquitylates the CTD of Rpb1 and triggers proteasomal degradation in a DNA damage-independent manner⁷⁰. This is thought to be a mechanism to regulate Rpb1 levels. In yeast, two ubiquitylation sites in the CTD tip region were identified, which are

targeted by the ubiquitin ligase Asr1⁷¹. However, Rpb1 remained extensively ubiquitylated upon Asr1 deletion, arguing for a redundant ubiquitin ligase for these sites. Simultaneously, the RNAPII subunit Rpb2 is ubiquitylated by Asr1 as well. Monoubiquitylation of Rpb1 and Rpb2 by Asr1 triggers removal of the RNAPII subunits Rpb4 and Rpb7 from the complex. Since Asr1 targets Rpb1, which is phosphorylated at Ser5, it was suggested that monoubiquitylation by Asr1 triggers RNAPII complex disassembly after abortive and cryptic transcription events⁷¹.

Apart from the above-mentioned CTD modifications, other lysine residues in the catalytic core region are targeted for ubiquitylation to trigger proteasomal degradation (described in section 2.4.4 in more detail). In addition, the catalytic core domain is also targeted for SUMOylation by the SUMO ligase Siz1 together with the SUMO-conjugating enzyme Ubc9⁷². SUMOylation of Rpb1 is induced upon DNA damage or transcriptional impairment, but has not been linked to Rpb1 ubiquitylation or proteasomal degradation so far. Instead, this modification is thought to restrain the DNA damage checkpoint response induced by a stalled RNAPII complex⁷².

2.4.2 Ubiquitin and the Small Ubiquitin-Like Modifier (SUMO)

Ubiquitin (Ub) and other ubiquitin-like modifiers are covalently conjugated to substrate proteins and thereby affect their activity, localization, folding or stability⁷³. The small ubiquitin-like modifier (SUMO) shares several similarities with ubiquitin (Figure 3). It is transcribed as an inactive precursor and needs proteolytic cleavage to expose a C-terminal double glycine motif that is required for conjugation⁷⁴. Similar to ubiquitin, the attachment of SUMO to substrates requires the action of three enzymes. The activating enzyme (also called E1) forms a thioester bond with the C-terminal carboxy group of Ub/SUMO in an ATP-dependent manner. Next, Ub/SUMO is transferred to the catalytic cysteine of the conjugating enzyme (E2) by transesterification. Finally, Ub/SUMO is transferred to a lysine within the substrate protein forming an isopeptide bond with its C-terminal glycine residue. The last step is usually facilitated by Ub/SUMO ligases (E3)⁷⁵.

While 11 ubiquitin E2s and 60-100 of ubiquitin E3 enzymes mediate ubiquitylation in yeast, only one SUMO E2 (Ubc9) and four SUMO E3 enzymes (Siz1, Siz2, Mms21 and Zip3) have been identified⁷⁶. Substrate specificity in the ubiquitin pathway is achieved through enzyme diversification, while in the case of SUMO distinct cellular localizations of the conjugating enzymes are thought to provide specificity to the SUMO system^{77,78}.

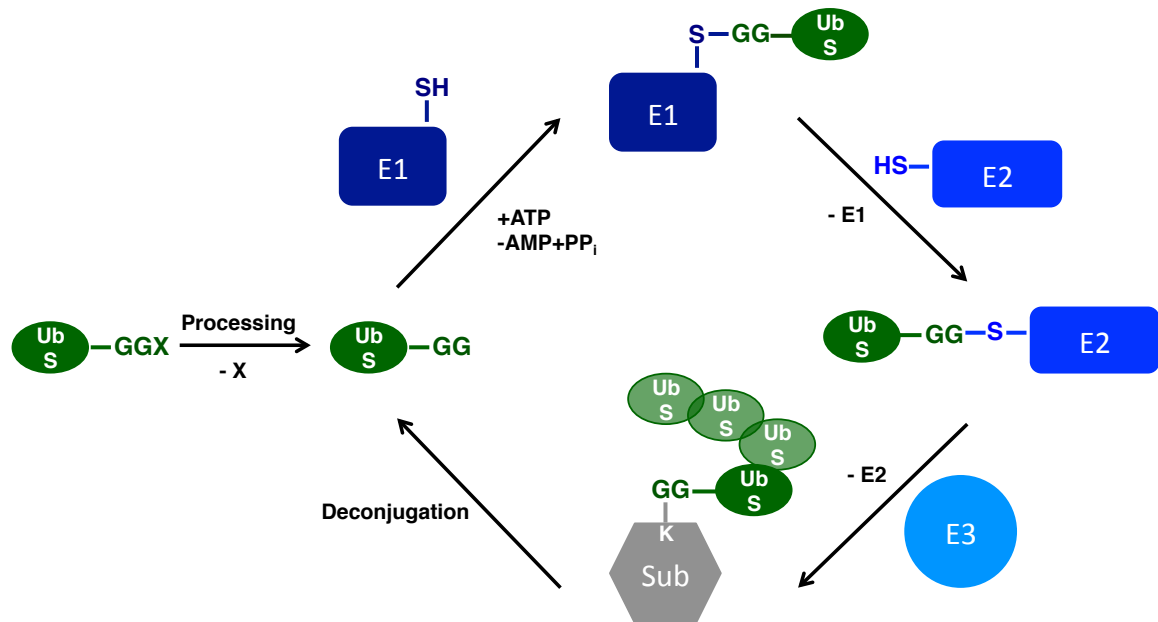


Figure 3: The ubiquitin and SUMO conjugation and deconjugation system.

Ubiquitin (Ub) and the small ubiquitin-like modifier (SUMO) (S) are synthesized as inactive precursors with a C-terminal extension (X). Proteolytic cleavage results in the exposure of the C-terminal double glycine motif (GG). Conjugation of both modifiers to substrate proteins (Sub) implies the action of three enzymes. First, the activating enzyme (E1) forms a thioester bond with the C-terminus of the modifier in an ATP-dependent manner. Second, the modifier is transferred to a cysteine of the conjugating enzyme (E2). Finally the ligase (E3) promotes E2-substrate interaction and facilitates the binding of the modifier to an internal lysine (K) residue of the substrate. However, special ubiquitin ligases can also form a thioester bond with ubiquitin before ubiquitin is transferred to the substrate. To assemble polyubiquitin/SUMO chains, several conjugation rounds are necessary. Ubiquitin/SUMO-attachment is a reversible process and can be reversed by isopeptidases, which hydrolyze the peptide bond between the modifier and the substrate.

Attachment of Ub/SUMO is a reversible process. While several ubiquitin-specific proteases (UBPs) hydrolyze the peptide bond between ubiquitin and substrate proteins, only two SUMO isopeptidases, Ulp1 and Ulp2, reverse SUMO modifications. Moreover, Ulp1 is also required for SUMO maturation at the nuclear envelope⁷⁹.

Substrate proteins can be modified by a single Ub/SUMO entity at individual or several different lysine residues, termed mono- and multiubiquitylation/SUMOylation, respectively. However, Ub/SUMO can also be attached to lysine residues on ubiquitin or SUMO, resulting in chain formation (polyubiquitylation/SUMOylation). All seven internal lysines of ubiquitin (K6, K11, K27, K29, K33, K48 and K63) are used for chain formation *in vivo*⁸⁰. These ubiquitin polymers can be composed of a single or mixed linkage types, resulting in homotypic/heterotypic or even branched chains. Mono/polyubiquitylated

substrates are subsequently recognized by partner proteins harboring ubiquitin-binding domains (UBDs) or by specific ubiquitin receptors⁸¹⁻⁸³. The yeast SUMO protein (encoded by a single gene *SMT3*) harbors nine lysines (K11, K15, K19, K27, K38, K40, K41, K54, K58), however, only the first three are efficiently used for chain formation^{84,85}. While multiple UBDs exist, SUMOylated proteins are recognized by a short stretch of hydrophobic amino acids termed SUMO-interacting motif (SIM). These motifs have been found in a variety of proteins, including SUMO ligases, SUMO-targeted ubiquitin ligases and other SUMO-binding proteins⁸⁶.

2.4.3 Functions of Ubiquitylation and SUMOylation

Covalent attachment of ubiquitin to substrate proteins can have proteolytic or non-proteolytic outcomes. Best studied is the proteolytic degradation of preferentially polyubiquitylated proteins by the 26S proteasome.

The proteasome is a multi-subunit protease complex consisting of a 20S core particle and a 19S regulatory particle⁸⁷. Proteolytic cleavage is performed in the cavity of the 20S particle, which exhibits a barrel-like structure. The 19S unit is located at each end of the 20S particle. The 19S particle mediates substrate recognition, protein unfolding, deubiquitylation and entry into the 20S particle in an ATP-dependent manner⁸⁸. While attachment of a single ubiquitin moiety in most cases is insufficient, preferentially K48- and K29-linked polyubiquitin chains target proteins to the proteasome, although exceptions are known⁸⁹⁻⁹¹. Protein degradation by the proteasome is important for several cellular pathways, among them protein quality control, cell cycle regulation or antigen production for MHC recognition⁹². Moreover, non-proteolytic functions of ubiquitin are implicated in DNA repair (see above section 2.2), gene transcription, endocytosis, protein-protein interaction, enzyme activation and cell signaling⁹³⁻⁹⁶.

Most known SUMOylated substrates are located in the nucleus and are implicated in DNA repair, gene transcription, replication or chromatin organization^{97,98}, but cytosolic, mitochondrial, plasma membrane- or ER-bound proteins can be SUMOylated as well⁷⁵. The attachment of SUMO can influence stability, folding, activity, localization or protein-protein interaction properties of the substrate protein⁹⁹. However, the underlying molecular consequences are diverse. SUMOylation can prevent other posttranslational modifications, like ubiquitylation, by competing for the same acceptor lysine. In addition,

the newly attached binding surface of SUMO itself can inhibit or foster protein-protein interactions⁷⁷. SUMOylation frequently targets multi-subunit complexes or protein groups that act in the same pathway. This so-called 'protein-group SUMOylation' takes place upon heat-shock or DNA damage induction^{78,100}. Protein-group SUMOylation might provide protein complex stability mediated by SUMO-SIM interactions, thereby enhancing its activity.

There are two different fates for SUMO-modified proteins. First, modified proteins can be deSUMOylated and recycled to the non-modified state. Second, SUMOylated proteins can be further modified with ubiquitin by SUMO-targeted ubiquitin ligases (STUbLs), which can subsequently trigger proteasomal degradation^{77,101}. This special class of enzymes provides an important link between the SUMO and the ubiquitin system and will be described later in section 2.4.5 more precisely.

2.4.4 Mechanism of Proteasomal Degradation of Rpb1

The sequential action of different enzymes on Rpb1 upon DNA damage is illustrated in Figure 4. First, the ubiquitin ligase Rsp5 was implicated in Rpb1 turnover¹⁰²⁻¹⁰⁶. *In vitro* studies revealed that Rsp5 binds the carboxy-terminal domain (CTD) of Rpb1 via the WW domain and is able to monoubiquitylate Rpb1 in a DNA damage-independent manner. Based on *in vitro* studies it was proposed that Rsp5 together with the ubiquitin-conjugating enzymes Ubc4/Ubc5 attaches K63-linked polyubiquitin chains to Rpb1¹⁰⁷. However, Rpb1 modified by K63 chains is not targeted for degradation but is rather a substrate of the ubiquitin protease Ubp2¹⁰⁷⁻¹⁰⁹. Ubp2 hydrolyzes the K63-linked chains resulting again in monoubiquitylated Rpb1. It was proposed that this might be a proofreading mechanism to avoid premature Rpb1 proteolysis. To trigger turnover, monoubiquitylated Rpb1 is targeted by a cullin-based ubiquitin ligase complex, composed of Elc1, Ela1, Cul3 and Roc1. *In vitro* studies revealed that this ligase adds K48-linked chains to monoubiquitylated Rpb1¹⁰⁷. Deletion of the non-essential subunits Elc1, Ela1 or Cul3 results in a delay in Rpb1 turnover after DNA damage^{110,111}. However, whether the present monoubiquitin is extended or whether the Elc1-Cul3 complex targets another lysine within Rpb1 is unclear. Two lysine residues (K330 and K695) within Rpb1 were identified to be modified by Rsp5¹¹². DNA damage-induced ubiquitylation was highly reduced upon mutation of the coding sequences for both lysines. However, mutation of the coding

sequence of K330 alone was suggested to abolish Rpb1 degradation. Moreover, crystal-structure analysis of RNAPII demonstrated that K695 lies in a region where the non-essential subunit Rpb9 binds Rpb1^{112,113}. However, to avoid degradation, Rpb1 modified by K48-linked ubiquitin chains can be rescued by deubiquitylation mediated by the ubiquitin protease Ubp3¹¹⁴. Finally, clearance of polyubiquitylated Rpb1 from the DNA is dependent on the ATPase Cdc48¹¹⁵. Cdc48 together with the adaptor proteins Ubx4/Ubx5 mediates extraction of Rpb1 from the chromatin-bound RNAPII complex for subsequent delivery to the proteasome for degradation^{115,116}. Recently, the chromatin remodeling complex INO80 has been implicated in Cdc48 binding. It was suggested that INO80 facilitates degradation of chromatin-bound Rpb1 through nucleosome remodeling¹¹⁷.

In human cells, Nedd4, the human homolog of Rsp5, binds and monoubiquitylates Rpb1 *in vitro*^{105,118}. This monoubiquitylation is thought to be important to trigger polyubiquitylation by the Elongin A/B/C ligase, which is the human homolog of yeast Elc1/Ela1, suggesting that this is a evolutionary conserved mechanism¹¹⁹. However, Rsp5 preferentially binds Rpb1 phosphorylated at Ser2 on the CTD. Further, Rsp5 binding is blocked if Rpb1 is phosphorylated at Ser5^{103,120}. In contrast, Elongin A/B/C binds preferentially Ser5 phosphorylated Rpb1¹¹⁹.

Moreover, although CSB and Rad26 both contribute to TCR, they have seemingly opposite effects on Rpb1 stability comparing yeast with human cells. While Rad26 has been described to counteract Rpb1 degradation, CSB induces Rpb1 turnover upon DNA damage¹²¹⁻¹²³.

Additionally, Rad26 interacts with the degradation factor 1 (Def1), which cycles between the nucleus and the cytoplasm¹²¹. Upon DNA damage, Def1 has been suggested to be monoubiquitylated by Rsp5 and cleaved by the proteasome. The processed version is retained in the nucleus and mediates binding between the Elc1-Cul3 ligase and Rpb1 to support its degradation^{120,124}. Rad26 has been proposed to antagonize Def1 function to allow repair by the TCR machinery without the necessity to remove RNAPII. However, the underlying mechanism is unclear and recent data contradict this model¹²⁵. Interestingly CSB, but not Rad26, is targeted for degradation in a CSA and Cdc48-dependent manner upon UV light irradiation^{122,126}.

Taken together, Rpb1 seems to be targeted for proteasomal degradation after DNA damage to allow DNA damage repair. However, several ubiquitin ligases also target Rpb1 in a DNA damage-independent manner and their functions on Rpb1 were previously analyzed by *in vitro* studies. Further, Rsp5 acts also on other proteins implicated in Rpb1

degradation. This makes a conclusive interpretation of data difficult, as indirect effects cannot be ruled out. Since Rpb1 is also SUMOylated upon DNA damage, it remains a possibility that it is a substrate for the so-called SUMO-targeted ubiquitin ligases.

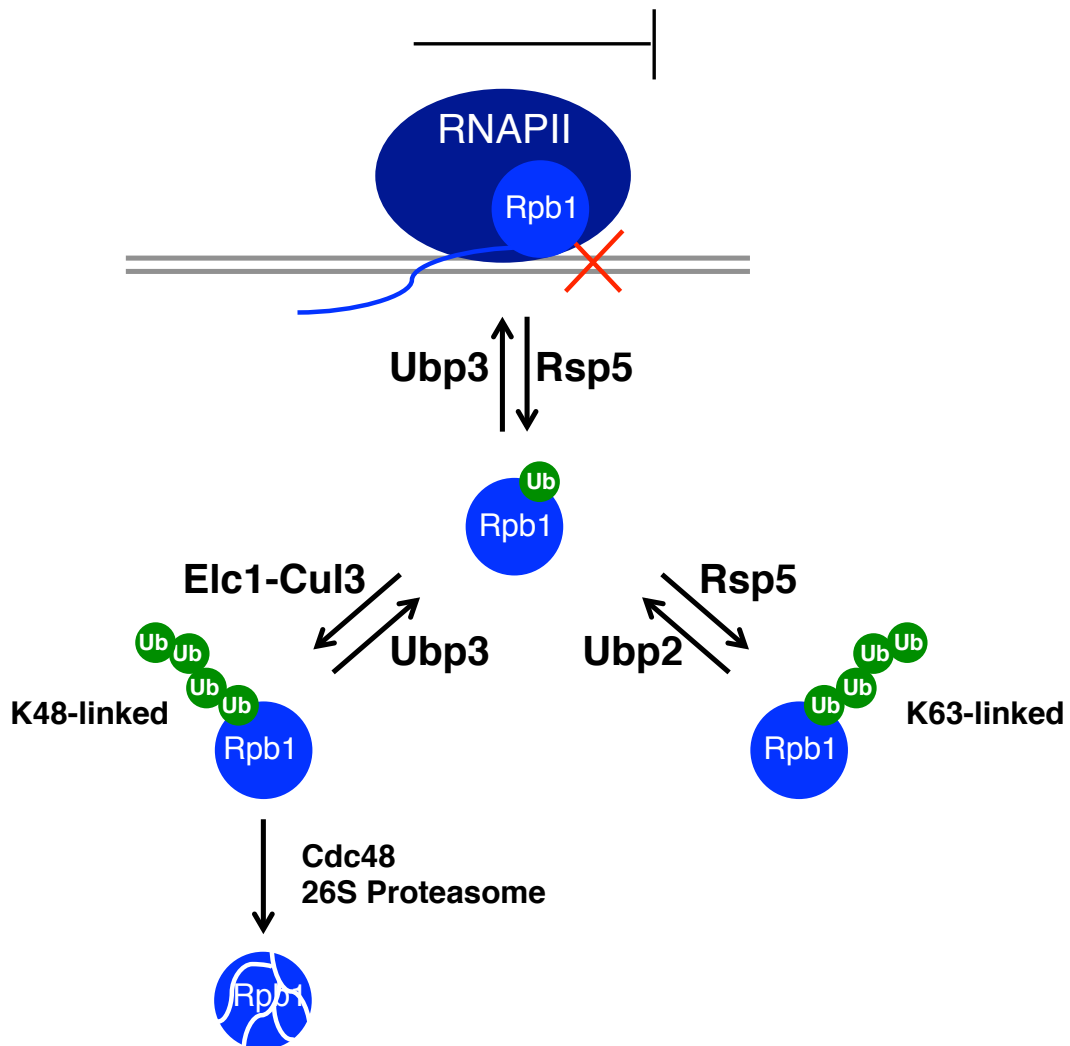


Figure 4: Targeting of stalled RNA polymerase II for proteasomal degradation.

RNA polymerase II (RNAPII) stalls at DNA lesions and is targeted for removal to allow lesion repair. The largest subunit, Rpb1, is first monoubiquitylated (Ub) by the ubiquitin ligase Rsp5, which can further attach K63-linked ubiquitin chains (right part). This is thought to be a protein quality control mechanism to avoid unwanted Rpb1 degradation and can be reversed by the deubiquitylation enzyme Ubp2. Ubp2 trims K63-linked chains resulting in monoubiquitylated Rpb1. To trigger degradation, the ubiquitin ligase complex E1c1-Cul3 attaches K48-linked chains (left part). This triggers recruitment of the segregase Cdc48 to deliver polyubiquitylated Rpb1 to the proteasome for degradation. Consequently, it is thought that the RNAPII complex will disassemble and liberate the DNA for repair. However, Ubp3 can rescue Rpb1 from degradation by complete hydrolysis of the ubiquitin chain.

2.4.5 SUMO-Targeted Ubiquitin Ligases (STUbLs)

SUMO-targeted ubiquitin ligases (STUbLs) harbor several SUMO-interacting motifs (SIMs), which allow the enzyme to recognize and bind SUMOylated proteins (Figure 5). Attachment of polyubiquitin chains to the SUMOylated substrates typically leads to proteasomal degradation¹²⁷. So far, several enzymes were shown to function as STUbLs. All of them are RING domain ubiquitin ligases possessing several SIMs. RING-type ubiquitin ligases facilitate the transfer of ubiquitin to its substrate protein by bringing the substrate protein and the E2-ubiquitin intermediate in close proximity¹²⁸.

In yeast, the ubiquitin ligase and DNA-dependent ATPase Ris1 was shown to promote degradation of certain SUMOylated proteins¹²⁹. These proteins were implicated in mating type silencing, replication stress response, inhibition of non-homologous end-joining of telomeres and chromosome segregation¹³⁰⁻¹³⁴.

The heterodimer Slx5/Slx8 is another STUbL, which shares sequence homology with STUbLs from fission yeast and humans. Both, Slx5 and Slx8, have a C-terminal RING domain and Slx5 additionally harbors multiple SIMs while Slx8 has a DNA-binding domain and a putative SIM. Data suggest that Slx5 is important for recognition of the substrate, which is subsequently ubiquitylated by Slx8^{135,136}. However, substrate SUMOylation is not a strict prerequisite to recruit Slx5/Slx8 since other structural features might also be recognized^{134,136}. Moreover, after recruitment of Slx5/Slx8, other adjacent proteins can also be ubiquitylated *in trans*¹³⁴. Recently, Slx5/Slx8 was shown to function in DSB repair at the nuclear periphery^{137,138}. Binding of the DSB to the nuclear pore complex (NPC) is thought to be mediated through Slx5/Slx8, which binds the nuclear pore protein Nup84 but also the damaged DNA. However, the underlying mechanism is unclear. It was proposed that a SUMOylated protein might accumulate at collapsed forks and appropriate repair requires Slx5/Slx8-dependent ubiquitylation and proteasomal degradation of this substrate^{137,138}.

Similar to budding yeast Slx5/Slx8, also the fission yeast STUbL Slx8/Rfp1/Rfp2 and the human homolog RNF4 function in genome stability and DNA repair^{137,139-141}. Intriguingly, RNF4 may also play a non-proteolytic role in DNA damage response, as it catalyzes K63-linked polyubiquitin chains. Further, RNF4 is recruited to promyelocytic leukaemia (PML) bodies. Induced by arsenic, RNF4 targets SUMOylated PML proteins for ubiquitylation and subsequent proteasomal degradation, which in turn leads to the disassembly of PML bodies^{142,143}. Interestingly, a non-proteolytic function was also suggested for the human STUbL RNF111, which targets SUMOylated XPC to attach K63-

linked ubiquitin chains¹⁴⁴⁻¹⁴⁶. XPC, which functions in the nucleotide excision repair pathway, gets SUMOylated upon UV light treatment. Subsequently, RNF11-dependent ubiquitylation triggers dissociation of XPC from the DNA to promote DNA lesion repair. However, XPC is not targeted for degradation but rather gets recycled by deubiquitylation^{147,148}.

Recently, the ubiquitin ligase Rad18 has been suggested to belong to the STUbL family as well. Rad18 is recruited to SUMOylated PCNA and governs translesion synthesis during replication stress^{16,149} (see above section 2.2).

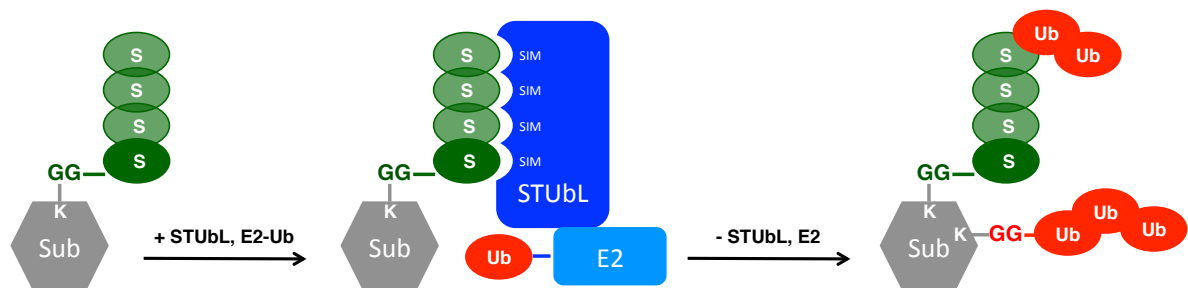


Figure 5: Model for the action of SUMO-targeted ubiquitin ligases (STUbLs).

SUMOylated (S) substrates (Sub) are recognized by multiple SUMO-interacting motifs (SIMs) of the STUbLs. In most cases, the RING domain containing STUbL (like Slx5/Slx8) promotes attachment of ubiquitin (Ub) moieties by facilitating the interaction between the ubiquitin-conjugating enzyme (E2) and the substrate. Ubiquitin can be attached either to the preexisting SUMO chain or to a lysine (K) within the substrate. Usually, the (poly)ubiquitylated substrates are targeted for proteasomal degradation.

The conserved AAA-type ATPase Cdc48 (p97 in humans) typically targets ubiquitylated proteins, but also participates in the SUMO pathway¹⁵⁰. Cdc48 uses ATP hydrolysis to segregate these substrates from their cellular compartment such as chromatin, cellular membranes or protein complexes¹⁵¹. The fate of the segregated proteins is further determined by so-called substrate processing co-factors¹⁵⁰. Usually, proteins bound to Cdc48 are delivered for proteasomal degradation^{115,152}. Since Cdc48 also targets SUMOylated proteins and associates with a number of ubiquitin ligases, it was considered to be a multi-subunit STUbL^{77,153,154}.

3 Aims of this Study

Rpb1, the largest subunit of RNA polymerase II, is targeted for proteasomal degradation upon DNA damage. Rpb1 degradation seems to be important to remove DNA damage-stalled RNAPII complexes from chromatin to allow for DNA repair⁵². The model proposed so far is highly complicated and implicates ubiquitylation of Rpb1 by two distinct ubiquitin ligases acting in a sequential mode¹⁰⁷.

However, initial experiments in our laboratory failed to reproduce the phenotype of Rpb1 degradation upon DNA damage using the same setup described by other groups¹²¹. Only when we used an antibody recognizing the elongating pool of RNAPII we were able to reproduce Rpb1 turnover in WT cells. We also found that the so far described ubiquitin ligases are not implicated in Rpb1 degradation.

Using our experimental setup, we aimed to elucidate the mechanism by which elongating RNAPII is degraded and which enzymes are involved in this pathway. Moreover, it was suggested that DNA damage not only triggers Rpb1 ubiquitylation but also Rpb1 SUMOylation⁷². However, so far the fate of SUMOylated Rpb1 was enigmatic. Another aim was therefore to elucidate how the posttranslational modification SUMO contributes to Rpb1 regulation upon DNA damage.

4 Results

4.1 DNA damage-induced degradation of Rpb1 from the elongating pool of RNA polymerase II

To monitor degradation after DNA damage induction, Rpb1 protein levels can be detected using several commercially available antibodies. Most of them are raised against the carboxy-terminal domain (CTD) of Rpb1, which is targeted for posttranslational modifications during the transcriptional cycle⁵⁹. However, using antibodies which recognize specific modifications of the CTD of Rpb1, one can distinguish between RNAPII complexes at different transcriptional stages.

To monitor Rpb1 turnover, cells were irradiated with UV light followed by a recovery phase. After irradiation, cells were kept in the dark to avoid DNA repair by the light-activated enzyme photolyase, thereby triggering transcriptional stalling. The Rpb1 protein levels were measured after various recovery time points. For western blot (WB) analysis we compared antibodies recognizing distinct pools of RNAPII. The monoclonal antibodies 4H8 and 8WG16 preferentially recognize the unmodified CTD of Rpb1 and therefore detect the whole pool of RNAPII, chromatin-bound or -unbound. Moreover, we also used antibodies recognizing the CTD phosphorylated on the serine at position two (S2P), characterizing the elongating pool of RNAPII, or position five (S5P), marking the transcription initiating pool of RNAPII. In contrast to previous work we observed almost no turnover of Rpb1 using antibodies recognizing the whole pool of RNAPII (Figure 6, 8WG16 and 4H8). However, we were able to detect robust Rpb1 turnover when we monitored Rpb1 with the S2P-specific antibody, which recognizes Rpb1 actively transcribing DNA. Surprisingly, Rpb1 turnover seemed to be highly specific for this elongating pool, since the transcription initiating pool of RNAPII was not affected by DNA damage-induced degradation (Figure 6, S5P).

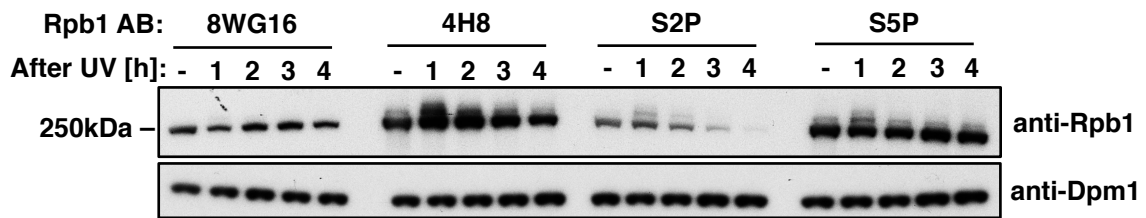


Figure 6: Rpb1 is degraded preferentially from the elongating pool of RNAPII upon DNA damage.

Rpb1 protein levels after UV light treatment (400 J/m^2) followed by a recovery phase of 4 hours in YPD medium. For the recovery phase cells were kept in the dark. For the western blots (WB) antibodies (AB) against the C-terminal domain (CTD) of Rpb1 were used. The S2P- or S5P-specific antibody recognizes phosphorylated serine-2 or serine-5 in the CTD of Rpb1, 8WG16 and 4H8 recognize the CTD independent of any modification. Dpm1 served as loading control.

To exclude that turnover of Rpb1 was masked by newly translated Rpb1, we also monitored Rpb1 levels after UV light in the presence of the protein synthesis inhibitor cycloheximide (CHX) (Figure 7A). Again, we hardly detected any decay in Rpb1 levels using the whole pool antibody 8WG16, but with the S2P-specific antibody (Figure 7A, compare upper and lower panel CHX+UV). Note that Rpb1 turnover was substantially lower in UV light-unchallenged cells (Figure 7A, CHX). Besides UV light irradiation we also introduced DNA lesions using the mutagenic compound 4-nitroquinoline 1-oxide (4NQO). 4NQO was described to induce DNA damage through reactive oxygen species and to activate the same repair mechanism as UV light treatment¹⁵⁵. Independent of the DNA damage source, UV light or 4NQO, Rpb1 was preferentially degraded from the elongating pool of RNAPII in various different yeast backgrounds (Figure 7B and Figure 7C). This further strengthens the fact that the preferential degradation of the elongating pool of RNAPII reflects a common mechanism upon DNA damage.

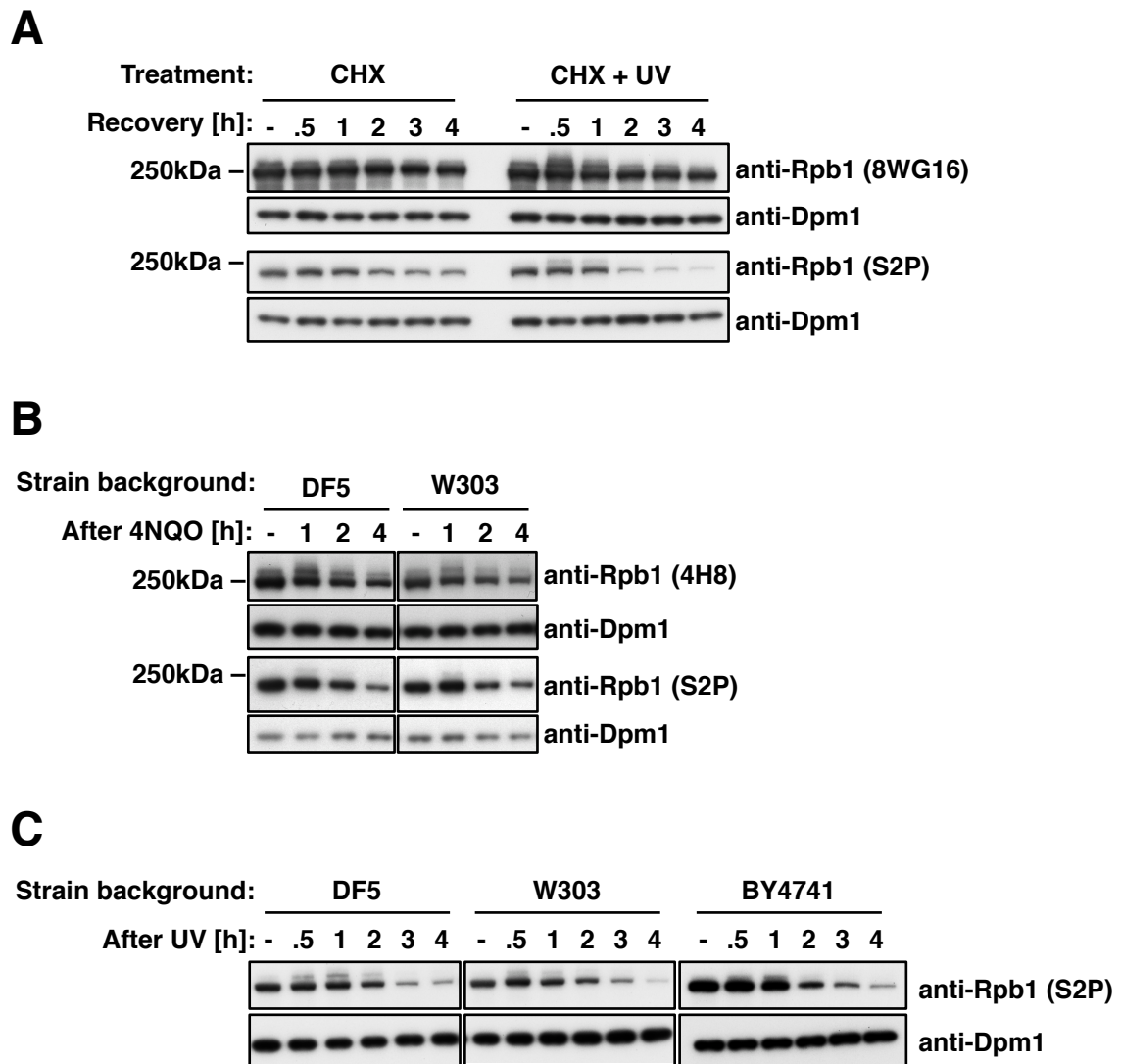


Figure 7: Rpb1 is degraded from the elongating pool of RNAPII independent of the DNA damage source or the yeast background.

(A) Rpb1 protein levels in untreated (CHX) or UV light-treated (CHX+UV) (400 J/m^2) WT cells followed by a recovery phase in YPD supplemented with cycloheximide (CHX) ($100 \mu\text{g/ml}$). For the WB the S2P-specific and the 8WG16 antibodies were used to detect Rpb1. Dpm1 served as loading control.

(B) Rpb1 protein levels after 4-nitroquinoline 1-oxide (4NQO) ($10 \mu\text{g/ml}$) treatment in different yeast background WT cells (DF5 and W303) followed by a recovery phase in YPD medium. Rpb1 was detected with the 8WG16 or S2P-specific antibody. Dpm1 served as loading control.

(C) Rpb1 protein levels in different yeast background WT cells (DF5, W303 and BY4741) after UV light treatment (400 J/m^2) followed by a recovery phase of 4 hours in YPD medium. Rpb1 was detected using the S2P-specific antibody. Dpm1 served as loading control.

4.2 Degradation of Rpb1 is dependent on the proteasome and the ubiquitin/SUMO-specific segregase Cdc48

It was described previously that turnover of Rpb1 upon stalling at DNA lesion sites relies on the ubiquitin proteasome system (UPS) and the ubiquitin/SUMO-specific segregase Cdc48¹¹⁵. To confirm this involvement also for the elongating pool of Rpb1, we followed Rpb1 levels after UV light irradiation using the S2P-specific antibody. In agreement with previous work, we noticed Rpb1 accumulation in mutants defective in proteasome activity (Figure 8A, hypomorphic mutant *cim3-1*) or in the ubiquitin/SUMO-specific segregase Cdc48 (Figure 8B, hypomorphic mutants *cdc48-6* and *cdc48-3*).

Given that (poly)ubiquitylated substrates are often targeted for proteasomal degradation, we wondered whether polyubiquitylated species of Rpb1 could be detected after DNA damage induction. To test this, we immunoprecipitated Rpb1 from UV light-treated (+) and -untreated (–) cells using the S2P-specific antibody and analyzed the samples by western blotting. Indeed, Rpb1 immunoprecipitated from UV light-treated cells was cross-reactive with a ubiquitin-specific antibody (Ub) (Figure 8C, WT). Considering that attachment of polyubiquitin chains to a substrate protein results in various slower-migrating species, the here-detected Rpb1 was rather monoubiquitylated than polyubiquitylated. Moreover, this pool of ubiquitylated Rpb1 was not enriched in Cdc48 mutant cells after UV light treatment (Figure 8C, *cdc48-6*). Presumably, Cdc48 does not target the identified monoubiquitylated pool of Rpb1.

Usually polyubiquitylated species are difficult to detect because the conjugates are subsequently degraded by the proteasome. Therefore, we used the hypomorphic proteasome mutant *cim3-1* to prolong the half-life of polyubiquitylated Rpb1 species and probed immunoprecipitated Rpb1 for ubiquitin (Figure 8C, *cim3-1*). In contrast to WT cells we could not detect ubiquitylated Rpb1 species even after UV light treatment. This could result from very low immunoprecipitation efficiency of Rpb1 in *cim3-1* cells (Figure 8C, compare middle panel of WT with *cim3-1* cells).

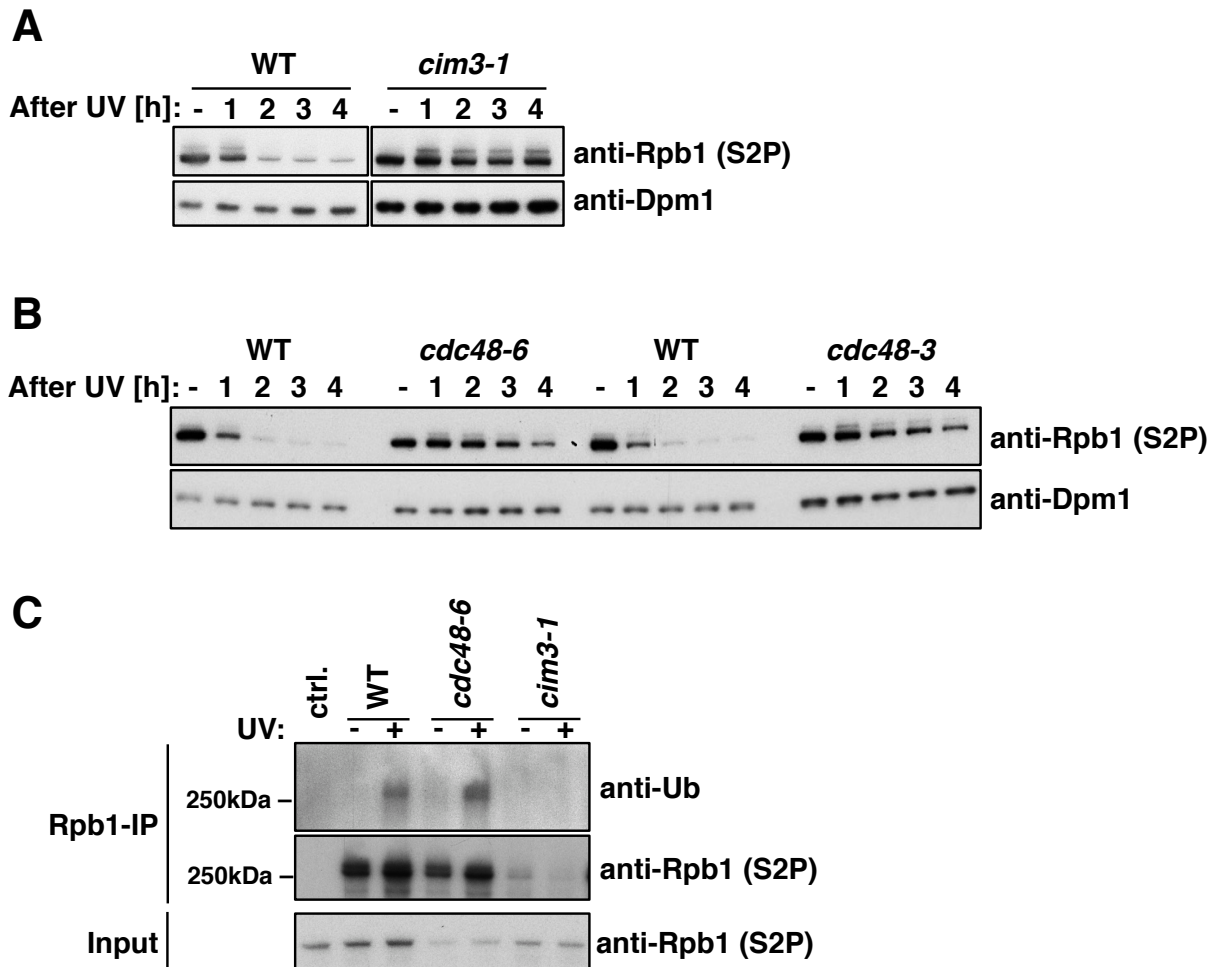


Figure 8: Rpb1 degradation is dependent on the proteasome and the segregase Cdc48.

(A) Rpb1 protein levels in WT and the proteasome mutant *cim3-1* after UV light treatment (400 J/m^2). Cells were shifted to 37°C for 1 hour before UV light irradiation and for the recovery phase in YPD medium. Rpb1 was detected using the S2P-specific antibody. Dpm1 served as loading control.

(B) Rpb1 protein levels in WT, *cdc48-6* and *cdc48-3* cells after UV light treatment (400 J/m^2). Cells were shifted to 37°C for 1 hour before UV light irradiation and for the recovery phase in YPD medium. Rpb1 was detected using the S2P-specific antibody. Dpm1 served as loading control.

(C) WT, *cdc48-6* and *cim3-1* cells were shifted to 37°C for 1 hour before being either UV light-irradiated (+) or not (-). Rpb1 was immunoprecipitated (Rpb1-IP) with the antibody S2P and ubiquitylated species of Rpb1 were detected using a ubiquitin-specific antibody. Sepharose beads without addition of the Rpb1 antibody served as background-binding control (ctrl.).

4.3 Rpb1 ubiquitylation upon DNA damage involves the ubiquitin ligases Rsp5 and Elc1-Cul3

To address which enzymes are crucial for the observed ubiquitin modification of Rpb1 after DNA damage treatment, we tested the ubiquitin ligases Rsp5 and the Elc1-Cul3 ligase complex (Cul3-Roc1-Elc1-Ela1) that were previously described to mediate Rpb1 degradation¹⁰⁷.

First, we compared Rpb1 ubiquitylation in WT cells with cells expressing a mutant allele of *RSP5* (Figure 9A, hypomorphic mutant *rsp5-1*). As seen before, Rpb1 ubiquitylation was induced following UV light treatment in WT cells, but was completely absent in cells expressing a mutant allele of *RSP5* (Figure 9A, left panels). Additionally, we used cells deficient in *RSP5* (Δ *rsp5* cells) to exclude indirect effects from the hypomorphic mutant *rsp5-1*. As reported previously¹⁵⁶, Δ *rsp5* cells are unviable but can be rescued by addition of oleic acid to the medium or overexpression of *OLE1*, a fatty acid desaturase and crucial target of Rsp5-mediated regulation. Following Rpb1 ubiquitylation in WT and Δ *rsp5* cells after UV light treatment, we confirmed previous results that cells deficient in *RSP5* are unable to ubiquitylate Rpb1^{103,104} (Figure 9A).

Next, we analyzed the second ubiquitin ligase described to act on Rpb1^{110,111}. Three components of the Elc1-Cul3 ligase complex can be deleted, without influencing cell viability. We used cells deficient in the subunits Elongin C, Elongin A or Cullin 3 (Figure 9B, Δ *elc1*, Δ *ela1*, Δ *cul3*) and probed for Rpb1 ubiquitylation by western blotting. Again, we could detect ubiquitylation of Rpb1 in WT cells, which was induced after UV light treatment. However, deletion of any component of the Elc1-Cul3 ligase complex abolished specifically the UV light-induced Rpb1 ubiquitylation (Figure 9B).

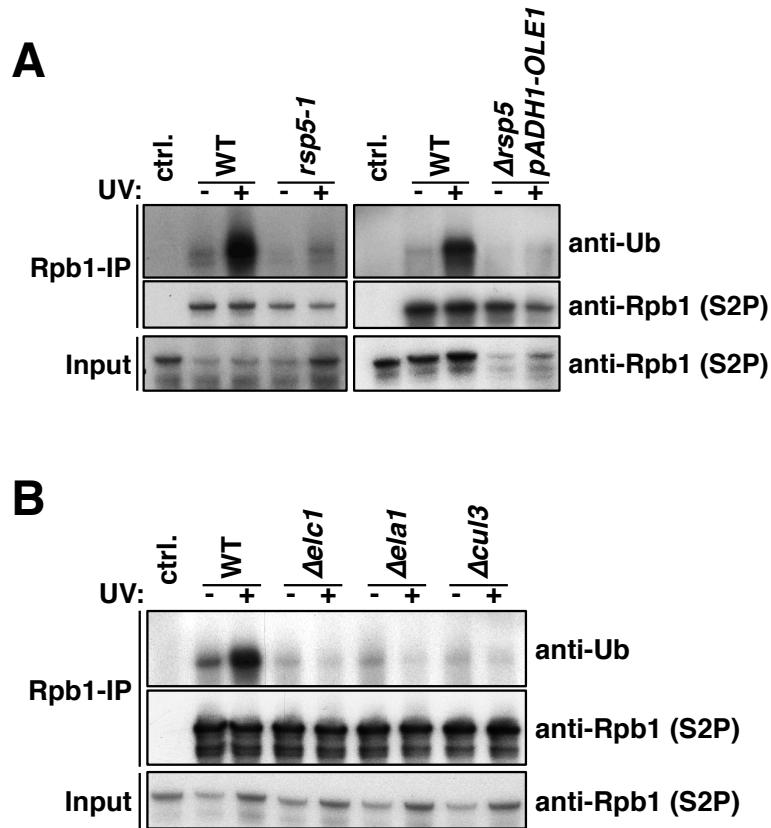


Figure 9: Rpb1 is ubiquitylated upon DNA damage involving the ubiquitin ligases Rsp5 and E1c1-Cul3. (A) UV light-irradiated (+) and non-irradiated (-) WT, *rsp5-1* and Δ *rsp5* (Δ *rsp5* *YCplac111pADH1-OLE1*) cells were lysed and Rpb1 was immunoprecipitated (Rpb1-IP) with antibody S2P. Ubiquitylated species of Rpb1 were detected with the P4D1 antibody. Sepharose beads without addition of the Rpb1 antibody served as background-binding control (ctrl.). Previous to UV light treatment, *rsp5-1* and the corresponding WT cells were shifted to 37°C. (B) Same procedure as described in (A) for WT, Δ *elc1*, Δ *ela1* and Δ *cul3* cells.

Given that the two previously identified ubiquitin ligases were not only described to be important for DNA damage-induced Rpb1 ubiquitylation but also for promoting Rpb1 degradation, we followed Rpb1 protein decay after UV light treatment in WT and cells deficient for Rsp5 or the E1c1-Cul3 ligase complex. Surprisingly, we detected turnover of Rpb1 in all tested cells of the previously described ubiquitin ligases similar to WT cells (Figure 10). Again, Rpb1 turnover was better detectable with the S2P-specific antibody compared to a whole pool RNAPII antibody (Figure 10A, compare 4H8 and S2P).

Hence, although the ubiquitin ligase Rsp5 and the E1c1-Cul3 ligase complex indeed contribute to Rpb1 ubiquitylation as described previously, they do not seem to be crucial for proteasomal degradation of Rpb1.

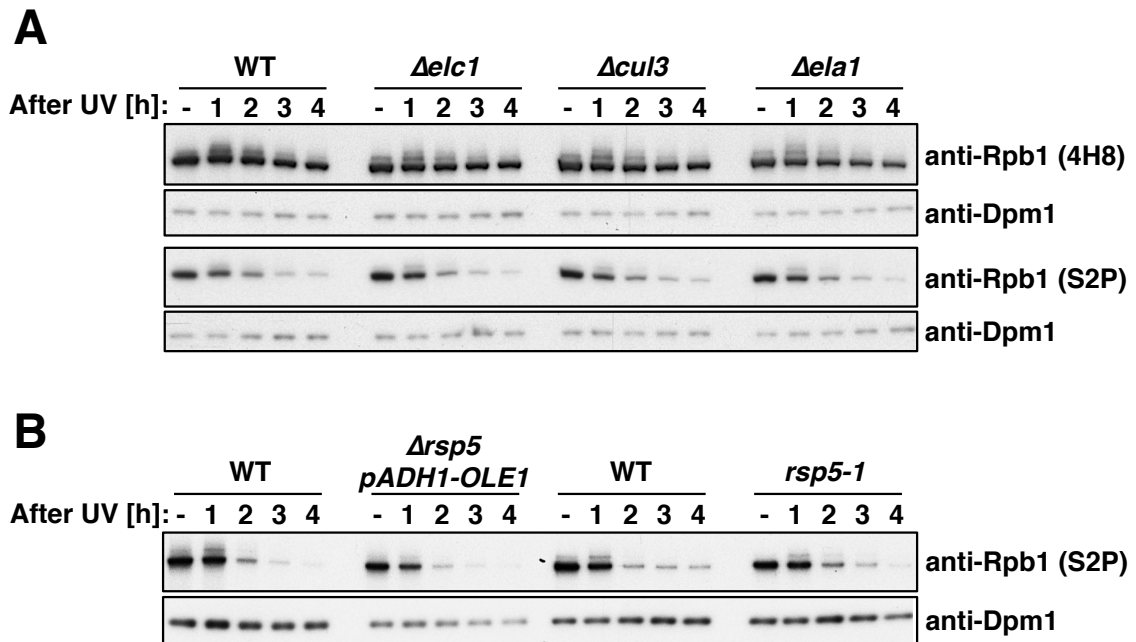


Figure 10: Rpb1 monoubiquitylation by Rsp5 or the Eic1-Cul3 complex does not trigger Rpb1 degradation upon DNA damage.

(A) Rpb1 protein levels in WT, $\Delta elc1$, $\Delta ela1$ and $\Delta cul3$ cells after UV light treatment (400 J/m^2) followed by a recovery phase of 4 hours in YPD medium. Rpb1 was detected with the 4H8 or S2P-specific antibody. Dpm1 served as loading control.

(B) Rpb1 protein levels in WT, *rsp5-1* and $\Delta rsp5$ ($\Delta rsp5$ *YCplac111pADH1-OLE1*) cells after UV light treatment (400 J/m^2). Previous to UV light treatment and for the recovery phase, *rsp5-1* and the corresponding WT cells were shifted to 37°C . Rpb1 was detected using the S2P-specific antibody. Dpm1 served as loading control.

4.4 Rpb1 is SUMOylated upon DNA damage and thereby marked for degradation

Because the previously described ubiquitin ligases are not implicated in Rpb1 degradation we were wondering by which pathway elongating Rpb1 is degraded. In our degradation assays we consistently observed a slower migrating band, which was cross-reactive with the S2P-specific antibody as well as with the whole pool Rpb1 antibodies (exemplified in Figure 10A). This slower migrating band appeared especially at early time points after recovery from DNA damage treatment. Since Rpb1 was not only described before to be ubiquitylated but also modified by SUMO⁷², we first wanted to confirm this observation. Indeed, we could detect Rpb1 species cross-reactive with a SUMO-specific antibody, especially after UV light irradiation (Figure 11A). Furthermore, in a hypomorphic mutant of the SUMO-conjugating gene *UBC9* (*ubc9^{ts}* cells), SUMOylation of Rpb1 was lost. Similarly, cells deleted either for the SUMO ligase gene *SIZ1* or *SIZ2*, showed reduced SUMOylation of Rpb1, with *SIZ1* having the major impact on Rpb1 SUMOylation.

Next, we asked whether the slower migrating band detected in our turnover assays corresponded to SUMOylated Rpb1. To this end, we expressed SUMO as a protein fusion with GFP to generate a larger form (GFP-SUMO), which resulted indeed in an upshift of the slower migrating band (Figure 11B). Moreover, in this Rpb1 degradation assay we observed that the amount of SUMOylated Rpb1 peaked roughly 1 hour after recovery from UV light treatment and dropped gradually during the recovery process.

Given that Rpb1 SUMOylation can be induced by DNA damage, and more interestingly, that we observed a decay of SUMOylated Rpb1 species following recovery from DNA damage, we asked whether SUMOylation influences Rpb1 degradation. To address this possibility, we compared UV light-induced Rpb1 decay in WT and mutant cells of the SUMO pathway. Strikingly, Rpb1 decay was almost abolished in cells defective in Ubc9 and Siz1 activity (Figure 11C and 11D), enzymes that were previously shown to perform Rpb1 SUMOylation (Figure 11A). In line with this finding, the slower migrating band in our decay assays, which corresponded to SUMOylated Rpb1, was not detectable in Ubc9- or Siz1-deficient cells. This finding provides first evidence that SUMOylation rather than ubiquitylation is the crucial initial modification needed for the observed degradation of elongating Rpb1.

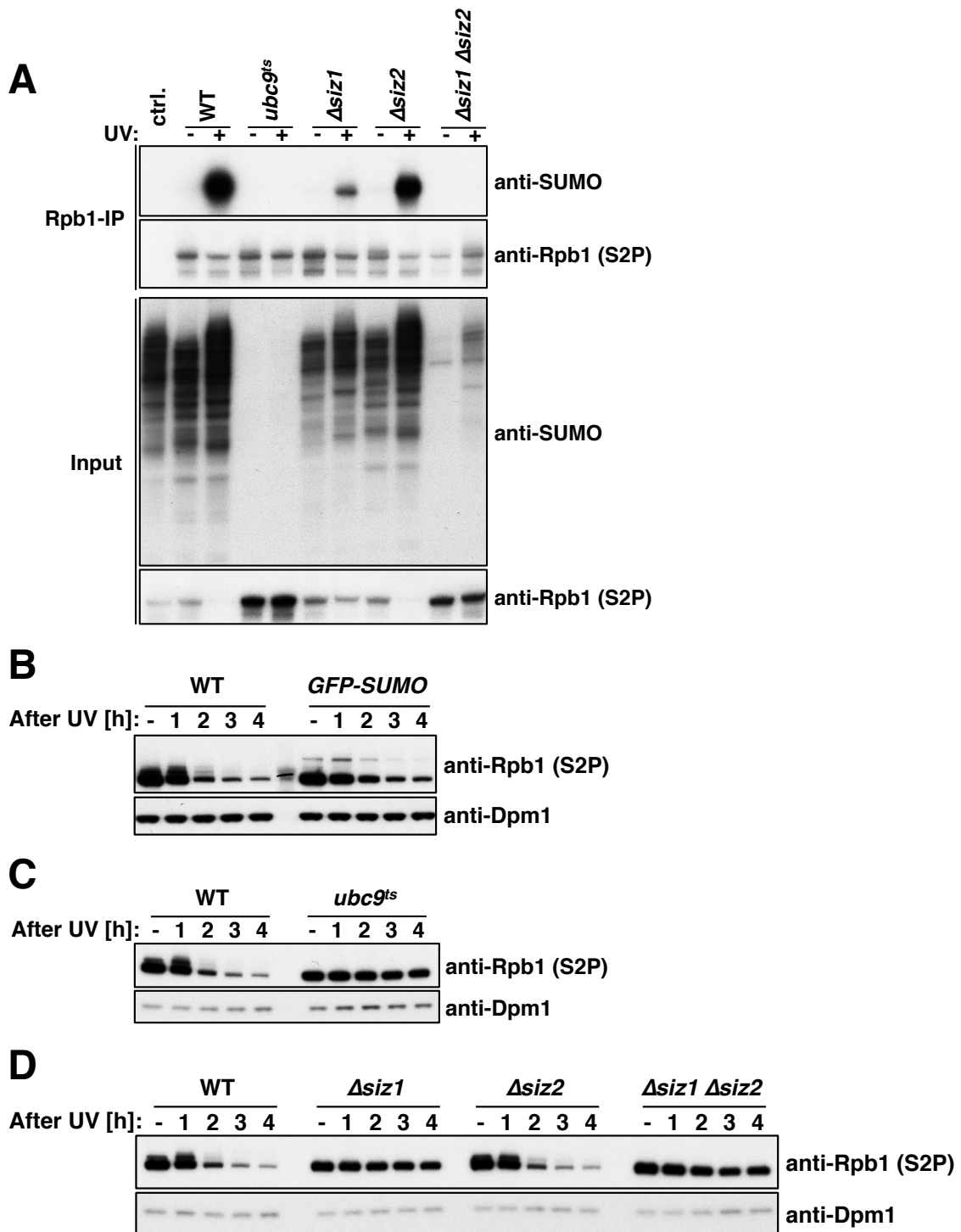


Figure 11: DNA damage-induced SUMOylation of elongating Rpb1 triggers proteasomal degradation.

(A) Western blot analysis of immunoprecipitated Rpb1 (Rpb1-IP) using the S2P-specific antibody from WT, *ubc9*, Δ *siz1*, Δ *siz2* and Δ *siz1* Δ *siz2* cells. Cells were shifted to 37°C before treatment with (+) or without (-) UV light. SUMOylated Rpb1 species were detected with a SUMO-specific antibody. Sepharose beads without addition of the S2P-specific antibody served as background-binding control (ctrl.).

(B) Rpb1 protein levels in WT and in mutant cells expressing GFP-tagged SUMO (under the *ADH1* promoter) after UV light treatment (400 J/m²) following recovery in YPD medium. Rpb1 was detected with the S2P-specific antibody. Dpm1 served as loading control.

(C) Same experimental setup as in (A). WT and *ubc9* cells were shifted to 37°C for 1 hour before UV light irradiation.

(D) Same experimental setup as in (A) with WT, Δ *siz1*, Δ *siz2* and Δ *siz1* Δ *siz2* cells.

4.5 Rpb1 SUMOylation is not restricted to previously identified lysine residues

To study the function of protein SUMOylation or ubiquitylation, modification has to be abolished by either depletion of the corresponding enzymes or, more directly, by changing the codons for the targeted lysine (K) residues to an arginine (R) codon. Several lysines within Rpb1 have been described to be crucial for modification by SUMO or ubiquitin^{72,112}. Since SUMOylation triggers Rpb1 degradation, we wondered whether mutation of previously identified SUMOylation sites (K217 and K1487) or even ubiquitylation sites (K330 and K695) had an impact on Rpb1 stability. We therefore expressed different mutant variants of Rpb1, with the specific lysine residues mutated to arginine, and tested first whether these mutant variants could be targeted for SUMOylation or ubiquitylation.

However, the immunoprecipitated Rpb1 mutant variants were still reactive with SUMO- or ubiquitin-specific antibodies comparable to the corresponding WT control (Figure 12A). Thus, as it is already described for other substrates, also in the case of Rpb1 the SUMO- and ubiquitin-machinery seem to target several lysine residues for modification, and mutation of one lysine residue does not abolish Rpb1 SUMOylation or ubiquitylation. In line with this finding, changing the codons for previously identified SUMOylation sites to arginine codons (K217R and K1487R) did not abolish DNA damage-induced degradation of Rpb1 (Figure 12B).

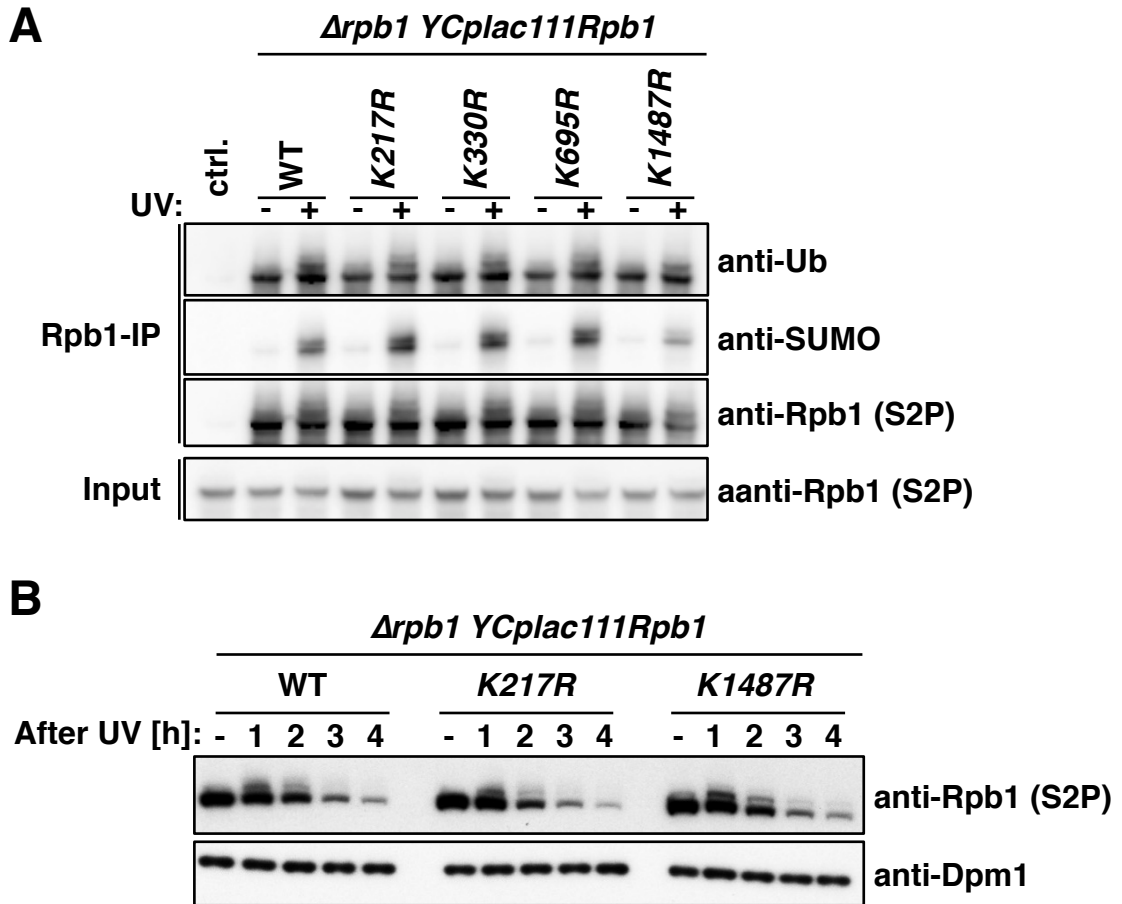


Figure 12: Rpb1 SUMOylation is not restricted to previously identified lysine residues.

(A) Rpb1 was expressed in *Δrpb1* cells under its endogenous promoter as a WT version or the mutant versions *K217R*, *K1487R* (previously identified SUMOylation sites) and *K330R*, *K695R* (previously identified ubiquitylation sites). Cells were either UV light-irradiated (+) or not irradiated (-), lysed and Rpb1 was immunoprecipitated using the S2P-specific antibody. First, SUMOylated Rpb1 species were detected with an anti-SUMO antibody. The PVDF membrane was cleared from the anti-SUMO antibody and ubiquitylated species of Rpb1 were detected with an anti-Ub antibody (P4D1). Sepharose beads without addition of the S2P-specific antibody served as background-binding control (ctrl.).

(B) Western blot analysis of Rpb1 protein levels in mutant versions *K217R*, *K1487R* of Rpb1 and the corresponding WT cells, treated with UV light and recovered in YPD medium. Rpb1 was detected with the anti-S2P antibody. Dpm1 served as loading control.

4.6 Degradation of Rpb1 is mediated by a SUMO-dependent pathway involving the SUMO-targeted ubiquitin ligase Slx5/Slx8

Because of the finding that Rpb1 is SUMOylated upon DNA damage and is targeted for proteasomal degradation we assumed that this degradation pathway might involve the SUMO-targeted ubiquitin ligases (STUbLs). Indeed, Rpb1 decay after UV light treatment was abolished when we used mutant cells deficient in the heterodimeric yeast STUbL Slx5/Slx8. Moreover, the slower migrating species, which corresponded to SUMOylated Rpb1, accumulated significantly in this mutant background (Figure 13A).

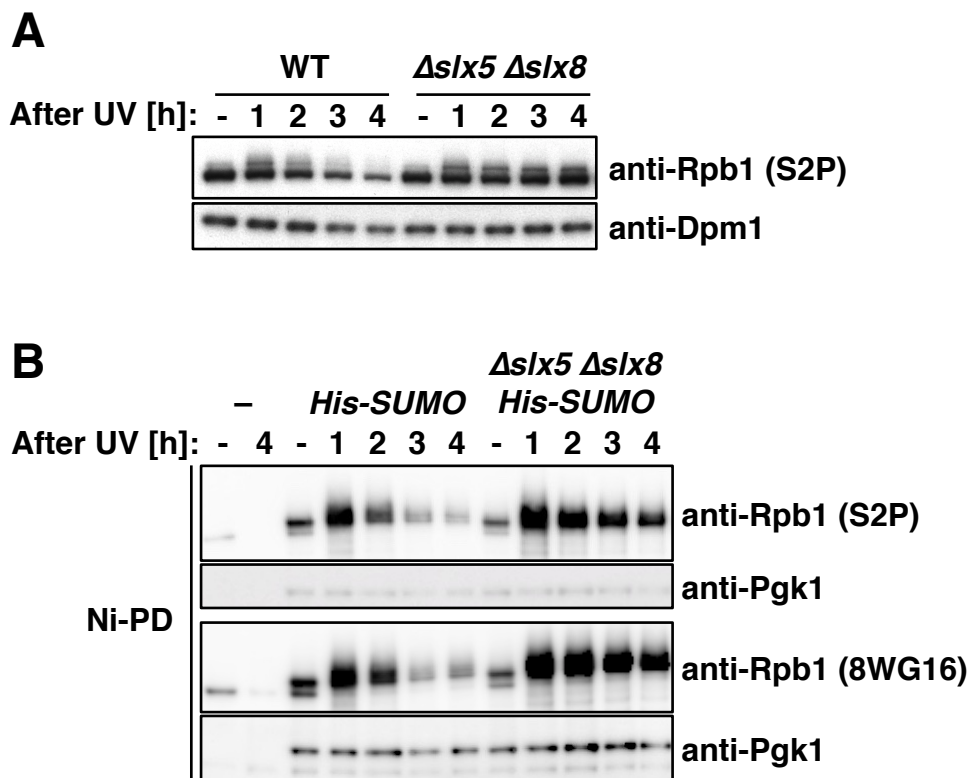


Figure 13: The SUMO-targeted ubiquitin ligase (STUbL) Slx5/Slx8 is involved in Rpb1 degradation.

(A) Rpb1 protein levels in WT and $\Delta slx5 \Delta slx8$ cells after UV light treatment (400 J/m^2) followed by a recovery time course in YPD medium over 4 hours. Rpb1 was detected with the anti-S2P antibody. Dpm1 levels served as loading control.

(B) Denaturing Ni-NTA pull-down (Ni-PD) was performed to isolate His-SUMO conjugates from UV light-treated (400 J/m^2) WT and $\Delta slx5 \Delta slx8$ cells following recovery in YPD medium. SUMOylated species of Rpb1 were detected with the S2P-specific antibody or the whole pool Rpb1 antibody 8WG16. SUMOylated Pgk1 served as pull-down control.

To confirm this finding, we enriched SUMOylated proteins using denaturing His-SUMO Ni-NTA pulldown assays¹⁵⁷. SUMOylated proteins from WT and STUbL-deficient cells before UV light treatment and after different recovery time points were probed with the Rpb1 elongation-specific antibody (S2P) or a whole pool antibody (8WG16) (Figure 13B). In line with our previous findings, SUMOylated species of Rpb1 peaked especially one hour after UV light treatment and dropped gradually during the recovery phase in WT cells. However, degradation of SUMOylated Rpb1 species was significantly delayed in Slx5/Slx8-deficient cells (Figure 13B). Notably, we could observe that specifically SUMOylated Rpb1 species were subjected for degradation by Slx5/Slx8, independent of the antibody used for Rpb1 detection (Figure 13B, compare S2P and 8WG16).

4.7 The kinases CTDK1 and Bur1/Bur2 are not degraded upon DNA damage

In most of our degradation assays we used the S2P-specific antibody in order to detect specifically the elongating pool of Rpb1. To substantiate the idea that the observed decay of Rpb1 is indeed protein turnover, we thought to address alternative explanations for the observed decay of the signal through DNA damage-induced dephosphorylation of Rpb1. One possible scenario would be DNA damage-induced proteasomal degradation of the kinases that mediate serine 2 phosphorylation. In that hypothetical case, the CTD of Rpb1 would not longer be phosphorylated at serine 2, resulting in a loss of the S2P signal in our analysis. We thus tested whether the stability of both kinases, CTDK1 and Bur1, is affected by UV light treatment.

First, we expressed epitope-tagged versions of all subunits of the CTDK1 complex as well as of Bur1 and its cyclin Bur2. This allowed us to follow protein levels after UV light treatment using an antibody against the epitope tag (HA), since commercial antibodies are not available for all kinase subunits. Interestingly, while most of the subunits were stable upon DNA damage, only HA-tagged versions of the subunits Ctk1 and Bur1 were unstable following recovery from DNA damage (Figure 14A and 14B). To exclude that the epitope tag interferes with protein function and causes artificial instability we additionally used antibodies against endogenous Ctk1 or Bur1 and followed protein levels in WT cells (Figure 14C and 14D).

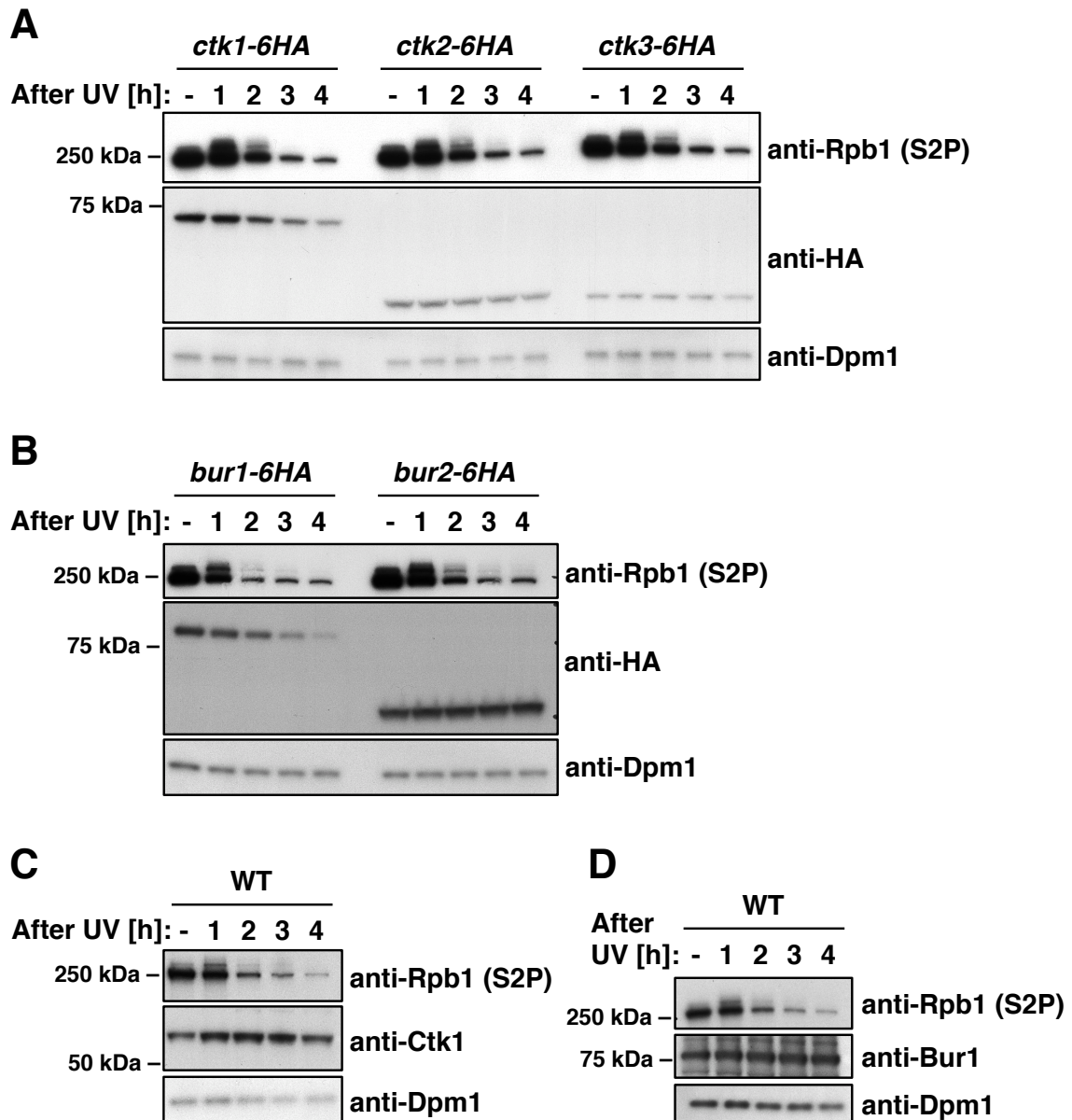


Figure 14: The kinase complex CTDK1 and Bur1 or Bur2 are not targeted for degradation.

(A) Cells with HA-tagged *ctk1*, *ctk2* or *ctk3* were UV light-treated (400 J/m^2) followed by a recovery time course in YPD medium over 4 hours. Rpb1 levels were detected with an anti-S2P antibody. Ctk1, Ctk2 and Ctk3 levels were detected with an anti-HA antibody in the corresponding cells. Dpm1 levels served as loading control.

(B) Cells with HA-tagged *bur1* and *bur2* were UV light-treated (400 J/m^2) followed by a recovery time course in YPD medium over 4 hours. Rpb1 levels were detected with the anti-S2P antibody. Bur1 and Bur2 levels were detected with an anti-HA antibody in the corresponding cells. Dpm1 levels served as loading control.

(C/D) WT cells were UV light-treated (400 J/m^2), followed by a recovery time course in YPD medium over 4 hours. Rpb1 protein levels were detected with the S2P-specific antibody. Ctk1 and Bur1 were detected with an anti-Ctk1 and anti-Bur1 antibody. Dpm1 levels served as loading control.

Strikingly, endogenous levels of Ctk1 and Bur1 were stable after UV light treatment, whereas Rpb1 levels dropped. This suggests that a C-terminal HA-fusion of Ctk1 and Bur1 cause protein instability. Most importantly, the stability of the endogenous proteins confirms that Rpb1 decay after DNA damage is not connected to serine 2 kinase levels.

4.8 Transcription-coupled repair (TCR) is important for DNA damage-induced Rpb1 degradation

Stalled RNA polymerases activate mainly the transcription-coupled repair (TCR) branch, which was shown to influence Rpb1 degradation in mammalian cells¹¹⁸. To investigate whether TCR influences Rpb1 degradation also in yeast, we compared UV light-induced Rpb1 decay in WT and mutant cells defective in two branches of TCR ($\Delta rad26$, $\Delta rpb9$).

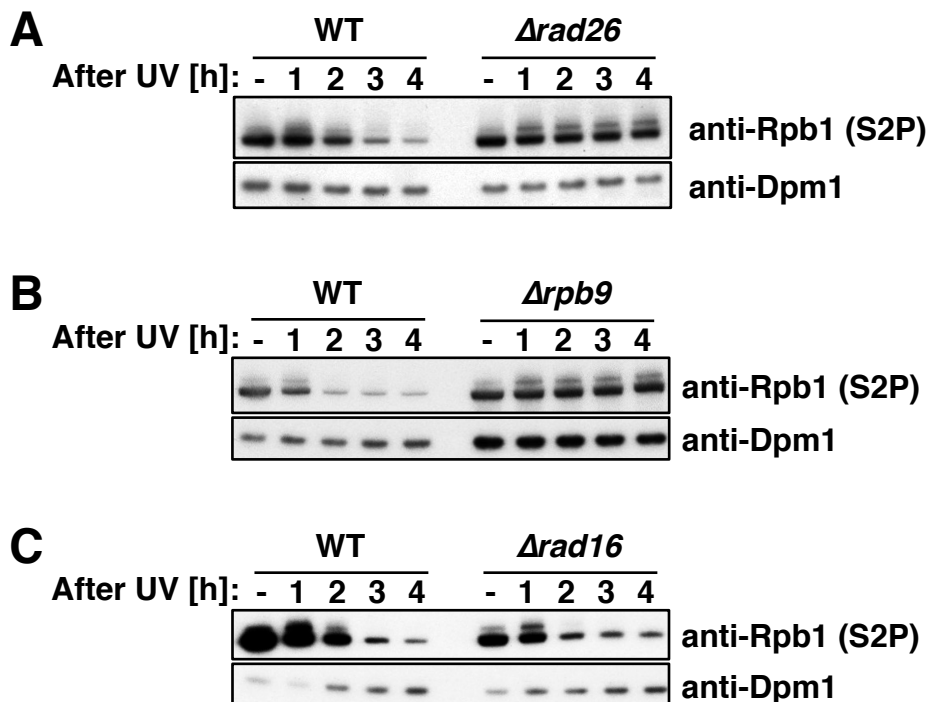


Figure 15: Transcription-coupled repair is important for DNA damage-induced Rpb1 degradation. (A/B/C) Rpb1 levels in WT, $\Delta rad26$, $\Delta rpb9$, and $\Delta rad16$ cells after UV light treatment (400 J/m^2) followed by a recovery time course in YPD medium over 4 hours. Rpb1 was detected with the anti-S2P antibody. Dpm1 levels served as loading control.

Indeed, cells deficient in the DNA-dependent remodeler Rad26 or the non-essential RNAPII subunit Rpb9 were unable to degrade Rpb1 (Figure 15A and 15B). As a control, mutant cells defective in the global-genome (GG) NER branch ($\Delta rad16$) showed Rpb1 decay indistinguishable from WT cells (Figure 15C). Interestingly, Rpb1 was SUMOylated in TCR-deficient cells, as the slower migrating band is still detectable. Thus, a stalled RNAPII complex likely recruits enzymes of the TCR pathway via SUMOylated Rpb1. However, how enzymes of the TCR pathway trigger subsequent Rpb1 degradation is still not known so far.

4.9 RNAPII accumulates on chromatin after DNA damage if Rpb1 is not removed by proteasomal degradation

According to our model, stalled RNAPII is cleared from damaged DNA by a SUMO-dependent pathway, which involves active TCR not only for DNA lesion removal but also for the Rpb1 degradation mechanism itself. Previous work showed that cells deficient in TCR ($\Delta rad26$) show higher chromatin occupancy of RNAPII after DNA damage induction¹²⁵. Following this work, we next asked whether RNAPII also accumulates on chromatin when we abolish Rpb1 SUMOylation and consequently SUMO-dependent Rpb1 degradation. Therefore, we performed chromatin immunoprecipitation (ChIP) studies after UV light treatment and measured Rpb1 levels at two different regions of the highly transcribed *RPB2* gene. In line with previous work and our degradation analysis, Rpb1 levels on chromatin dropped over time following recovery from UV light treatment (Figure 16A and 16B). By contrast, Rpb1 signals persisted and even rose over time in $\Delta siz1$ as well as in $\Delta rad26$ cells, arguing for a direct involvement in the turnover process of stalled RNAPII. This effect was much stronger for a region in close proximity to the transcriptional start site (TSS) (Figure 16A and 16D; *RPB2*-Region1) compared to a region further downstream (Figure 16B and 16D, *RPB2*-Region2). Moreover, when we monitored Rpb1 occupancy on the *ACT1* gene at a region further downstream of the TSS (Figure 16C and 16D), Rpb1 signals dropped in WT cells following exposure to UV light but to a lower extent in $\Delta siz1$ and $\Delta rad26$ mutant cells (Figure 16C). From these data we interpret that RNAPII accumulates on chromatin upon DNA damage induction if Rpb1 is not SUMOylated and subsequently removed from the stalled complex. Moreover, Rad26

is indeed necessary to promote Rpb1 removal from chromatin. However, accumulation of RNAPII seems to be biased towards regions in close proximity to the TSS. To further analyze this phenomenon, a genome-wide Rpb1-ChIP approach would be best suited.

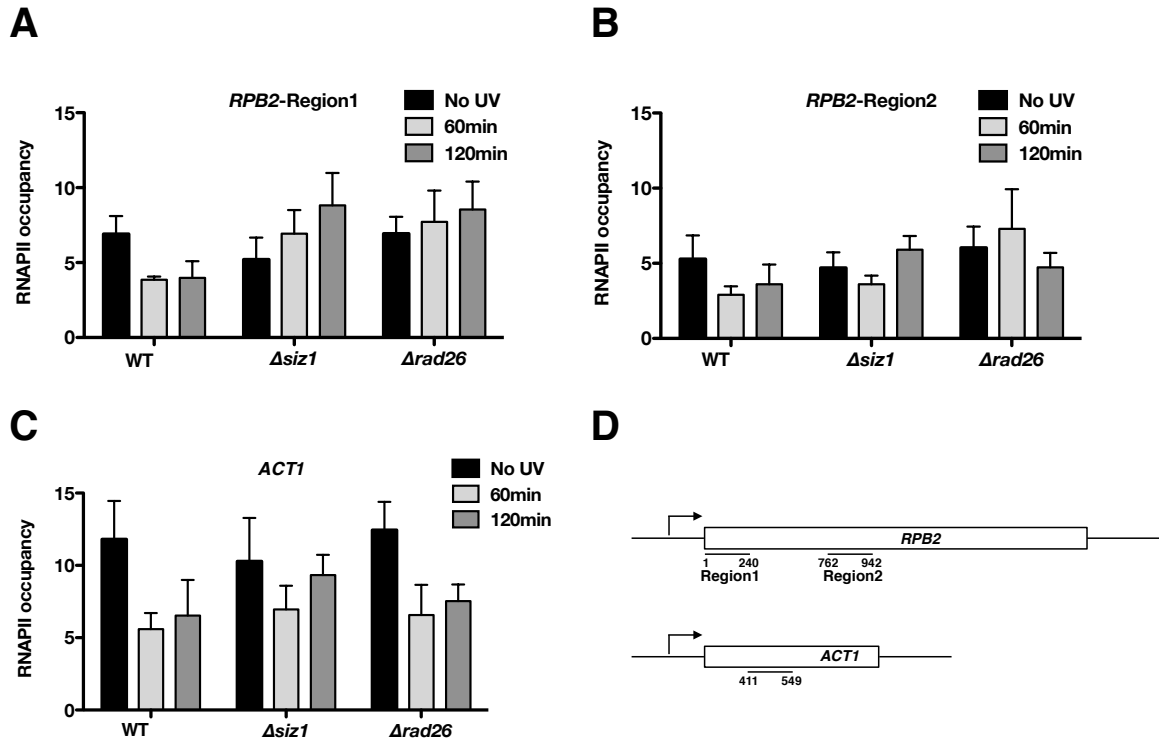


Figure 16: RNAPII occupancy on chromatin after DNA damage.

(A/B/C) Chromatin immunoprecipitation (ChIP) studies in different regions of the *RPB2* locus and at the *ACT1* locus. Cells were irradiated with UV light (100 J/m^2) and incubated for different repair times as indicated. Rpb1 was immunoprecipitated with 8WG16 antibody or control IgG2a, followed by quantitative PCR amplification using primers for the *RPB2* locus in WT, $\Delta siz1$ and $\Delta rad26$ cells. The values given for all tested regions are calculated by normalizing the ChIP-PCR signal with the IgG2a PCR signal and input PCR signal.

(D) Schematic overview of primer sets used for the ChIP analysis within the *RPB2* or *ACT1* locus. Numbers correspond to nucleotides of the open reading frame.

4.10 Interference with the nuclear pore complex influences Rpb1 degradation

Degradation of Rpb1 critically depends on SUMOylation, which recruits the heterodimeric STUbL Slx5/Slx8 and presumably also factors of the TCR pathway. It has been suggested that a large fraction of the Slx5/Slx8 protein pool co-localizes with the nuclear pore complex (NPC) and especially binds the nuclear pore protein Nup84¹³⁷. Nup84 and Slx5/Slx8 were previously described to be important to tether damaged DNA to the nuclear periphery for DNA repair. We thus wondered whether Rpb1 degradation would be mediated in proximity of nuclear pores.

When we performed Rpb1 decay analysis in Nup84-deficient cells ($\Delta nup84$) we observed no Rpb1 degradation (Figure 17A). Surprisingly, we also found that SUMOylation of Rpb1 was absent in Nup84-deficient cells. Moreover, we were unable to detect SUMOylated Rpb1 after UV light treatment in these cells (Figure 17B). Interestingly, overall protein SUMOylation was not affected in Nup84-deficient cells (Figure 17B, compare input levels). However, in Nup84-deficient cells, not only the organization of the NPC is affected, but also the localization of Ulp1, a SUMO protease important for SUMO maturation at the nuclear pore^{79,158}. Ulp1 mislocalization was also observed in cells deficient for the nuclear basket proteins Mlp1 and Mlp2. Strikingly, Rpb1 degradation was also abolished in $\Delta mlp1 \Delta mlp2$ cells (Figure 17C), possibly because Rpb1 SUMOylation is impaired as well. From these preliminary experiments we speculate that interference with the NPC causes an impairment of Rpb1 SUMOylation and thereby leads indirectly to Rpb1 stabilization after DNA damage.

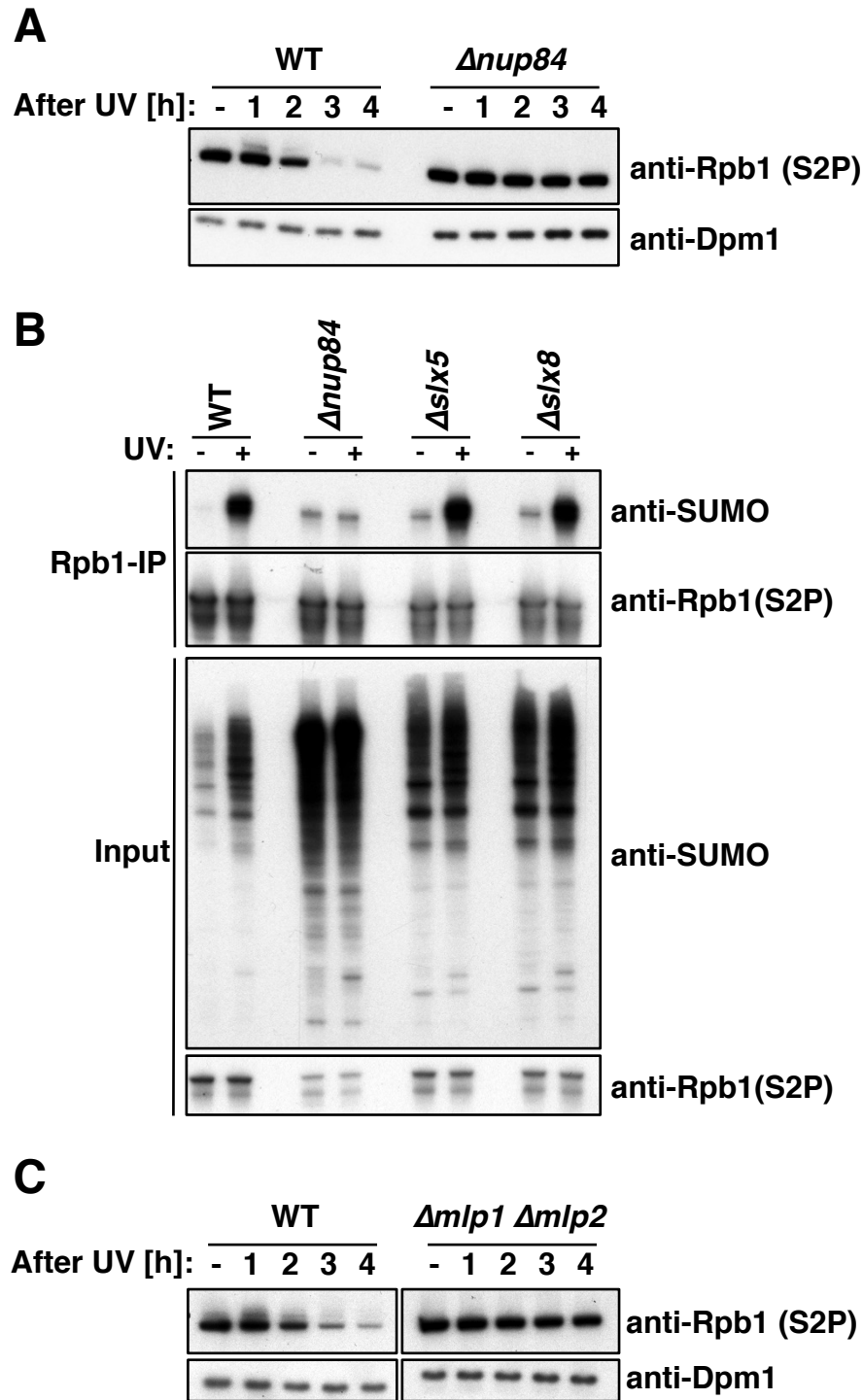


Figure 17: Interference with the nuclear pore complex abolishes Rpb1 SUMOylation and degradation.
(A/B) Rpb1 protein levels in WT and $\Delta nup84$ or $\Delta mlp1 \Delta mlp2$ cells after UV light treatment (400 J/m^2) followed by a recovery time course in YPD medium over 4 hours. Rpb1 was detected with the anti-S2P antibody. Dpm1 levels served as loading control.
(C) UV light-irradiated (+) and not irradiated (-) WT, $\Delta nup84$, $\Delta slx5$ and $\Delta slx8$ cells were lysed and Rpb1 was immunoprecipitated (Rpb1-IP) with antibody S2P. SUMOylated species of Rpb1 were detected with a self-made anti-SUMO antibody.

5 Discussion

The previously described mechanism for RNA polymerase II (RNAPII) removal from the DNA upon prolonged stalling implicates many factors, which were discovered over a long period and finally combined in one complex unifying model^{107,124}. However, most studies did not distinguish between the chromatin-engaged or -unengaged pools of RNAPII, because antibodies recognizing potentially all forms of Rpb1 were used in these studies. These data might be difficult to interpret because various degradation pathways might act on different pools of Rpb1, which even can take place simultaneously. Although previous groups reported⁵³ that the chromatin-engaged elongating pool of RNAPII is affected by stalling and therefore only this pool should be removed from the DNA by proteasomal degradation, in this study we used for the first time different antibodies against Rpb1. This enables us to distinguish between transcriptional initiating and elongating RNAPII. In this study we describe a different pathway for the removal of stalled RNA polymerase II from DNA. This stepwise mechanism involves initial Rpb1 SUMOylation followed by ubiquitylation by a SUMO-targeted ubiquitin ligase (STUbL) and subsequent proteasomal degradation.

5.1 Potential loss of Rpb1 phosphorylation after DNA damage

In this study the identification of new players in the Rpb1 degradation pathway was possible by using the S2P-specific Rpb1 antibody, which was described to recognize carboxy-terminal domain (CTD) repeats with phosphorylated serine 2. However, Rpb1 decay after DNA damage treatment might also be interpreted as phosphorylation loss of Rpb1 CTD. This is unlikely to be the case for the following reasons: First, we and others showed that the known kinases CTDK1 and Bur1, responsible for serine 2 phosphorylation, are not degraded upon DNA damage induction¹⁵⁹. Nevertheless, a so far uncharacterized kinase might act on the CTD of Rpb1 upon DNA damage. However, this hypothetical kinase then must be activated and at the same time degraded upon DNA damage, which appears unlikely.

Second and even more speculative, the phosphatase Fcp1, which dephosphorylates the CTD at serine 2, might get activated upon DNA damage. In this

speculative model DNA damage would trigger degradation of a hypothetical Fcp1 inhibitor. However, such an inhibitor of Fcp1 has so far not been described.

On the contrary, our ChIP or His-SUMO pulldown data strongly support our interpretation that the observed Rpb1 decay is indeed degradation of the elongating form of Rpb1. In the ChIP experiments we observed that Rpb1 accumulates on the chromatin if the SUMOylation system is impaired, which is in line with our decay analysis. Moreover, in our His-SUMO pulldown experiments we found that specifically the SUMOylated form of Rpb1 is targeted for degradation independent of the antibody used for Rpb1 detection.

5.2 Rpb1 is degraded in a SUMOylation- and ubiquitylation-dependent manner

It is well established that Rpb1 is SUMOylated specifically upon DNA damage treatment, but the purpose of this modification remained so far enigmatic⁷². The biochemical data presented in this study allow us to propose a stepwise model, by which Rpb1 is first SUMOylated and subsequently ubiquitylated to trigger proteasomal degradation (Figure 18). The elongating RNAPII complex is forced to stall at DNA lesion sites, which triggers recruitment of the SUMO-conjugating enzyme Ubc9 and the SUMO ligases Siz1 and Siz2. Consequently, the catalytic subunit of RNAPII, Rpb1, is SUMOylated upon DNA damage treatment⁷². How the SUMO machinery recognizes a prolonged stalled RNAPII complex is, however, unknown. It is established that Siz1 and Siz2 localize to DNA via their SAP domain and act *e.g.* on proteins linked to DNA repair⁷⁷. For instance, several proteins involved in the NER pathway were shown to be SUMOylated after UV light treatment by Siz1 or Siz2^{78,160}. Interestingly, UV light treatment can either induce *de novo* SUMOylation of several NER factors or increase the SUMOylation pattern of others. Among them are the RNAPII subunits Rpb1 and Rpb4, which are already SUMOylated even in untreated cells^{78,160}. However, UV light-induced SUMOylation of Rpb1 and potentially other RNAPII subunits might recruit DNA repair factors via SUMO-SIM interactions. In turn, these repair factors would also be SUMOylated to foster protein-protein interactions and create a DNA damage repair hot spot⁷⁸.

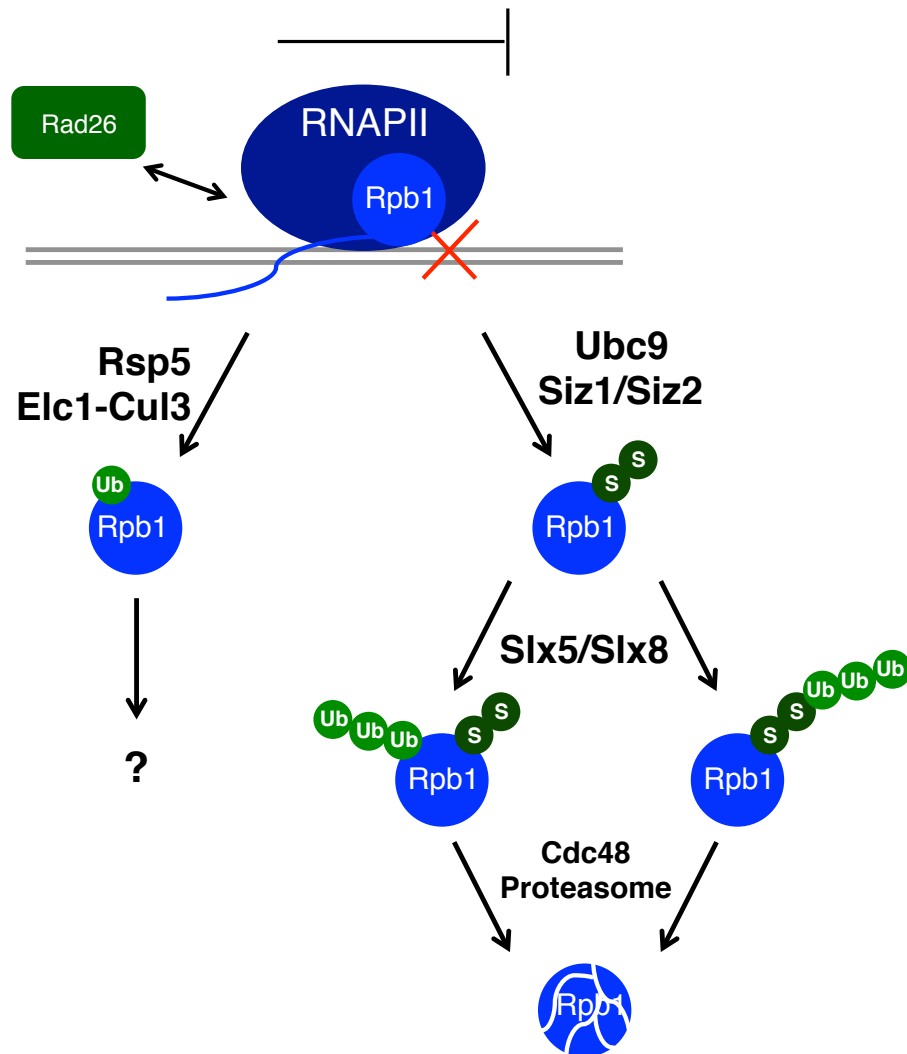


Figure 18: Model of SUMO-dependent degradation of Rpb1.

RNA polymerase II stalls at DNA lesion sites and is recognized by the remodeler Rad26 and subsequently targeted by the SUMO machinery. Rpb1 is SUMOylated (S) by the SUMO-conjugating enzyme Ubc9 together with the SUMO ligases Siz1 and Siz2 at potentially several lysine residues. SUMOylated Rpb1 recruits the SUMO-targeted ubiquitin ligase Slx5/Slx8 for subsequent polyubiquitylation. Slx5/Slx8 either extends the SUMO-chain with ubiquitin (Ub) entities or targets another lysine within Rpb1. Polyubiquitylated (and SUMOylated) Rpb1 is targeted by Cdc48 likely for extraction from the RNAPII complex and for delivery to the proteasome. Rpb1 is also targeted by the previous identified ubiquitin ligases Rsp5 and Elc1-Cul3 for monoubiquitylation, but the function is unknown so far.

Moreover, whether SUMOylated Rpb1 is further targeted for degradation might depend on the ability of the recruited repair machinery to remove the DNA damage in the context of a stalled RNAPII^{49,161}. Only if this is not possible, DNA has to be cleared from the stalled RNAPII complex to make the DNA lesion accessible for repair. In that case, we assume that the STUbL Slx5/Slx8 is recruited to these damaged sites to target Rpb1 and potentially also other proteins for polyubiquitylation. Since we were not able to detect a direct binding between Rpb1 and Slx5/Slx8, this interaction could be very transient or might occur upon Rpb1 SUMOylation. From our His-SUMO pulldown experiment we know that Slx5/Slx8 preferentially targets SUMOylated Rpb1 for ubiquitylation, which in turn triggers degradation. Moreover, Slx5/Slx8 might attach ubiquitin entities to the preexisted SUMO-chain¹⁶² or to other lysine residues within Rpb1 (Figure 18).

Our finding that Slx5/Slx8 is involved in Rpb1 ubiquitylation and degradation reveals striking parallels to other DNA damage repair pathways. Persistent DNA breaks and collapsed replication forks are targeted to the nuclear periphery in a Slx5/Slx8-dependent manner^{137,163-165}. Thus, Slx5/Slx8 associates with nuclear pore proteins like Nup84. Although in most cases the targeted substrates are still unknown, it was suggested that Slx5/Slx8 targets SUMOylated proteins for ubiquitylation to trigger proteasomal degradation thereby facilitating DNA damage repair^{137,138,165}. In line with this, also Rpb1 degradation is dependent on an intact nuclear pore complex.

5.3 Influence of the nuclear pore complex on Rpb1 degradation

In this study we showed that UV light-induced SUMOylation of Rpb1 was abolished in cells deficient in the nuclear pore proteins Nup84 or Mlp1 and Mlp2. As a consequence, DNA damage-induced degradation of Rpb1 was inhibited. This might be due to the following reasons: First, the SUMO-specific protease Ulp1 is located at the nuclear periphery where it functions in SUMO maturation. Deletion of the nuclear basket proteins Nup84 or Mlp1/Mlp2 leads to Ulp1 mislocalization and consequently might interfere with SUMO maturation and the SUMO metabolism^{158,166}. However, although UV light-induced Rpb1 SUMOylation was abolished, overall protein SUMOylation was not affected, arguing against a limited SUMO pool. Moreover, if Ulp1 is not tethered to the NPC, it could also deSUMOylate Rpb1. So far it is unclear whether Rpb1 is in general a substrate of SUMO

proteases after DNA damage treatment. Our initial results showed that Rpb1 SUMOylation is not enriched in mutants of the SUMO protease Ulp1 or Ulp2 (data not shown). However, further experiments are necessary to elucidate whether a mislocalization of Ulp1 leads to Rpb1 deSUMOylation.

Second, interference with the NPC leads not only to mislocalization of Ulp1 but also of Slx5/Slx8^{101,164}. As described for other potential substrates, recognition of SUMOylated Rpb1 by Slx5/Slx8 is important for subsequent ubiquitylation and degradation. Whether the catalytic activity of Slx5/Slx8 relies on the localization to the NPC is still unknown. A separation-of-function protein variant of Slx5/Slx8, which cannot localize to the NPC but displays ubiquitylation function would help to investigate whether localization to the NPC is important for Rpb1 SUMOylation and subsequent degradation.

Finally, SUMOylation and degradation of Rpb1 might occur in close proximity to the NPC. Considering that gene transcription occurs in the vicinity of the NPC to facilitate the coordination between mRNA maturation and export^{167,168}, degradation of a stalled RNAPII at the nuclear pore represents an attractive hypothesis.

5.4 Rpb1 is monoubiquitylated by previously identified ubiquitin ligases

During this study we could confirm that Rpb1 is indeed a target of the ubiquitin ligases Rsp5 and Elc1-Cul3¹⁰⁷. However, deletion of the corresponding genes did not abolish degradation of the elongating form of Rpb1 after DNA damage. Moreover, when we performed Rpb1 immunoprecipitation assays only the monoubiquitylated form of Rpb1 was detectable, and both ubiquitin ligases seem to contribute to this modification. Since Rpb1 is highly regulated by posttranslational modifications during transcription, monoubiquitylation of Rpb1 performed by Rsp5 and Elc1-Cul3 might be important to control other cellular activities.

Rsp5 was recently implicated in the clearance of misfolded proteins from the cytoplasm upon heat-shock induction¹⁶⁹. Since *RSP5* deletion is lethal¹⁵⁶, most studies to analyze Rpb1 decay were performed with temperature-sensitive mutants^{105,107}. In these mutants, Rsp5 function is diminished at elevated temperatures. Consequently, shifts to a higher temperature would induced protein misfolding and trigger the Rsp5-dependent clearance pathway. Also Rpb1 with its highly repetitive and unstructured CTD might have

a high propensity for misfolding and could be targeted by Rsp5 for protein quality control. Interestingly, our initial data revealed that Rpb1 is also monoubiquitylated after heat-shock treatment in an Rsp5-dependent manner (data not shown). It would be interesting to see whether specifically the cytosolic pool of Rpb1 is targeted for Rsp5-dependent ubiquitylation and degradation upon heat-shock.

Moreover, ubiquitylation of Rpb1 by Rsp5 is dependent on binding to the CTD of Rpb1^{103,106}. By doing so Rsp5 competes for binding with the isomerase Ess1. Both enzymes were shown to bind to Rpb1's CTD via their WW-domain and thereby presumably regulate RNAPII levels available for transcription^{104,170}. It was proposed that binding of Ess1 to the CTD enhances transcription whereas Rsp5 binding counteracts somehow this effect perhaps through Rpb1 degradation. Since Rsp5 localizes primarily to the cytosol, it was suggested that Rpb1 would be exported from the nucleus and targeted for ubiquitylation and degradation in the cytoplasm. From our data, we know that ubiquitylation of Rpb1 by Rsp5 upon UV light or heat-shock treatment does not lead to degradation of the elongating pool. Potentially this modification might block re-import of RNAPII to the nucleus, thereby counteracting transcription until DNA repair is finished.

Furthermore, we could not abolish Rpb1 monoubiquitylation by interfering with the previously described ubiquitylation sites K330 or K695¹¹². However, so far we cannot exclude that a mutant variant of Rpb1, in which both lysines are replaced by arginines, would abolish UV light-induced Rpb1 monoubiquitylation. An alternative explanation is that these sites are prone for modification after DNA damage-induction by other means than UV light. Moreover, K695 is located in a region where Rpb9, a non-essential subunit of RNAPII, binds¹¹³. Ubiquitylation at this site could be used to control Rpb9 binding and thereby its function.

5.5 Role of Rad26 in RNAPII removal from chromatin upon DNA damage

The transcription-coupled repair (TCR) factor Rad26 and its human homolog Cockayne syndrome (CS) protein B were previously described to act on stalled RNAPII. It is assumed that Rad26 and CSB are recruited to and travel with the elongating RNAPII, but how these factors recognize a stalled RNAPII complexes is unknown^{40,41}. CSB, but apparently not Rad26, harbors a ubiquitin-binding domain (UBD) at the CTD, which is important for its function in the TCR pathway³⁸. However, potential binding substrates to this domain are unknown so far. Moreover, comparable to Rpb1, CSB itself was shown to be ubiquitylated and targeted by Cdc48 for proteasomal degradation at the end of the TCR process^{122,126}. Interestingly, instead of a UBD, Rad26 possesses several putative SUMO-interacting motifs (SIMs), which might be crucial for binding to SUMOylated Rpb1. Initial results suggest that mutation of SIMs at least at the very C-terminus of Rad26 does not impair Rpb1 degradation (data not shown). Moreover, in contrast to CSB, no direct interaction between Rad26 and Rpb1 was reported so far^{38,171}. This indicates that binding of Rad26 to the RNAPII complex might also be delivered through other subunits. Additionally, since Rad26/CSB belongs to the SWI2/SNF2 chromatin remodeling protein family, its potential function in chromatin remodeling does not necessarily require robust binding to Rpb1. Rather, Rad26/CSB might facilitate Rpb1 removal through chromatin remodeling, thereby increasing lesion accessibility to enhance TCR^{49,172}. Interestingly, the chromatin remodeling complex INO80 was recently implicated in Rpb1 removal¹¹⁷. This suggests that although transcription occurs on nucleosome-free DNA, chromatin remodeling indeed facilitates Rpb1 degradation.

Moreover, while CSB promotes Rpb1 degradation, Rad26 was reported to have a protective effect¹²¹. This is in conflict with our results and results obtained by others^{125,173}. We demonstrated that Rad26 function in a similar way as its human homolog, as *RAD26* deletion abolished specifically degradation of the elongating pool of Rpb1. These conflicting results might originate from the choice of antibodies used to follow Rpb1 degradation. Additionally, we and others found that deletion of Rad26 results in an accumulation of Rpb1 at chromatin, likely because the TCR pathway is blocked and degradation of Rpb1 is impaired¹²⁵.

5.6 Parallels of Rpb1 modification and degradation to other SUMO- and STUbL-dependent pathways

Targeting DNA damage-stalled RNAPII complexes for SUMOylation and subsequent proteasomal degradation through the action of the SUMO-targeted ubiquitin ligase (STUbL) seems to be another example how genome stability is preserved by ubiquitin and ubiquitin-like proteins.

Comparable to transcriptional stalling, also a stalled replication fork is controlled by the action of ubiquitin and the small ubiquitin-like modifier (SUMO). Modification of Rpb1 might resemble the complex modification pattern of PCNA, in which the two different modifiers control translesion synthesis, error-free DNA damage repair and inhibition of unwanted recombination^{13,16,174}. Moreover, stalled replication forks are targeted to the nuclear periphery in a Slx5/Slx8-dependent manner for DNA repair¹³⁷. Although the target substrate of Slx5/Slx8 at the stalled replication fork is so far uncharacterized, various other DNA-bound proteins were shown to be targeted by a two-step mechanism, implicating first SUMOylation followed by ubiquitylation and degradation to regulate and facilitate DNA damage repair^{133,138,175}.

Such a two-step mechanism resulting in SUMOylated and ubiquitylated substrates represents an elegant mode of action to recruit proteins containing ubiquitin-and/or SUMO-interacting motifs. For instance, the segregase Cdc48 together with its co-factor Ufd1 was shown to target both ubiquitylated and SUMOylated proteins and, more strikingly, also STUbL substrates^{153,154}. Cdc48 extracts proteins from their cellular environment and facilitates their deubiquitylation or degradation by the proteasome. Also in the case of Rpb1, SUMOylation might first recruit repair factors and Slx5/Slx8. Subsequently, Cdc48 is recruited to SUMOylated and ubiquitylated Rpb1 and helps to segregate it from the chromatin-bound RNAPII complex for proteasomal degradation, as described previously¹¹⁵.

Taken together, the mechanism for Rpb1 degradation upon DNA damage, described in this study, is distinctly different from the previously described¹⁰⁷. However, our new degradation model is supported by several lines of evidence and involves a similar set of factors, which are also implicated in removal of other chromatin-bound proteins. Moreover, this study expands the substrate spectra of the SUMO-targeted ubiquitin ligase Slx5/Slx8 by Rpb1 and helps to elucidate their mode of action.

6 Materials and Methods

6.1 Microbiological Techniques

If not otherwise indicated, all chemicals and reagents were obtained from Applied Biosystems, BD, Biomol, Bio-Rad, Enzo, GE Healthcare, Greiner Bio-One, Life, Merck, Millipore, New England Biolabs, Peqlab, Pierce, Promega, Roche, Roth, Serva, Sigma and Thermo Scientific. Enzymes and deoxynucleotide triphosphates (dNTPs) for molecular biology were purchased from NEB. DNA oligonucleotides for cloning were custom-made by Eurofins MWG. For all procedures described, sterile flasks, sterile and de-ionized water as well as sterile solutions were used. Microbiological, molecular biological and biochemical techniques described below were derived from standard protocols¹⁷⁶.

6.1.1 *Escherichia coli* (*E. coli*) Techniques

E. coli Strains

Strain	Genotype	Reference
XL1-Blue	hsd R17 rec A1 end A1 gyrA46 thi-1 sup E44 relA1 lac [F' pro AB lacI ^q ZΔ M15 Tn10 (Tet ^r)]	Stratagene

E. coli Media

LB-medium/plates: 1% Trypton (Difco)
 0.5% yeast extract (Difco)
 1% NaCl
 1.5% agar - for plates
 sterilized by autoclaving

For plasmid selection 100 µg/ml ampicillin or 30 µg/ml kanamycin were added.

Preparation of competent *E. coli* cells

LB medium was inoculated with a single colony and grown at 37°C with constantly shaking to produce an overnight culture. The main culture was inoculated with an OD₆₀₀ of 0.05 and 1 L was harvested at an OD₆₀₀ of 0.5 by centrifugation (15 min, 4000 g, 4°C). All further steps were performed at 4°C with pre-chilled solutions. The pellet was washed with 250 ml and afterwards with 125 ml of 10% glycerol. The pellet was resuspended in 2 ml of 10% glycerol. Aliquots were frozen on dry ice and stored at -80°C.

Transformation of plasmid DNA into competent *E. coli* cells

For transformation of expression vectors into *E. coli* electroporation was used. Competent cells were thawed on ice and 50 µl were mixed with either 10 ng plasmid DNA or half of a ligation mixture. The cell/DNA suspension was electroporated in a pre-chilled cuvette (0.1 cm gap) with a pulse of 1.8 kV at a resistance of 200 Ω using a GenePulser Xcell electroporator. The mixture was plated onto selective medium.

6.1.2 *Saccharomyces cerevisiae* (*S. cerevisiae*) Techniques

S. cerevisiae Strains

Strain	Genotype	Reference
W303	<i>leu2-3,112 ade2-1 can1-100 his3-11,15 ura3-1 trp1-1 RAD5</i>	Jentsch strain collection
BY4741	<i>ura3Δ0 leu2Δ0 his3Δ1 met15 Δ0</i>	177
DF5	<i>his3Δ200 leu2-3,11 lys2-801 trp1-1 ura3-52</i>	178
Y0933	RC757 <i>Mat alpha, his6 met1 sst2-1 cyh2 can1</i>	Jentsch strain collection
Y0934	RH448 <i>Mat a, leu2 his4 lys2 ura3 bar1</i>	Jentsch strain collection
YIH516	DF5 <i>elc1::hphNT1</i>	This study
MJK110	DF5 <i>ela1::hphNT1</i>	This study
MJK108	DF5 <i>cul3::hphNT1</i>	This study
Y2240	DF5 <i>rsp5::HIS3 YCplac111-pADH1-OLE1</i>	Jentsch strain collection
FW1808	<i>his4-912 ΔR5, lys2-128Δ, ura3-52, rsp5-1</i>	106
Y0554	DF5 <i>cim3-1, ura3-52, leu2Δ1</i>	179

Materials and Methods

Y0649	DF5 <i>cdc48-6</i>	154
Y3784	DF5 <i>cdc48-3</i>	Jentsch strain collection
MJK369	DF5 <i>pADH-GFP-Smt3::natNT2</i>	Jentsch strain collection
Y0174	DF5 <i>ubc9Δ::TRP1 leu2::ubc9Pro-Ser::LEU2</i>	180
Y1558	DF5 <i>siz1::HIS3MX6</i>	J. Stingele
Y3619	DF5 <i>siz2::HIS3MX4</i>	J. Stingele
YJS	DF5 <i>siz1::HIS3MX6 siz2::HIS3MX4</i>	J. Stingele
YIH443	DF5 <i>slx5::HIS3MX6 slx8::hphNT1</i>	This study
MJK116	DF5 <i>rpb1::hphNT1 YCplac111-rpb1::LEU</i>	Jentsch strain collection
MJK117	DF5 <i>rpb1::hphNT1 YCplac111-rpb1K330R::LEU</i>	Jentsch strain collection
MJK151	DF5 <i>rpb1::hphNT1 YCplac111-rpb1K217R::LEU</i>	Jentsch strain collection
MJK155	DF5 <i>rpb1::hphNT1 YCplac111-rpb1K1487R::LEU</i>	Jentsch strain collection
YIH607	DF5 <i>rpb1::hphNT1 YCplac111-rpb1K695R::LEU</i>	This study
YIH590	DF5 <i>Ylplac211-pADH-His-Smt3-tADH::URA3</i>	F. Paasch
YIH599	DF5 <i>slx5::natNT2 slx8::hphNT1 Ylplac211-pADH-His-Smt3-tADH::URA3</i>	This study
YIH677	DF5 <i>rad26::kanMX4</i>	This study
YIH475	DF5 <i>rpb9::natNT2</i>	This study
YIH363	DF5 <i>rad16::hphNT1</i>	This study
MJK619	DF5 <i>nup84::kanMX6</i>	M. Kern
YIH465	DF5 <i>mlp1::hphNT1 mlp2::natNT2</i>	This study
YIH543	DF5 <i>ctk1-6HA::kanMX4</i>	This study
YIH545	DF5 <i>ctk2-6HA::kanMX4</i>	This study
YIH547	DF5 <i>ctk3-6HA::kanMX4</i>	This study
YIH549	DF5 <i>bur1-6HA::kanMX4</i>	This study
YIH551	DF5 <i>bur2-6HA::kanMX4</i>	This study

S. cerevisiae Vectors

Name	Type	Reference
<i>YCplac111</i>	Integrative	¹⁸¹

***S. cerevisiae* Plasmids**

Name	Plasmid	Reference
pMJK44	<i>YCplac111rpb1</i>	M. Kern
pIH31	<i>YCplac111rpb1K695R::LEU</i>	This study
pMJK62	<i>YCplac111-rpb1K217R::LEU</i>	M. Kern
pMJK63	<i>YCplac111-rpb1K1487R::LEU</i>	M. Kern
pMJK46	<i>YCplac111rpb1K330R::LEU</i>	M. Kern

***S. cerevisiae* Media and Solutions**

YPD medium/plates:	1% yeast extract 2% bacto-peptone 2% glucose 2% agar (only for plates) sterilized by autoclaving
YPD G418/NAT/Hph Plates:	after autoclaving, YPD medium containing 2% agar was cooled to 50°C before addition of 200 mg/L G418 (geneticine disulfate; Sigma), 100 mg/L NAT (noursethricin, HKI Jena) or 500 mg/L Hph (hygromycin B, PAA Laboratories)
SC medium/plates:	0.67% yeast extract 0.2% amino acid drop-out mix 2% glucose 2% agar (only for plates) sterilized by autoclaving
Amino acid drop-out mix:	20 mg Ade, Ura, Trp, His 30 mg Arg, Tyr, Leu, Lys 50 mg Phe 100 mg Glu, Asp 150 mg Val 200 mg Thr 400 mg Ser
Sporulation medium:	2% (w/v) KAc sterilized by autoclaving

Materials and Methods

SORB Buffer:	100 mM LiOAc 10 mM Tris-HCl, pH 8.0 1 mM EDTA, pH 8.0 1 M sorbitol sterilized by filtration
PEG Solution:	100 mM LiOAc 10 mM Tris-HCl, pH 8.0 1 mM EDTA, pH 8.0 40% (w/v) PEG-3350 sterilized by filtration stored at 4 °C
Zymolyase 100T solution:	0.9 M sorbitol 0.1 M Tris-HCl, pH 8.0 0.2 M EDTA, pH 8.0 50 mM DTT 0.5 mg/ml Zymolyase 100T

Cultivation and storage of *S. cerevisiae* cells

Yeast cells were either cultivated on agar plates or in liquid cultures. For growth on agar plates cells were streaked from a glycerol stock using a sterile toothpick or a glass pipette. For a liquid culture 5-25 ml of YPD were inoculated with typically one single colony from a freshly streaked agar plate and grown overnight. The main culture was inoculated from the overnight culture to an OD₆₀₀ of 0.1-0.2 in baffled flasks (size ≥ 3x liquid culture volume). The cultures were grown to mid-log phase (OD₆₀₀ of 0.6-1) under constantly shaking on a shaking platform (150-200 rpm). The optical density was determined using a photometer, whereby OD₆₀₀ of 1 corresponds to approximately 1.5 x 10⁷ cells/ml. Cultures and plates were incubated at 30°C for growth.

Agar plates and overnight cultures of temperature-sensitive cells were incubated at the permissive temperature of 25°C. The main culture was grown at 30°C (semi-permissive temperature) to an OD₆₀₀ of 0.6-0.8 and switched to 37°C (non-permissive temperature) for at least 1 hour. Agar plates were sealed with parafilm for short-term storage (1-2 weeks) at 4°C. For long-term storage at -80°C, glycerol stocks were prepared by freezing cells from stationary phase (OD₆₀₀ ≥ 3) in 15% glycerol.

Preparation of competent *S. cerevisiae* cells

Cells from a mid-log phase culture (50 ml of OD₆₀₀ of 0.6-1) were harvested by centrifugation (5 min, 500 g) and washed once with 25 ml of cold sterile water and afterwards with 10 ml of cold SORB buffer. The pellet was resuspended in 360 μ l of SORB buffer and 40 μ l carrier DNA (denatured salmon or herring sperm DNA, 10 mg/ml Invitrogen). Aliquots of 55 μ l of competent cells were stored at -80°C.

Transformation of DNA into competent *S. cerevisiae* cells

For transformation, 0.2 μ g of a circular plasmid or 2 μ g of a linearized plasmid or PCR product were mixed with either 10 μ l or 50 μ l of competent yeast cells and incubated in 6 volumes of PEG buffer at room temperature. After 30 min, DMSO was added to a final concentration of 10% and the reaction was incubated at 42°C for 12 min (heat-shock). In case of temperature-sensitive strains the heat-shock was reduced to 8 min. Afterwards, the cells were centrifuged (2 min, 380 g) and resuspended in 100 μ l of sterile water and plated onto SC selection plates. In case of G418 (*kanMX6*), hygromycin (*hphNT1*) or nourseothricin (*natNT2*) resistance, the pellet was resuspended in 2 ml of YPD and incubated at 25°C for at least 1 hour while shaking before plating on SC selection plates. Plates were incubated at 25°C for 2-3 days and replica plated to eliminate false-positive colonies.

Genetic manipulation of *S. cerevisiae* cells

A PCR-based method was used to construct strains with epitope tagged genes or gene deletions^{182,183}. In Brief, a PCR product was generated using selection cassettes, which harbors either only a selection marker (deletion) or selection marker and epitope sequence and is flanked by genomic targeting sequences. After transformation into competent yeast cells, the PCR product was integrated into the genome by homologous recombination. Correct integration of the PCR product was analyzed by colony PCR (section 6.2.4). Epitope-tagged proteins were additionally tested by western blot analysis.

Mating type analysis of haploid yeast strains

The yeast tester strains RC634 (Mat a) and RC75-7 (Mat α), which are hypersensitive to the pheromone secreted by yeast of the opposite mating type, were used for mating type identification of haploid strains. Therefore, several colonies of a freshly streaked tester strain were resuspended in 2 ml sterile water and mixed with 100 ml of 1% agar (1% w/v water, pre-cooled to 50°C). Pre-warmed YPD plates were covered with 7 ml of the cell-agar suspension and allowed to dry. For analysis, strains were replica-plated or streaked on the tester plates and incubated at 30°C overnight. Growth of the tester strain is inhibited by a strain of the opposing mating type, which results in a free region around the streaked strain.

Mating, sporulation and tetrad analysis

One colony of freshly streaked yeast strains of the opposite mating type were resuspended in 100 μ l water and plated on pre-warmed YPD plates. After incubation overnight at 30°C, cells were analyzed for selection markers (if available) or for diploid cells. For sporulation, 300 μ l of an overnight culture of the selected diploid cells was washed three times with cold water and once with sporulation medium. The final pellet was resuspended in 3 ml of sporulation medium and grown at 25°C for at least 3 days in a culture tube while shaking. The sporulated diploid cells were incubated 1:1 with Zymolyase 100T solution for 8 min at room temperature. Tetrad dissection was performed with a micromanipulator (Singer MSM Systems) on YPD plates. After incubation for 2-4 days at 25°C, the mating type and genotype was analyzed by replica plating on mating tester and selection plates, respectively.

6.2 Molecular Biological Techniques

6.2.1 General Buffers and Solutions

TE buffer	10 mM Tris/HCl, pH 8.0 1 mM EDTA
TBE buffer (5x)	90 mM Tris 90 mM boric acid 2.5 mM EDTA, pH 8.0
DNA loading dye (6x)	0.5% SDS 0.25% (w/v) bromophenol blue 0.25% glycerol 25 mM EDTA, pH 8.0

6.2.2 Purification of DNA

Isolation of plasmid DNA from *E. coli*

A 5 ml LB overnight culture was used to isolate plasmid DNA using a commercial available kit (AccuPrep Plasmid Mini Extraction Kit, Bioneer). Purification was performed closely to the manufacturers instruction.

Isolation of genomic DNA from *S. cerevisiae*

Genomic DNA was isolated from an overnight culture or from colonies of a freshly streaked plate using a commercial available kit (Master Pure Yeast DNA Purification Kit, Epicentre). Purification was performed as described in the manufacturers instruction.

Determination of DNA concentration

DNA concentrations were determined photometrically using a NanoDrop ND-1000 spectrophotometer (PeqLab). Thereby, the absorbance was measured at a wavelength of 260nm. An OD₂₆₀ of 1 corresponds to a concentration of 50 µg/ml of double stranded DNA.

6.2.3 Molecular Cloning

Digestion of DNA with restriction enzymes

Restriction enzymes from New England Biolabs were used according to manufacturers instruction. Typically 2 μg of DNA was digested in a 30-40 μl reaction at 37°C for 2 hours or overnight. To avoid re-ligation of plasmid DNA the 5'-end was dephosphorylated by incubation of the reaction with 1 μl calf intestinal phosphatase (CIP, New England Biolabs) at 37°C for 1 hour.

Separation of DNA by agarose gel electrophoresis

Sample DNA was mixed with 6x loading dye and loaded on a 0.8% agarose gel, containing 0.5 $\mu\text{g}/\text{ml}$ ethidium bromide. Electroporesis was performed at 120 V in TBE buffer. DNA was visualized with a UV transilluminator (324 nm). The size was estimated by comparison with a 1 kb DNA ladder marker (Invitrogen).

Purification of DNA fragments from agarose gels

The band of interest was excised from the agarose gel using a sterile razor blade. The DNA was purified using a commercial available kit (QIAquick Gel Extraction Kit, Qiagen). Purification was performed as described in the manufacturers instruction.

Ligation of DNA fragments

The digested and dephosphorylated plasmid was incubated with the digested DNA insert together with T4 DNA ligase (New England Biolab) in a 20 μl reaction for 20 min at 25°C. The ration between plasmid and insert was 1:3 (Insert = (bp Insert / bp plasmid) x 300 ng). Afterwards the T4 DNA ligase was heat inactivated by incubation at 65°C for 10 min. Prior to transformation in electrocompetent *E. coli* cells, the reaction was dialyzed against deionized water on a nitrocellulose filter (pore size 0.05 μm , Millipore) for 10min.

DNA sequencing

DNA sequencing was performed by MWG Eurofins. A 17 μl reaction containing 15 μl purified DNA (50 ng/ μl plasmid DNA, 1-10 ng/ μl PCR product) together with 2 μl sequencing primer (10 μM) was send to Eurofins.

6.2.4 Polymerase Chain Reaction (PCR)

For amplification of DNA fragments from genomic DNA, targeting cassettes for gene deletion or epitope tagging or to test for genomic recombination events PCR was used. Oligonucleotides (primers) were designed and purchased from MWG Eurofins. Reactions were prepared on ice and carried out in a Veriti® Thermal Cycler (Thermo Fischer).

Amplification of genomic DNA fragments

The Phusion™ DNA polymerase was used for DNA fragment amplification from genomic DNA.

Reaction Mix	μ l	Thermocycler		
5x HF buffer	10	98°C	1 min	1x
dNTP Mix (10 mM each)	1	98°C	20 sec	
template gen. DNA (200ng/ μ l)	1	60°C	20 sec	25x
Primer1	3	72°C	40 sec/1kb	
Primer2	3	72°C	10 min	1x
H ₂ O	31.5	4°C	∞	1x
Phusion™ DNA Polymerase	0.5			

Amplification of targeting cassettes

For gene deletions the plasmids *pFA6a-natNT2*, *pFA6a-hphNT1* or *pFA6a-HIS3MX6* were used. According to the epitope tag different *pYM* plasmids were used as templates^{182,183}. The PCR product was analyzed by gel electrophoresis, purified from the agarose gel and further used for transformation in competent yeast cells.

Reaction Mix	μ l	Thermocycler		
10x Thermo Pol Buffer	10	95°C	5 min	1x
dNTP Mix (10 mM each)	3	95°C	30 sec	
cassette plasmid (100 μ g/ml)	1	54°C	30 sec	10x
Primer1	3	68°C	2 min 40 sec	
Primer2	3	95°C	30 sec	
H ₂ O	74.5	54°C	30 sec	20x
Vent DNA Polymerase	2.1	68°C	2 min 40 sec +	
Taq DNA Polymerase	2.4		20 s/cycle	
		68°C	5 min	1x
		4°C	∞	

PCR screening of genomic recombination events (Colony PCR)

To confirm whether a PCR product was integrated into the correct chromosomal location, a PCR based strategy was used. Therefore, one colony was resuspended in 20 μ l of 0.02 M NaOH, glass beads were added (425-600 nm, Sigma) and the mixture was boiled for 5 min at 99°C. From the supernatant 1.6 μ l were used as template for the PCR reaction.

Reaction Mix	μ l	Thermocycler		
10x Thermo Pol Buffer	2	94°C	5 min	1x
dNTP Mix (10 mM each)	0.7	94°C	30 sec	
template mixture	1.6	55°C	30 sec	30x
Primer1	1.3	72°C	1 min	
Primer2	1.3	72°C	5 min	1x
H ₂ O	12.9	4°C	∞	
Taq DNA Polymerase	0.2			

6.3 Biochemical Techniques

6.3.1 General Buffers and Solutions

PBS	10 mM phosphate, pH 7.4 137 mM NaCl 2.7 mM KCl
HU sample buffer	200 mM Tris, pH 6.8 8 M urea 5% (w/v) SDS 1 mM EDTA 1.5% (w/v) DTT 0.1% (w/v) bromophenol blue
2x Lämmli buffer	125 mM Tris/HCl, pH 6.8 4% SDS 20% glycerol 0.01% bromophenol blue 2.5% β -ME

MOPS running buffer	50 mM MOPS 50 mM Tris 3.5 mM SDS 1 mM EDTA
Blotting buffer	5% (v/v) 20x SWIFT™ Western buffer 10% (v/v) methanol
TBS-T	25 mM Tris/HCl pH 7.5 137 mM NaCl 2.6 mM KCl 0.1% Tween 20

6.3.2 Protein Methods

DNA damage treatment of yeast cells

DNA damage was induced by UV-C light or 4-nitroquinoline 1-oxide (4NQO) treatment. For UV light treatment cells were grown to mid-log phase (OD_{600} of 0.8-1) and 30-50 OD_{600} were harvested by centrifugation (5 min, 500 g) in a 50 ml Falcon tube. The pellet was washed once with 40 ml PBS buffer and the final pellet was resuspended in 40 ml PBS buffer. UV light irradiation was performed in 140-mm culture dishes with a dose of 400 J/m² (BS04-irradiation chamber, Dr. Gröbel UV-Elektronik GmbH) in the dark. The cell suspension was collected in a dark 50 ml Falcon tube and centrifuged 5 min at 500 g. For recovery from the UV light treatment the cell pellet was resuspended in 30 ml YPD and incubated for 4 h at 30°C or 37°C while shaking. Every hour a sample of 0.8 OD_{600} cells was harvested, pelleted, frozen in liquid nitrogen and stored at -80°C. For Rpb1 decay analysis the pellet was lysed by TCA-precipitation and analyzed by western blot.

For 4NQO treatment, cells were grown to mid-log phase (OD_{600} of 0.8-1) and 4NQO was added (10 μ g/ml in DMSO). For Rpb1 decay analysis samples were harvested and treated as described above.

Preparation of denatured protein extracts (TCA-precipitation)

Small-scale cell amounts were lysed under denaturing conditions. Usually pellets (0.8-1 OD₆₀₀) were incubated in 150 μ l of lysis buffer (1.85 M NaOH, 7.5% β -mercaptoethanol) for 15 min on ice. After addition of 150 μ l of 55% (w/v) trichloroacetic acid (TCA), the reaction was incubated a second time for 15 min on ice. The precipitated material was collected by sequential centrifugation (30 min/10 min, 18.000 g, 4°C). After removal of the supernatant, the pellet was resuspended in 40 μ l HU-buffer and analyzed by western blot.

Rpb1-Immunoprecipitation (Rpb1-IP)

For immunoprecipitation about 50 OD₆₀₀ cells were resuspended in 800 μ l lysis buffer (lysis buffer: 50 mM HEPES pH 7.5, 140 mM NaCl, 1 mM EDTA, 1% TritonX-100, 0.1% Na-Deoxycholate, 10 mM NEM, complete protease inhibitors) and lysed with a bead-beater (MM301, Retsch) using zirconia/silica beads (BioSpec Inc.). To shear the DNA and release protein bound to it, lysates were transferred to hard plastic Sumilon 15 ml centrifuge tubes (Sumitomo Bakelite Co.) by piggyback elution and the volume was adjusted to 1 ml with lysis buffer. Sonication (water/ice bath sonication: Bioruptor UCD-200, Diagenode) was performed with 10 times 30 sec cycles (with 30 sec breaks in between) and afterwards centrifuged at 18,000 g for 10 min. As an input sample 20 μ l of the supernatant were boiled (95°C, 5 min) in 2x Lämmli buffer. For Immunoprecipitation 500 μ l of the extract were incubated with 4 μ l of anti-Rpb1 antibodies (3E10) for 1.5 hour at 4°C on a rotation wheel followed by addition of 100 μ l equilibrated Protein A Sepharose CL-4B 50/50 slurry (GE Healthcare) for 30 min. The beads were washed 3-times with lysis buffer and boiled (95°C, 5 min) in 30 μ l 2x Lämmli buffer. Usually 10 μ l of the supernatant were analyzed by western blot.

Ni-NTA pulldown (Ni-PD)

Ni-NTA PDs under denaturing conditions were performed under modified conditions as previously described¹⁵⁷. 50OD₆₀₀ of UV light-treated and -untreated cells were harvested, washed with water, pelleted by centrifugation, frozen in liquid nitrogen, and stored for some days at -80°C.

The frozen pellet was resuspended in cold lysis buffer (lysis buffer: 1.85 M NaOH, 7.5% β -mercaptoethanol) to a final volume of 6 ml. After 15 min on ice, an equal volume of cold 55% TCA was added and kept on ice for another 15 min. Proteins were pelleted by centrifugation at 3500 g for 5 min (4°C), and the pellet was washed twice with cold water.

Subsequently, the pellet was thoroughly resuspended in 12 ml of Buffer A plus 0.05% Tween20 (Buffer A: 6 M guanidinium chloride, 100 mM NaH₂PO₄, 10 mM Tris; pH adjusted to pH 8.0 with NaOH). After transfer into centrifuge tubes, the suspensions were shaken for 1 hour at 180 rpm at room temperature for resolubilization. Insoluble material was removed by centrifugation (20 min, 4°C, 23.000 g), and the clear supernatant was transferred into a fresh tube. After adding imidazole to a final concentration of 20 mM, 200 μ l of Ni-NTA agarose slurry (Qiagen) was added to the tubes for the protein pull-down, and the sample was incubated on a rotating wheel at 4°C overnight. The material was then poured into a column, washed with 50 ml of Buffer A plus 0.05% Tween20, and subsequently with 50 ml of Buffer C plus 0.05% Tween20 (Buffer C: 8 M urea, 100 mM NaH₂PO₄, 10 mM Tris/HCl; pH adjusted to pH 6.3 with HCl). Proteins bound to the Ni-NTA column were eluted with 1 ml of elution buffer (elution buffer: Buffer C, 0.05% Tween20, 250 mM imidazole) into a 2 ml tube. Eluted proteins were precipitated by addition of 1 ml of 55% TCA, incubation for 10 min and centrifugation at 20.000 g for 30 min. The pellet was boiled in 30 μ l HU-Buffer for 10 min at 65°C. Samples were analyzed by western blot.

SDS-polyacrylamide gel electrophoresis (SDS-PAGE)

Proteins were separated using pre-cast 4-12% gradient NuPAGE Bis-Tris polyacrylamide gels (Invitrogen). Electrophoresis was performed in cold MOPS running buffer at 120 V for 10 min followed by 200 V for 1-1.5 hours under cooling conditions. Protein size was estimated by comparison with the Precision Plus Protein All Blue Standard (Bio-Rad) molecular weight marker.

Immuno-blot analysis (western blot)

Proteins separated by SDS-PAGE were transferred to a polyvinylidene fluoride membrane (Immobilion-P, Millipore). Therefore, the membrane was activated in 100% methanol for 1 min. The transfer was performed in cold SWIFT blotting buffer at 80 V for 2 hours at 4°C using a wet tank system (GE Healthcare). Afterwards, the membrane was blocked for 20 min with 5% skim milk powder dissolved in TBS-T. Incubation with the primary antibody (dissolved in TBS-T, 5% skim milk powder, 0.02% NaN₃) was performed overnight at 4°C. The membrane was washed 3 times with 10 ml TBS-T before incubated with HRP-coupled secondary antibody (dissolved in TBS-T, 5% skim milk powder) for 60 min. Unbound antibody was removed by 3 washing steps with 10 ml of TBS-T for 10 min. To detect the chemiluminescence signal the ECL, ECL-plus or ECL advanced kit (GE

Healthcare) was used. The membrane was incubated with the solutions as described by the manufacturers instruction and visualized by exposure to a chemiluminescence film (Amersham Hyperfilm ECL, GE Healthcare) or using a luminescent image analyzer (LAS-3000, Fujifilm).

For sequential usage of the membrane, antibodies were removed from the membrane by incubation with 10 ml of Restore™ PLUS western blot stripping buffer (Thermo Scientific) for 15 min. The membrane was washed with 10 ml TBS-T for 5 min, blocked and incubation with a primary antibody, as described above.

Primary Antibodies

Specificity	Type	Reference
anti-Rpb1 (3E10)	rat, monoclonal	Millipore
anti-Rpb1 (8WG16)	mouse, monoclonal	Abcam
anti-Rpb1 (4H8)	mouse, monoclonal	Cell Signaling
anti-SUMO	rabbit, polyclonal	¹⁶
anti-Ub (P4D1)	mouse, monoclonal	Santa Cruz Biotechnology
anti-Dpm1	mouse, monoclonal	Life Technologies
anti-Pgk1	mouse, monoclonal	Life Technologies
anti-Ctk1	rabbit, polyclonal	Abcam
anti-Bur1	rabbit, polyclonal	¹⁸⁴
anti-HA	mouse, monoclonal	Santa Cruz Biotechnology

Secondary Antibodies

Specificity	Type	Reference
anti-mouse	HRP-coupled IgG	Dianova
anti-rabbit	HRP-coupled IgG	Dianova
anti-rat	HRP-coupled IgG	Dianova

6.3.3 Chromatin Methods

Chromatin immunoprecipitation (ChIP)

ChIP was performed as described previously¹⁸⁵. Mid-log phase yeast cells were treated with or without UV light (100 J/m²) and allowed to repair for indicated time in the dark. Cells were cross-linked with 1% formaldehyde for 15 min and quenched with 125 mM glycylglycine for at least 10 min. Cells were pelleted (5 min, 5000 g, 4°C) and washed once with cold TBS. The pellet was frozen in liquid nitrogen and stored for some days at -80°C.

Cell lysis was performed in 800 μ l lysis buffer (lysis buffer: 50 mM HEPES, pH 7.5, 140 mM NaCl, 1 mM EDTA, 1% TritonX-100, 0.1% sodium deoxycholate, 1 mM PMSF, complete protease inhibitors) using zirconia/silica beads (BioSpec Inc.) in a multi-tube beat-beater (MM301, Retsch GmbH). The reaction was shaken 6 times for 3 min with a frequency of 30/s with 3 min cooling intervals. The supernatant was transferred to a hard plastic Sumilon 15 ml centrifuge tubes (Sumitomo Bakelite Co.) by piggyback elution and the volume was adjusted to 1 ml with lysis buffer. Sonication (water/ice bath sonication: Bioruptor UCD-200, Diagenode) was performed with 40 times 30 sec cycles (with 30 sec breaks in between) at an output of 200 W to shear the DNA to an average size of 250-500 bp. Beat beating and sonication was performed in the cold room (4°C). The solution was transferred into a 2 ml tube, adjusted to 2 ml with lysis buffer and centrifuged (14,000 g, 15 min). As an input sample 90 μ l of the supernatant was stored at -80°C. For immunoprecipitation 900 μ l of the supernatant were incubated either with 4 μ l anti-Rpb1 (8WG16, Abcam) antibody or with 2 μ l IgG2a (Bethyl Laboratories, Inc.) overnight with head-over-tail rotation at 4°C. Equilibrated Protein A Sepharose CL-4B 50/50 slurry (GE Healthcare) was added (100 μ l per sample) and incubated with head-over-tail rotation for 1 hour at 4°C. The beads were washed once with lysis buffer, wash buffer 1 (wash buffer 1: 50 mM HEPES, pH 7.5, 500 mM NaCl, 1 mM EDTA, 1% TritonX-100, 0.1% sodium deoxycholate, 1 mM PMSF), wash buffer 2 (wash buffer 2: 10 mM Tris/HCl, pH 8.0, 250 mM LiCl, 0.5% NP-50, 0.5% sodium deoxycholate, 1 mM EDTA) and TE (Tris/HCl, pH 8.0). The beads were resuspended in 100 μ l TE containing 20 μ g RNase A and incubated for 30 min at 37°C. After removal of the RNase A mixture from the beads, elution was performed with 500 μ l elution buffer (1% SDS, 0.1 M NaHCO₃) for 15 min with head-over-tail rotation at room temperature. The supernatant was transferred to a new 1.5 ml tube. The input samples were thawed and mixed with 410 μ l of elution buffer. To revert cross-links, 20 μ l of 5 M NaCl was added to IP and Input samples and incubated for at least 5 hours at 65°C. To precipitate the DNA, 1 ml of 99% ethanol was added to the samples

and incubated at -20°C overnight. The mixture was centrifuged (14.000 g, 15 min) and the pellet was washed once with 70% ethanol. The dry pellet was resuspended in 100 μ l TE buffer. Proteinase K digestion was performed for 30 min at 50°C. Input and ChIP samples were purified using the QIAquick PCR purification Kit (Qiagen). Samples were analyzed by RTq-PCR.

Quantitative real-time PCR (RTqPCR)

ChIP samples were analyzed by RT-qPCR using the 2x KAPA SYBR FAST qPCR Master Mix (PeqLab) and the LightCycler 480 System (Roche). Therefore, 2 μ l of the ChIP sample (undiluted) or input sample (1:10 diluted) were mixed with 18 μ l of Master Mix. For each sample triplicates in a 384-well LightCycler plate were tested. To determine the DNA concentration a dilution series for each primer pair was generated from the input sample (1:5, 1:50, 1:500, 1:5000) and used as a standard. DNA concentration was quantified from the LightCycler PCR amplification curves using the second derivate maximum. As a control for primer specificity a melting curve analysis was performed to determine whether only one PCR product was amplified.

For normalization the values for each strain and each time point were calculated by normalizing the ChIP-PCR signal with the IgG2a PCR signal and input PCR signal. All data in Figure 16 are depicted as the mean \pm SEM (standard error of the mean) of 3 independent ChIP experiments.

Reaction Mix	μ l	LightCycler		
2x KAPA SYBR FAST	10	95°C	3 min	1x
Primer1 (10 μ M)	0.4	95°C	10 sec	40x
Primer2 (10 μ M)	0.4	57°C	20 sec	
H ₂ O	7.2	72°C	1 sec	
ChIP sample	2	Melting curve analysis		
		4°C	∞	

Primers used for RTqPCR

Name	Sequence	Gene	Reference
IH_268 for	ATGTCAGACCTTGCAAACCTCAG	<i>RPB2</i>	¹²⁵
IH_269 rev	TTCGGTAGTATGTTGAGCCA	<i>RPB2</i>	¹²⁵
IH_270 for	TCAAGTCAAGCTTTATGGTCGT	<i>RPB2</i>	¹²⁵
IH_271 rev	AAGCATTTCCAGCATTTGCC	<i>RPB2</i>	¹²⁵
IH_274 for	CGTCGGTAGACCAAGACACC	<i>ACT1</i>	This study
IH_275 rev	TCCCAGTTGGTGACAATACCG	<i>ACT1</i>	This study

6.4 Computer-aided Analysis

For literature review the National Centre for Biotechnology Information (<http://www.ncbi.nlm.nih.gov>) and Papers3 (<http://www.papersapp.com>) were used. For sequence research the electronic database provided by the *Saccharomyces* Genome Database (www.yeastgenome.org) was used. The DNA-Star software (DNA Star Inc.) was used for DNA sequence analysis as well as for DNA restriction enzyme maps. The contrast for western blot images was adjusted linearly using Adobe Photoshop (Adobe Systems Inc.). Figures were designed and labeled using Adobe Power Point (Adobe Systems Inc.). ChIP data representation and statistics were done with GraphPad Prism (GraphPad Software, Inc.). The Microsoft Office software package (Microsoft Corp.) was used for text and table generation.

7 References

1. Hoeijmakers, J. H. Genome maintenance mechanisms for preventing cancer. *Nature* **411**, 366–374 (2001).
2. Edenberg, E. R., Downey, M. & Toczyski, D. Polymerase stalling during replication, transcription and translation. *Curr. Biol.* **24**, R445–52 (2014).
3. Vijg, J. & Suh, Y. Genome instability and aging. *Annu. Rev. Physiol.* **75**, 645–668 (2013).
4. Branzei, D. & Foiani, M. Maintaining genome stability at the replication fork. *Nat. Rev. Mol. Cell Biol.* **11**, 208–219 (2010).
5. Nospikel, T. & Hanawalt, P. C. DNA repair in terminally differentiated cells. *DNA Repair (Amst.)* **1**, 59–75 (2002).
6. Tercero, J. A., Longhese, M. P. & Diffley, J. F. X. A central role for DNA replication forks in checkpoint activation and response. *Mol. Cell* **11**, 1323–1336 (2003).
7. Alabert, C. & Groth, A. Chromatin replication and epigenome maintenance. *Nat. Rev. Mol. Cell Biol.* **13**, 153–167 (2012).
8. Azvolinsky, A., Giresi, P. G., Lieb, J. D. & Zakian, V. A. Highly transcribed RNA polymerase II genes are impediments to replication fork progression in *Saccharomyces cerevisiae*. *Mol. Cell* **34**, 722–734 (2009).
9. Blastyák, A. DNA replication: damage tolerance at the assembly line. *Trends Biochem. Sci.* **39**, 301–304 (2014).
10. Cobb, J. A., Bjergbaek, L., Shimada, K., Frei, C. & Gasser, S. M. DNA polymerase stabilization at stalled replication forks requires Mec1 and the RecQ helicase Sgs1. *EMBO J.* **22**, 4325–4336 (2003).
11. Lucca, C. *et al.* Checkpoint-mediated control of replisome-fork association and signalling in response to replication pausing. *Oncogene* **23**, 1206–1213 (2004).
12. Cobb, J. A. *et al.* Replisome instability, fork collapse, and gross chromosomal rearrangements arise synergistically from Mec1 kinase and RecQ helicase mutations. *Genes Dev.* **19**, 3055–3069 (2005).
13. Moldovan, G.-L., Pfander, B. & Jentsch, S. PCNA, the maestro of the replication fork. *Cell* **129**, 665–679 (2007).
14. Davies, A. A., Huttner, D., Daigaku, Y., Chen, S. & Ulrich, H. D. Activation of ubiquitin-dependent DNA damage bypass is mediated by replication protein a. *Mol. Cell* **29**, 625–636 (2008).
15. Bienko, M. *et al.* Ubiquitin-binding domains in Y-family polymerases regulate translesion synthesis. *Science* **310**, 1821–1824 (2005).
16. Hoege, C., Pfander, B., Moldovan, G.-L., Pyrowolakis, G. & Jentsch, S. RAD6-dependent DNA repair is linked to modification of PCNA by ubiquitin and SUMO. *Nature* **419**, 135–141 (2002).
17. Branzei, D. Ubiquitin family modifications and template switching. *FEBS Letters* **585**, 2810–2817 (2011).

References

18. Daraba, A., Gali, V. K., Halmai, M., Haracska, L. & Unk, I. Def1 promotes the degradation of Pol3 for polymerase exchange to occur during DNA-damage--induced mutagenesis in *Saccharomyces cerevisiae*. *PLoS Biol.* **12**, e1001771 (2014).
19. Brueckner, F., Hennecke, U., Carell, T. & Cramer, P. CPD damage recognition by transcribing RNA polymerase II. *Science* **315**, 859–862 (2007).
20. Derheimer, F. A. *et al.* RPA and ATR link transcriptional stress to p53. *PNAS* **104**, 12778–12783 (2007).
21. Livingstone-Zatchej, M., Meier, A., Suter, B. & Thoma, F. RNA polymerase II transcription inhibits DNA repair by photolyase in the transcribed strand of active yeast genes. *Nucleic Acids Res.* **25**, 3795–3800 (1997).
22. Marteijn, J. A., Lans, H., Vermeulen, W. & Hoeijmakers, J. H. J. Understanding nucleotide excision repair and its roles in cancer and ageing. *Nat. Rev. Mol. Cell Biol.* **15**, 465–481 (2014).
23. Spivak, G. Nucleotide excision repair in humans. *DNA Repair (Amst.)* **36**, 13–18 (2015).
24. Dupuy, A. & Sarasin, A. DNA damage and gene therapy of xeroderma pigmentosum, a human DNA repair-deficient disease. *Mutat. Res.* **776**, 2–8 (2015).
25. Vermeulen, W. & Fousteri, M. Mammalian transcription-coupled excision repair. *Cold Spring Harb Perspect Biol* **5**, a012625 (2013).
26. Theil, A. F., Hoeijmakers, J. H. J. & Vermeulen, W. TTDA: big impact of a small protein. *Experimental Cell Research* **329**, 61–68 (2014).
27. Min, J.-H. & Pavletich, N. P. Recognition of DNA damage by the Rad4 nucleotide excision repair protein. *Nature* **449**, 570–575 (2007).
28. Fei, J. *et al.* Regulation of nucleotide excision repair by UV-DDB: prioritization of damage recognition to internucleosomal DNA. *PLoS Biol.* **9**, e1001183 (2011).
29. Oksenyich, V., Bernardes de Jesus, B., Zhovmer, A., Egly, J. M. & Coin, F. Molecular insights into the recruitment of TFIIH to sites of DNA damage. *EMBO J.* **28**, 2971–2980 (2009).
30. Compe, E. & Egly, J. M. TFIIH: when transcription met DNA repair. *Nat. Rev. Mol. Cell Biol.* **13**, 343–354 (2012).
31. Fagbemi, A. F., Orelli, B. & Schärer, O. D. Regulation of endonuclease activity in human nucleotide excision repair. *DNA Repair (Amst.)* **10**, 722–729 (2011).
32. Moser, J. *et al.* Sealing of chromosomal DNA nicks during nucleotide excision repair requires XRCC1 and DNA ligase III alpha in a cell-cycle-specific manner. *Mol. Cell* **27**, 311–323 (2007).
33. Ogi, T. *et al.* Three DNA polymerases, recruited by different mechanisms, carry out NER repair synthesis in human cells. *Mol. Cell* **37**, 714–727 (2010).
34. Fousteri, M., Vermeulen, W., van Zeeland, A. A. & Mullenders, L. H. F. Cockayne syndrome A and B proteins differentially regulate recruitment of chromatin remodeling and repair factors to stalled RNA polymerase II in vivo. *Mol. Cell* **23**, 471–482 (2006).

References

35. Schwertman, P. *et al.* UV-sensitive syndrome protein UVSSA recruits USP7 to regulate transcription-coupled repair. *Nat. Genet.* **44**, 598–602 (2012).
36. van Gool, A. J. *et al.* RAD26, the functional *S. cerevisiae* homolog of the Cockayne syndrome B gene ERCC6. *EMBO J.* **13**, 5361–5369 (1994).
37. Li, S., Chen, X., Ruggiero, C., Ding, B. & Smerdon, M. J. Modulation of Rad26- and Rpb9-mediated DNA repair by different promoter elements. *J. Biol. Chem.* **281**, 36643–36651 (2006).
38. Li, S. Transcription coupled nucleotide excision repair in the yeast *Saccharomyces cerevisiae*: The ambiguous role of Rad26. *DNA Repair (Amst.)* **36**, 43–48 (2015).
39. Li, S. & Smerdon, M. J. Rpb4 and Rpb9 mediate subpathways of transcription-coupled DNA repair in *Saccharomyces cerevisiae*. *EMBO J.* **21**, 5921–5929 (2002).
40. Van Den Boom, V. *et al.* DNA damage stabilizes interaction of CSB with the transcription elongation machinery. *J Cell Biol* **166**, 27–36 (2004).
41. Malik, S. *et al.* Rad26p, a transcription-coupled repair factor, is recruited to the site of DNA lesion in an elongating RNA polymerase II-dependent manner in vivo. *Nucleic Acids Res.* **38**, 1461–1477 (2010).
42. Taschner, M. *et al.* A role for checkpoint kinase-dependent Rad26 phosphorylation in transcription-coupled DNA repair in *Saccharomyces cerevisiae*. *Mol. Cell. Biol.* **30**, 436–446 (2010).
43. Tornaletti, S., Reines, D. & Hanawalt, P. C. Structural Characterization of RNA Polymerase II Complexes Arrested by a Cyclobutane Pyrimidine Dimer in the Transcribed Strand of Template DNA. *J. Biol. Chem.* **274**, 24124–24130 (1999).
44. Hara, R., Selby, C. P., Liu, M., Price, D. H. & Sancar, A. Human transcription release factor 2 dissociates RNA polymerases I and II stalled at a cyclobutane thymine dimer. *J. Biol. Chem.* **274**, 24779–24786 (1999).
45. Tremblay, M. *et al.* UV light-induced DNA lesions cause dissociation of yeast RNA polymerases-I and establishment of a specialized chromatin structure at rRNA genes. *Nucleic Acids Res.* **42**, 380–395 (2014).
46. Sigurdsson, S., Dirac-Svejstrup, A. B. & Svejstrup, J. Q. Evidence that Transcript Cleavage Is Essential for RNA Polymerase II Transcription and Cell Viability. *Mol. Cell* **38**, 202–210 (2010).
47. Cheung, A. C. M. & Cramer, P. Structural basis of RNA polymerase II backtracking, arrest and reactivation. *Nature* **471**, 249–253 (2011).
48. Epshtein, V. *et al.* UvrD facilitates DNA repair by pulling RNA polymerase backwards. *Nature* **505**, 372–377 (2014).
49. Donahue, B. A., Yin, S., Taylor, J. S., Reines, D. & Hanawalt, P. C. Transcript cleavage by RNA polymerase II arrested by a cyclobutane pyrimidine dimer in the DNA template. *PNAS* **91**, 8502–8506 (1994).
50. Citterio, E. *et al.* ATP-dependent chromatin remodeling by the Cockayne syndrome B DNA repair-transcription-coupling factor. *Mol. Cell. Biol.* **20**, 7643–7653 (2000).

References

51. Beerens, N., Hoeijmakers, J. H. J., Kanaar, R., Vermeulen, W. & Wyman, C. The CSB protein actively wraps DNA. *J. Biol. Chem.* **280**, 4722–4729 (2005).
52. Wilson, M. D., Harreman, M. & Svejstrup, J. Q. Ubiquitylation and degradation of elongating RNA polymerase II: the last resort. *Biochim. Biophys. Acta* **1829**, 151–157 (2013).
53. Malik, S., Bagla, S., Chaurasia, P., Duan, Z. & Bhaumik, S. R. Elongating RNA polymerase II is disassembled through specific degradation of its largest but not other subunits in response to DNA damage in vivo. *J. Biol. Chem.* **283**, 6897–6905 (2008).
54. Neil, H. *et al.* Widespread bidirectional promoters are the major source of cryptic transcripts in yeast. *Nature* **457**, 1038–1042 (2009).
55. van Dijk, E. L. *et al.* XUTs are a class of Xrn1-sensitive antisense regulatory non-coding RNA in yeast. *Nature* **475**, 114–117 (2011).
56. Tudek, A., Candelli, T. & Libri, D. Non-coding transcription by RNA polymerase II in yeast: Hasard or nécessité? *Biochimie* **117**, 28–36 (2015).
57. Hirose, Y. & Ohkuma, Y. Phosphorylation of the C-terminal domain of RNA polymerase II plays central roles in the integrated events of eucaryotic gene expression. *J. Biochem.* **141**, 601–608 (2007).
58. Eick, D. & Geyer, M. The RNA polymerase II carboxy-terminal domain (CTD) code. *Chem. Rev.* **113**, 8456–8490 (2013).
59. Srivastava, R. & Ahn, S. H. Modifications of RNA polymerase II CTD: Connections to the histone code and cellular function. *Biotechnol. Adv.* **33**, 856–872 (2015).
60. Schüller, R. *et al.* Heptad-Specific Phosphorylation of RNA Polymerase II CTD. *Mol. Cell* **61**, 305–314 (2016).
61. Suh, H. *et al.* Direct Analysis of Phosphorylation Sites on the Rpb1 C-Terminal Domain of RNA Polymerase II. *Mol. Cell* **61**, 297–304 (2016).
62. Hengartner, C. J. *et al.* Temporal regulation of RNA polymerase II by Srb10 and Kin28 cyclin-dependent kinases. *Mol. Cell* **2**, 43–53 (1998).
63. Bowman, E. A. & Kelly, W. G. RNA polymerase II transcription elongation and Pol II CTD Ser2 phosphorylation: A tail of two kinases. *Nucleus* **5**, 224–236 (2014).
64. Belakavadi, M. & Fondell, J. D. Cyclin-dependent kinase 8 positively cooperates with Mediator to promote thyroid hormone receptor-dependent transcriptional activation. *Mol. Cell. Biol.* **30**, 2437–2448 (2010).
65. Krishnamurthy, S., He, X., Reyes-Reyes, M., Moore, C. & Hampsey, M. Ssu72 Is an RNA polymerase II CTD phosphatase. *Mol. Cell* **14**, 387–394 (2004).
66. Mosley, A. L. *et al.* Rtr1 is a CTD phosphatase that regulates RNA polymerase II during the transition from serine 5 to serine 2 phosphorylation. *Mol. Cell* **34**, 168–178 (2009).
67. Cho, E. J., Kobor, M. S., Kim, M., Greenblatt, J. & Buratowski, S. Opposing effects of Ctk1 kinase and Fcp1 phosphatase at Ser 2 of the RNA polymerase II C-terminal domain. *Genes Dev.* **15**, 3319–3329 (2001).
68. Archambault, J. *et al.* An essential component of a C-terminal domain phosphatase that interacts with transcription factor IIF in *Saccharomyces cerevisiae*. *PNAS* **94**, 14300–14305 (1997).

References

69. Hsin, J.-P., Xiang, K. & Manley, J. L. Function and control of RNA polymerase II C-terminal domain phosphorylation in vertebrate transcription and RNA processing. *Mol. Cell. Biol.* **34**, 2488–2498 (2014).
70. Li, H. *et al.* Wwp2-mediated ubiquitination of the RNA polymerase II large subunit in mouse embryonic pluripotent stem cells. *Mol. Cell. Biol.* **27**, 5296–5305 (2007).
71. Daulny, A. *et al.* Modulation of RNA polymerase II subunit composition by ubiquitylation. *Proc. Natl. Acad. Sci. U.S.A.* **105**, 19649–19654 (2008).
72. Chen, X., Ding, B., LeJeune, D., Ruggiero, C. & Li, S. Rpb1 sumoylation in response to UV radiation or transcriptional impairment in yeast. *PLoS ONE* **4**, e5267 (2009).
73. Kerscher, O., Felberbaum, R. & Hochstrasser, M. Modification of proteins by ubiquitin and ubiquitin-like proteins. *Annu. Rev. Cell Dev. Biol.* **22**, 159–180 (2006).
74. Gareau, J. R. & Lima, C. D. The SUMO pathway: emerging mechanisms that shape specificity, conjugation and recognition. *Nat. Rev. Mol. Cell Biol.* **11**, 861–871 (2010).
75. Geiss-Friedlander, R. & Melchior, F. Concepts in sumoylation: a decade on. *Nat. Rev. Mol. Cell Biol.* **8**, 947–956 (2007).
76. Finley, D., Ulrich, H. D., Sommer, T. & Kaiser, P. The ubiquitin-proteasome system of *Saccharomyces cerevisiae*. *Genetics* **192**, 319–360 (2012).
77. Jentsch, S. & Psakhye, I. Control of nuclear activities by substrate-selective and protein-group SUMOylation. *Annu. Rev. Genet.* **47**, 167–186 (2013).
78. Psakhye, I. & Jentsch, S. Protein group modification and synergy in the SUMO pathway as exemplified in DNA repair. *Cell* **151**, 807–820 (2012).
79. Hickey, C. M., Wilson, N. R. & Hochstrasser, M. Function and regulation of SUMO proteases. *Nat. Rev. Mol. Cell Biol.* **13**, 755–766 (2012).
80. Kulathu, Y. & Komander, D. Atypical ubiquitylation - the unexplored world of polyubiquitin beyond Lys48 and Lys63 linkages. *Nat. Rev. Mol. Cell Biol.* **13**, 508–523 (2012).
81. Richly, H. *et al.* A series of ubiquitin binding factors connects CDC48/p97 to substrate multiubiquitylation and proteasomal targeting. *Cell* **120**, 73–84 (2005).
82. Dikic, I., Wakatsuki, S. & Walters, K. J. Ubiquitin-binding domains - from structures to functions. *Nat. Rev. Mol. Cell Biol.* **10**, 659–671 (2009).
83. Husnjak, K. & Dikic, I. Ubiquitin-binding proteins: decoders of ubiquitin-mediated cellular functions. *Annu. Rev. Biochem.* **81**, 291–322 (2012).
84. Ulrich, H. D. The fast-growing business of SUMO chains. *Mol. Cell* **32**, 301–305 (2008).
85. Srikumar, T. *et al.* Global analysis of SUMO chain function reveals multiple roles in chromatin regulation. *J Cell Biol* **201**, 145–163 (2013).
86. Kerscher, O. SUMO junction-what's your function? New insights through SUMO-interacting motifs. *EMBO reports* **8**, 550–555 (2007).
87. Matyskiela, M. E. & Martin, A. Design principles of a universal protein degradation machine. *J. Mol. Biol.* **425**, 199–213 (2013).

References

88. Verma, R., Oania, R., Graumann, J. & Deshaies, R. J. Multiubiquitin chain receptors define a layer of substrate selectivity in the ubiquitin-proteasome system. *Cell* **118**, 99–110 (2004).
89. Thrower, J. S., Hoffman, L., Rechsteiner, M. & Pickart, C. M. Recognition of the polyubiquitin proteolytic signal. *EMBO J.* **19**, 94–102 (2000).
90. Xu, P. *et al.* Quantitative proteomics reveals the function of unconventional ubiquitin chains in proteasomal degradation. *Cell* **137**, 133–145 (2009).
91. Saeki, Y. *et al.* Lysine 63-linked polyubiquitin chain may serve as a targeting signal for the 26S proteasome. *EMBO J.* **28**, 359–371 (2009).
92. Komander, D. & Rape, M. The ubiquitin code. *Annu. Rev. Biochem.* **81**, 203–229 (2012).
93. Mukhopadhyay, D. & Riezman, H. Proteasome-independent functions of ubiquitin in endocytosis and signaling. *Science* **315**, 201–205 (2007).
94. Chen, Z. J. & Sun, L. J. Nonproteolytic functions of ubiquitin in cell signaling. *Mol. Cell* **33**, 275–286 (2009).
95. Braun, S. & Madhani, H. D. Shaping the landscape: mechanistic consequences of ubiquitin modification of chromatin. *EMBO reports* **13**, 619–630 (2012).
96. Geng, F., Wenzel, S. & Tansey, W. P. Ubiquitin and proteasomes in transcription. *Annu. Rev. Biochem.* **81**, 177–201 (2012).
97. Bergink, S. & Jentsch, S. Principles of ubiquitin and SUMO modifications in DNA repair. *Nature* **458**, 461–467 (2009).
98. Rosonina, E., Duncan, S. M. & Manley, J. L. SUMO functions in constitutive transcription and during activation of inducible genes in yeast. *Genes Dev.* **24**, 1242–1252 (2010).
99. Zhao, J. Sumoylation regulates diverse biological processes. *Cell. Mol. Life Sci.* **64**, 3017–3033 (2007).
100. Hendriks, I. A. *et al.* Uncovering global SUMOylation signaling networks in a site-specific manner. *Nat Struct Mol Biol* **21**, 927–936 (2014).
101. Sriramachandran, A. M. & Dohmen, R. J. SUMO-targeted ubiquitin ligases. *Biochim. Biophys. Acta* **1843**, 75–85 (2014).
102. Mitsui, A. & Sharp, P. A. Ubiquitination of RNA polymerase II large subunit signaled by phosphorylation of carboxyl-terminal domain. *PNAS* **96**, 6054–6059 (1999).
103. Huibregtse, J. M., Yang, J. C. & Beaudenon, S. L. The large subunit of RNA polymerase II is a substrate of the Rsp5 ubiquitin-protein ligase. *PNAS* **94**, 3656–3661 (1997).
104. Chang, A., Cheang, S., Espanel, X. & Sudol, M. Rsp5 WW domains interact directly with the carboxyl-terminal domain of RNA polymerase II. *J. Biol. Chem.* **275**, 20562–20571 (2000).
105. Beaudenon, S. L., Huacani, M. R., Wang, G., McDonnell, D. P. & Huibregtse, J. M. Rsp5 ubiquitin-protein ligase mediates DNA damage-induced degradation of the large subunit of RNA polymerase II in *Saccharomyces cerevisiae*. *Mol. Cell. Biol.* **19**, 6972–6979 (1999).

References

106. Wang, G., Yang, J. & Huibregtse, J. M. Functional domains of the Rsp5 ubiquitin-protein ligase. *Mol. Cell. Biol.* **19**, 342–352 (1999).
107. Harreman, M. *et al.* Distinct ubiquitin ligases act sequentially for RNA polymerase II polyubiquitylation. *Proc. Natl. Acad. Sci. U.S.A.* **106**, 20705–20710 (2009).
108. Kee, Y., Lyon, N. & Huibregtse, J. M. The Rsp5 ubiquitin ligase is coupled to and antagonized by the Ubp2 deubiquitinating enzyme. *EMBO J.* **24**, 2414–2424 (2005).
109. Kee, Y., Muñoz, W., Lyon, N. & Huibregtse, J. M. The deubiquitinating enzyme Ubp2 modulates Rsp5-dependent Lys63-linked polyubiquitin conjugates in *Saccharomyces cerevisiae*. *J. Biol. Chem.* **281**, 36724–36731 (2006).
110. Ribar, B., Prakash, L. & Prakash, S. Requirement of ELC1 for RNA polymerase II polyubiquitylation and degradation in response to DNA damage in *Saccharomyces cerevisiae*. *Mol. Cell. Biol.* **26**, 3999–4005 (2006).
111. Ribar, B., Prakash, L. & Prakash, S. ELA1 and CUL3 are required along with ELC1 for RNA polymerase II polyubiquitylation and degradation in DNA-damaged yeast cells. *Mol. Cell. Biol.* **27**, 3211–3216 (2007).
112. Somesh, B. P. *et al.* Communication between distant sites in RNA polymerase II through ubiquitylation factors and the polymerase CTD. *Cell* **129**, 57–68 (2007).
113. Cramer, P., Bushnell, D. A. & Kornberg, R. D. Structural basis of transcription: RNA polymerase II at 2.8 angstrom resolution. *Science* **292**, 1863–1876 (2001).
114. Kvint, K. *et al.* Reversal of RNA polymerase II ubiquitylation by the ubiquitin protease Ubp3. *Mol. Cell* **30**, 498–506 (2008).
115. Verma, R., Oania, R., Fang, R., Smith, G. T. & Deshaies, R. J. Cdc48/p97 mediates UV-dependent turnover of RNA Pol II. *Mol. Cell* **41**, 82–92 (2011).
116. Gillette, T. G., Gonzalez, F., Delahodde, A., Johnston, S. A. & Kodadek, T. Physical and functional association of RNA polymerase II and the proteasome. *Proc. Natl. Acad. Sci. U.S.A.* **101**, 5904–5909 (2004).
117. Lafon, A. *et al.* INO80 Chromatin Remodeler Facilitates Release of RNA Polymerase II from Chromatin for Ubiquitin-Mediated Proteasomal Degradation. *Mol. Cell* **60**, 784–796 (2015).
118. Anindya, R., Aygün, O. & Svejstrup, J. Q. Damage-induced ubiquitylation of human RNA polymerase II by the ubiquitin ligase Nedd4, but not Cockayne syndrome proteins or BRCA1. *Mol. Cell* **28**, 386–397 (2007).
119. Yasukawa, T. *et al.* Mammalian Elongin A complex mediates DNA-damage-induced ubiquitylation and degradation of Rpb1. *EMBO J.* **27**, 3256–3266 (2008).
120. Somesh, B. P. *et al.* Multiple mechanisms confining RNA polymerase II ubiquitylation to polymerases undergoing transcriptional arrest. *Cell* **121**, 913–923 (2005).
121. Woudstra, E. C. *et al.* A Rad26-Def1 complex coordinates repair and RNA pol II proteolysis in response to DNA damage. *Nature* **415**, 929–933 (2002).
122. Groisman, R. *et al.* CSA-dependent degradation of CSB by the ubiquitin-proteasome pathway establishes a link between complementation factors of the Cockayne syndrome. *Genes Dev.* **20**, 1429–1434 (2006).

References

123. Rockx, D. A. *et al.* UV-induced inhibition of transcription involves repression of transcription initiation and phosphorylation of RNA polymerase II. *PNAS* **97**, 10503–10508 (2000).
124. Wilson, M. D. *et al.* Proteasome-mediated processing of Def1, a critical step in the cellular response to transcription stress. *Cell* **154**, 983–995 (2013).
125. Ghosh-Roy, S. *et al.* Rad26, the transcription-coupled repair factor in yeast, is required for removal of stalled RNA polymerase-II following UV irradiation. *PLoS ONE* **8**, e72090 (2013).
126. He, J., Zhu, Q., Wani, G., Sharma, N. & Wani, A. A. Valosin-containing Protein (VCP)/p97 Segregase Mediates Proteolytic Processing of Cockayne Syndrome Group B (CSB) in Damaged Chromatin. *J. Biol. Chem.* **291**, 7396–7408 (2016).
127. Praefcke, G. J. K., Hofmann, K. & Dohmen, R. J. SUMO playing tag with ubiquitin. *Trends Biochem. Sci.* **37**, 23–31 (2012).
128. Ozkan, E., Yu, H. & Deisenhofer, J. Mechanistic insight into the allosteric activation of a ubiquitin-conjugating enzyme by RING-type ubiquitin ligases. *PNAS* **102**, 18890–18895 (2005).
129. Uzunova, K. *et al.* Ubiquitin-dependent proteolytic control of SUMO conjugates. *J. Biol. Chem.* **282**, 34167–34175 (2007).
130. Zhang, Z. & Buchman, A. R. Identification of a member of a DNA-dependent ATPase family that causes interference with silencing. *Mol. Cell. Biol.* **17**, 5461–5472 (1997).
131. Hannich, J. T. *et al.* Defining the SUMO-modified proteome by multiple approaches in *Saccharomyces cerevisiae*. *J. Biol. Chem.* **280**, 4102–4110 (2005).
132. Cal-Bąkowska, M., Litwin, I., Bocer, T., Wysocki, R. & Dziadkowiec, D. The Swi2-Snf2-like protein Uls1 is involved in replication stress response. *Nucleic Acids Res.* **39**, 8765–8777 (2011).
133. Lescasse, R., Pobiega, S., Callebaut, I. & Marcand, S. End-joining inhibition at telomeres requires the translocase and polySUMO-dependent ubiquitin ligase Uls1. *EMBO J.* **32**, 805–815 (2013).
134. Schweiggert, J., Stevermann, L., Panigada, D., Kammerer, D. & Liakopoulos, D. Regulation of a Spindle Positioning Factor at Kinetochores by SUMO-Targeted Ubiquitin Ligases. *Dev. Cell* **36**, 415–427 (2016).
135. Xie, Y. *et al.* The yeast Hex3.Slx8 heterodimer is a ubiquitin ligase stimulated by substrate sumoylation. *J. Biol. Chem.* **282**, 34176–34184 (2007).
136. Xie, Y., Rubenstein, E. M., Matt, T. & Hochstrasser, M. SUMO-independent in vivo activity of a SUMO-targeted ubiquitin ligase toward a short-lived transcription factor. *Genes Dev.* **24**, 893–903 (2010).
137. Nagai, S. *et al.* Functional targeting of DNA damage to a nuclear pore-associated SUMO-dependent ubiquitin ligase. *Science* **322**, 597–602 (2008).
138. Horigome, C. *et al.* PolySUMOylation by Siz2 and Mms21 triggers relocation of DNA breaks to nuclear pores through the Slx5/Slx8 STUbL. *Genes Dev.* **30**, 931–945 (2016).

References

139. Sun, H., Leverson, J. D. & Hunter, T. Conserved function of RNF4 family proteins in eukaryotes: targeting a ubiquitin ligase to SUMOylated proteins. *EMBO J.* **26**, 4102–4112 (2007).
140. Bruderer, R. *et al.* Purification and identification of endogenous polySUMO conjugates. *EMBO reports* **12**, 142–148 (2011).
141. Yin, Y. *et al.* SUMO-targeted ubiquitin E3 ligase RNF4 is required for the response of human cells to DNA damage. *Genes Dev.* **26**, 1196–1208 (2012).
142. Lallemand-Breitenbach, V. *et al.* Arsenic degrades PML or PML-RARalpha through a SUMO-triggered RNF4/ubiquitin-mediated pathway. *Nat. Cell Biol.* **10**, 547–555 (2008).
143. Tatham, M. H. *et al.* RNF4 is a poly-SUMO-specific E3 ubiquitin ligase required for arsenic-induced PML degradation. *Nat. Cell Biol.* **10**, 538–546 (2008).
144. Wang, Q.-E. *et al.* DNA repair factor XPC is modified by SUMO-1 and ubiquitin following UV irradiation. *Nucleic Acids Res.* **33**, 4023–4034 (2005).
145. Wang, Q.-E. *et al.* Ubiquitylation-independent degradation of Xeroderma pigmentosum group C protein is required for efficient nucleotide excision repair. *Nucleic Acids Res.* **35**, 5338–5350 (2007).
146. Rütthemann, P., Balbo Pogliano, C. & Naegeli, H. Global-genome Nucleotide Excision Repair Controlled by Ubiquitin/Sumo Modifiers. *Front. Genet.* **7**, 68 (2016).
147. He, J. *et al.* Ubiquitin-specific protease 7 regulates nucleotide excision repair through deubiquitinating XPC protein and preventing XPC protein from undergoing ultraviolet light-induced and VCP/p97 protein-regulated proteolysis. *J. Biol. Chem.* **289**, 27278–27289 (2014).
148. Puumalainen, M.-R., Rütthemann, P., Min, J.-H. & Naegeli, H. Xeroderma pigmentosum group C sensor: unprecedented recognition strategy and tight spatiotemporal regulation. *Cell. Mol. Life Sci.* **73**, 547–566 (2016).
149. Parker, J. L. & Ulrich, H. D. A SUMO-interacting motif activates budding yeast ubiquitin ligase Rad18 towards SUMO-modified PCNA. *Nucleic Acids Res.* **40**, 11380–11388 (2012).
150. Jentsch, S. & Rumpf, S. Cdc48 (p97): a ‘molecular gearbox’ in the ubiquitin pathway? *Trends Biochem. Sci.* **32**, 6–11 (2007).
151. Pye, V. E. *et al.* Going through the motions: the ATPase cycle of p97. *J. Struct. Biol.* **156**, 12–28 (2006).
152. Stolz, A., Hilt, W., Buchberger, A. & Wolf, D. H. Cdc48: a power machine in protein degradation. *Trends Biochem. Sci.* **36**, 515–523 (2011).
153. Nie, M. *et al.* Dual recruitment of Cdc48 (p97)-Ufd1-Npl4 ubiquitin-selective segregase by small ubiquitin-like modifier protein (SUMO) and ubiquitin in SUMO-targeted ubiquitin ligase-mediated genome stability functions. *J. Biol. Chem.* **287**, 29610–29619 (2012).
154. Bergink, S. *et al.* Role of Cdc48/p97 as a SUMO-targeted segregase curbing Rad51-Rad52 interaction. *Nat. Cell Biol.* **15**, 526–532 (2013).

References

155. Ikenaga, M., Takebe, H. & Ishii, Y. Excision repair of DNA base damage in human cells treated with the chemical carcinogen 4-nitroquinoline 1-oxide. *Mutat. Res.* **43**, 415–427 (1977).
156. Hoppe, T. *et al.* Activation of a Membrane-Bound Transcription Factor by Regulated Ubiquitin/Proteasome-Dependent Processing. *Cell* **102**, 577–586 (2000).
157. Sacher, M., Pfander, B. & Jentsch, S. Identification of SUMO-protein conjugates. *Meth. Enzymol.* **399**, 392–404 (2005).
158. Texari, L. *et al.* The nuclear pore regulates GAL1 gene transcription by controlling the localization of the SUMO protease Ulp1. *Mol. Cell* **51**, 807–818 (2013).
159. Jeong, S.-J. *et al.* Role of RNA polymerase II carboxy terminal domain phosphorylation in DNA damage response. *J. Microbiol.* **43**, 516–522 (2005).
160. Silver, H. R., Nissley, J. A., Reed, S. H., Hou, Y.-M. & Johnson, E. S. A role for SUMO in nucleotide excision repair. *DNA Repair (Amst.)* **10**, 1243–1251 (2011).
161. Guintini, L., Charton, R., Peyresaubes, F., Thoma, F. & Conconi, A. Nucleosome positioning, nucleotide excision repair and photoreactivation in *Saccharomyces cerevisiae*. *DNA Repair (Amst.)* **36**, 98–104 (2015).
162. Mullen, J. R. & Brill, S. J. Activation of the Slx5-Slx8 ubiquitin ligase by poly-small ubiquitin-like modifier conjugates. *J. Biol. Chem.* **283**, 19912–19921 (2008).
163. Kalocsay, M., Hiller, N. J. & Jentsch, S. Chromosome-wide Rad51 spreading and SUMO-H2A.Z-dependent chromosome fixation in response to a persistent DNA double-strand break. *Mol. Cell* **33**, 335–343 (2009).
164. Cook, C. E., Hochstrasser, M. & Kerscher, O. The SUMO-targeted ubiquitin ligase subunit Slx5 resides in nuclear foci and at sites of DNA breaks. *Cell Cycle* **8**, 1080–1089 (2009).
165. Su, X. A., Dion, V., Gasser, S. M. & Freudenreich, C. H. Regulation of recombination at yeast nuclear pores controls repair and triplet repeat stability. *Genes Dev.* **29**, 1006–1017 (2015).
166. Zhao, X., Wu, C.-Y. & Blobel, G. Mlp-dependent anchorage and stabilization of a desumoylating enzyme is required to prevent clonal lethality. *J Cell Biol* **167**, 605–611 (2004).
167. Dieppois, G. & Stutz, F. Connecting the transcription site to the nuclear pore: a multi-tether process that regulates gene expression. *J Cell Sci* **123**, 1989–1999 (2010).
168. Texari, L. & Stutz, F. Sumoylation and transcription regulation at nuclear pores. *Chromosoma* **124**, 45–56 (2015).
169. Fang, N. N. *et al.* Rsp5/Nedd4 is the main ubiquitin ligase that targets cytosolic misfolded proteins following heat stress. *Nat. Cell Biol.* **16**, 1227–1237 (2014).
170. Wu, X., Chang, A., Sudol, M. & Hanes, S. D. Genetic interactions between the ESS1 prolyl-isomerase and the RSP5 ubiquitin ligase reveal opposing effects on RNA polymerase II function. *Curr. Genet.* **40**, 234–242 (2001).
171. Boeing, S. *et al.* Multiomic Analysis of the UV-Induced DNA Damage Response. *Cell Rep* **15**, 1597–1610 (2016).

References

172. Bucheli, M. & Sweder, K. In UV-irradiated *Saccharomyces cerevisiae*, overexpression of Swi2/Snf2 family member Rad26 increases transcription-coupled repair and repair of the non-transcribed strand. *Mol. Microbiol.* **52**, 1653–1663 (2004).
173. Tijsterman, M. & Brouwer, J. Rad26, the yeast homolog of the cockayne syndrome B gene product, counteracts inhibition of DNA repair due to RNA polymerase II transcription. *J. Biol. Chem.* **274**, 1199–1202 (1999).
174. Pfander, B., Moldovan, G.-L., Sacher, M., Hoegge, C. & Jentsch, S. SUMO-modified PCNA recruits Srs2 to prevent recombination during S phase. *Nature* **436**, 428–433 (2005).
175. Heideker, J., Prudden, J., Perry, J. J. P., Tainer, J. A. & Boddy, M. N. SUMO-targeted ubiquitin ligase, Rad60, and Nse2 SUMO ligase suppress spontaneous Top1-mediated DNA damage and genome instability. *PLoS Genetics* **7**, e1001320 (2011).
176. Camilo, C. M., Lima, G. M. A., Maluf, F. V., Guido, R. V. C. & Polikarpov, I. HTP-OligoDesigner: An Online Primer Design Tool for High-Throughput Gene Cloning and Site-Directed Mutagenesis. *J. Comput. Biol.* **23**, 27–29 (2016).
177. Brachmann, C. B. *et al.* Designer deletion strains derived from *Saccharomyces cerevisiae* S288C: a useful set of strains and plasmids for PCR-mediated gene disruption and other applications. *Yeast* **14**, 115–132 (1998).
178. Finley, D., Ozkaynak, E. & Varshavsky, A. The yeast polyubiquitin gene is essential for resistance to high temperatures, starvation, and other stresses. *Cell* **48**, 1035–1046 (1987).
179. Piwko, W. & Jentsch, S. Proteasome-mediated protein processing by bidirectional degradation initiated from an internal site. *Nat Struct Mol Biol* **13**, 691–697 (2006).
180. Seufert, W., Futcher, B. & Jentsch, S. Role of a ubiquitin-conjugating enzyme in degradation of S- and M-phase cyclins. *Nature* **373**, 78–81 (1995).
181. Gietz, R. D. & Sugino, A. New yeast-*Escherichia coli* shuttle vectors constructed with in vitro mutagenized yeast genes lacking six-base pair restriction sites. *Gene* **74**, 527–534 (1988).
182. Knop, M. *et al.* Epitope tagging of yeast genes using a PCR-based strategy: more tags and improved practical routines. *Yeast* **15**, 963–972 (1999).
183. Janke, C. *et al.* A versatile toolbox for PCR-based tagging of yeast genes: new fluorescent proteins, more markers and promoter substitution cassettes. *Yeast* **21**, 947–962 (2004).
184. Clausing, E. *et al.* The transcription elongation factor Bur1-Bur2 interacts with replication protein A and maintains genome stability during replication stress. *J. Biol. Chem.* **285**, 41665–41674 (2010).
185. Kuo, M. H. & Allis, C. D. In vivo cross-linking and immunoprecipitation for studying dynamic Protein:DNA associations in a chromatin environment. *Methods* **19**, 425–433 (1999).

8 Abbreviations

4-NQO	4-nitroquinoline 1-oxide	g	gravity
aa	amino acid(s)	G1	gap 1 phase of the cell cycle
AAA	ATPases associated with various cellular activities	G418	geneticine disulfate
Ac	acetate	Gal	galactose
ADP	adenosine 5'-diphosphate	GFP	green fluorescent protein
AMP	adenosine 5'-monophosphate	GGR	global genome repair
ATM	ataxia telangiectasia mutated	Glu	glutamate
ATP	adenosine 5'-triphosphate	h	hour(s)
ATR	ATM- and RAD3-related	HA	hemagglutinin epitope
bp	base pair(s)	HECT	homologous to the E6-AP carboxyl terminus
°C	degree celcius	His	histidine
Cdc	cell division cycle	HMGN	high mobility group nucleosome binding domain
CDK	cyclin-dependent kinase	Hph	hygromycin B
cDNA	complementary DNA	hphNT1	gene conferring resistance to hygromycin
CENT2	centrin2	HRP	horse radish peroxidase
ChIP	chromatin immunoprecipitation	I	isoleucine
CHX	cycloheximide	IgG	immunoglobulin G
CPD	cyclobutane pyrimidine dimer	IP	immunoprecipitation
CS	Cockayne syndrome	K	lysine
CTD	carboxy-terminal domain	kanMX6	gene conferring resistance to G418
CTDK	CTD kinase	kb	kilo base pair(s)
Cul	cullin	kDa	kilo Dalton
DMSO	dimethylsulfoxide	Kin	kinase
DNA	deoxyribonucleic acid	kV	kilo Volt
DUB	deubiquitylating enzyme	L	liter(s)
DSB	DNA double-strand break	LB	Luria-Bertani
DTT	dithiothreitol	Leu	leucine
E	glutamic acid	LMU	Ludwig-Maximilians-University Munich
<i>E. coli</i>	<i>Escherichia coli</i>	Log	logarithmic
e.g.	exempli gratia, for example	m	milli ($\times 10^{-3}$)
E1	activating enzyme	μ	micro ($\times 10^{-6}$)
E2	conjugating enzyme	M	molar
E3	ligase	μm	micrometre(s)
E4	chain elongating ligase	MAT	mating-type locus
EDTA	ethylenediaminetetraacetic acid	MAT α	MAT locus containing α information
Ela	elonginA	MAT β	MAT locus containing β information
Elc	elonginC	MAT γ	MAT locus containing γ information
ER	endoplasmic reticulum	MCM	minichromosome maintenance
ERAD	ER-associated degradation	min	minute(s)
ERCC1	excision repair cross-complementation group 1	MMS	methyl methanesulfonate
G	glycine		
g	gram		

Abbreviations

MPI	Max-Planck-Institute	SH	thiol group
MRN	serine/threonine kinase complex Mre11 Rad50 Nbs1	SIM	SUMO-interaction motif
mRNA	messenger ribonucleic acid	Siz	SAP and Miz-finger domain
MRX	serine/threonine kinase complex Mre11 Rad50 Xrs2	Smt	suppressor of Mif2
Myc	epitope from c-Myc	STUbL	SUMO-targeted ubiquitin ligase
n	nano ($\times 10^{-9}$)	Sub	substrate
NAT	nourseothricin	SUMO	small ubiquitin-like modifier
natNT2	gene conferring resistance to nourseothricin	Swi/Snf	switching defective/sucrose non-fermentable
NEM	N-ethylmaleimide	TBE	tris, boric acid, EDTA
NER	nucleotide excision repair	TBS-T	tris-buffered saline-Tween20
nm	nanometre(s)	TCA	trichloro acidic acid
NF κ B	nuclear factor κ -light-chain-enhancer of activated B cells	TCR	transcription coupled repair
NP-40	nonidet p-40	TDD	trichothiodystrophy
OD $_x$	optical density at x nm	TE	Tris EDTA
ORF	open reading frame	TFIIH	transcription factor II H
Ω	Ohm	TFIIS	transcription factor II S
PAGE	polyacrylamide gel electrophoresis	Thr	threonine
PBS	phosphate buffered saline	TLS	translesion synthesis
PCNA	proliferating cell nuclear antigen	Tris	Tris(hydroxymethyl)-aminomethane
PCR	polymerase chain reaction	Trp	tryptophan
PE	phosphatidylethanolamine	Tyr	tyrosine
PEG	polyethylene glycol	Ub	ubiquitin
Pgk1	phospho-glycerate kinase 1	Ubc	ubiquitin conjugating
PML	promyelocytic leukaemia	UBP	ubiquitin protease
PPi	pyrophosphate	UBD	ubiquitin-binding domain
Pol	polymerase	UBL	ubiquitin-like
Pro	proline	Ufd	ubiquitin-fusion degradation
PVDF	polyvinylidene fluoride	Ulp	UbL-specific protease
R	arginine	USP	ubiquitin-specific protease
Rad	radiation	UTR	untranslated region
RING	really interesting new gene	UV	ultraviolet
RNA	ribonucleic acid	UV-DDB	UV-damaged DNA-binding
RNAPII	RNA polymerase II	UVSSA	UV-stimulated scaffold A
ROS	reactive oxygen species	V	Volt
RPA	replication protein A	v/v	volume per volume
Rpb	RNA polymerase B	vs.	versus
rpm	rounds per minute	WB	western blot
RT-PCR	real-time PCR	WCE	whole cell extract
S	Svedberg	WT	wild-type
<i>S. cerevisiae</i>	<i>Saccharomyces cerevisiae</i>	w/v	weight per volume
Sc	synthetic complete	Wwp	WW domain protein
SDS	sodium dodecyl sulfate	XAB	XPA binding
sec	second(s)	XP	xeroderma pigmentosum
Ser	serine	Y	tyrosine
		YPD	yeast bactopectone dextrose
		β -Me	β -mercaptoethanol

